

**USING PERCOLATION TECHNIQUES
TO ESTIMATE INTERWELL CONNECTIVITY PROBABILITY**

A Thesis

by

WEIQIANG LI

Submitted to the Office of Graduate Studies of
Texas A&M University
in partial fulfillment of the requirements for the degree of
MASTER OF SCIENCE

August 2007

Major Subject: Petroleum Engineering

**USING PERCOLATION TECHNIQUES
TO ESTIMATE INTERWELL CONNECTIVITY PROBABILITY**

A Thesis

by

WEIQIANG LI

Submitted to the Office of Graduate Studies of
Texas A&M University
in partial fulfillment of the requirements for the degree of
MASTER OF SCIENCE

Approved by:

Chair of Committee, Jerry L. Jensen
Committee Members, Walter B. Ayers
Richard Gibson
Head of Department, Stephen A. Holditch

August 2007

Major Subject: Petroleum Engineering

ABSTRACT

Using Percolation Techniques
to Estimate Interwell Connectivity Probability. (August 2007)
Weiqiang Li, B.S., Shandong University of Technology, P. R. China
Chair of Advisory Committee: Dr. Jerry L. Jensen

Reservoir connectivity is often an important consideration for reservoir management. For example, connectivity is an important control on waterflood sweep efficiency and requires evaluation to optimize injection well rates. The uncertainty of sandbody distributions, however, can make interwell connectivity prediction extremely difficult. Percolation models are a useful tool to simulate sandbody connectivity behavior and can be used to estimate interwell connectivity. This study discusses the universal characteristics of different sandbody percolation models and develops an efficient percolation method to estimate interwell connectivity.

Using King and others results for fluid travel time between locations in a percolation model, we developed a method to estimate interwell connectivity. Three parameters are needed to use this approach: the sandbody occupied probability p_{sand} , the dimensionless reservoir length, and the well spacing. To evaluate this new percolation method, the procedure was coded using Visual Basic and Mathematica and the results compared to those from two other methods, a simple geometrical model and Monte Carlo simulation.

All these methods were applied to estimate interwell connectivity for the D1, D2, and D3 intervals in the Monument Butte field. The results suggest that the new percolation method can give reasonable effective-square sandbody dimensions and can estimate the interwell connectivity accurately for thin intervals with p_{sand} in the 60% to 80% range.

The proposed method requires that the reservoir interval for evaluation be sufficiently thin so that 2D percolation results can be applied. To extend the method to 3D cases, we propose an approach that can be used to estimate interwell connectivity for reservoirs having multiple, noncommunicating layers, and that considers the weight of each interval for multilayer estimation. This approach is applied to the three-layer case of Monument Butte field and the estimates showed the method gives useful results for well pattern design. For example, water saturation and interval thickness affect the weight of each interval to be included in the multilayer estimation.

For thick intervals or heterogeneous sandbody distributions, the percolation method developed here is not suitable because it assumes thin layers. Future percolation research will be needed to adapt this new percolation method.

DEDICATION

To my wife, my sister, my mother, and my father

ACKNOWLEDGEMENTS

I would like to thank the following people for their contributions toward the success of this thesis:

Dr. Jerry L. Jensen, for his support, valuable comments, and advice throughout all stages of this study;

Dr. Walter B. Ayers, for his guidance, encouragement, tireless effort, patience, and advice in helping me to complete this thesis;

Dr. Richard Gibson, for his interest, kindness and serving as a member of my advisory committee;

My many friends, for their help, concern, and encouragement all the time.

TABLE OF CONTENTS

	Page
ABSTRACT	iii
DEDICATION	v
ACKNOWLEDGEMENTS	vi
TABLE OF CONTENTS	vii
LIST OF FIGURES	ix
LIST OF TABLES	xii
CHAPTER I: INTRODUCTION	1
1.1 State of problem	1
1.2 What is percolation?	3
1.3 Literature review	7
1.3.1 Interwell connectivity study	7
1.3.2 Percolation study	9
1.4 Research procedure	11
1.5 Objective of this study	13
1.6 Outline of this thesis	14
CHAPTER II: PERCOLATION MODEL ANALYSIS	15
2.1 Relevance of percolation model to interwell connectivity	15
2.2 Infinite square sandbody model	16
2.3 Boundary effect analysis	20
2.4 Rectangular effect analysis	25
2.5 Orientation degree effect analysis	31
2.6 Discussion	36
CHAPTER III: INTERWELL CONNECTIVITY ESTIMATION ANALYSIS	40
3.1 King et al.'s (2002) process for breakthrough time estimation	40
3.2 Interwell estimation method based on King et al.'s (2002) process	45
3.2.1 Derivation of interwell connectivity estimation method	45
3.2.2 Generation of input parameters L and p_{sand}	49
3.3 Simple geometric model analysis	53
3.4 Monte Carlo simulation	60
CHAPTER IV: MULTILAYER ESTIMATION METHOD	63

	Page
CHAPTER V: APPLICATION TO FIELD DATA	67
5.1 Description of field data.....	67
5.2 Analysis and results	74
5.2.1 D1 interval.....	74
5.2.2 D2 interval.....	77
5.2.3 D3 interval.....	80
5.2.4 Multilayer estimation	84
5.3 Summary and discussion.....	87
CHAPTER VI: CONCLUSIONS	89
CHAPTER VII: RECOMMENDATIONS FOR FURTHER WORK.....	91
NOMENCLATURE.....	93
REFERENCES.....	95
APPENDIX A: VBA CODE FOR INPUTTING PARAMETER ESTIMATION.....	98
APPENDIX B: MATHEMATICA CODE FOR INTERWELL ESTIMATION	99
APPENDIX C: RESERVOIR PROPERTIES SUMMARY OF D1, D2 AND D3	101
VITA	104

LIST OF FIGURES

FIGURE	Page
1.1 The conventional workflow for interwell connectivity estimation by reservoir simulation.....	2
1.2 One example to show percolation phenomena.....	4
1.3 Basic percolation models	5
1.4 Site percolation model of porous media.....	6
2.1 Infinite square sandbody model	16
2.2 Square sandbody distribution simulation	18
2.3 Universal curve for percolation phenomenon (Modified from Gimmet, 1999)	19
2.4 Scatter points of $P(p_{\text{sand}}, L)$ against p_{sand} for a given L along with the average curve and error bars (Modified from Mashih, 2006)	21
2.5 Universal curves for finite square sandbody model	23
2.6 Rectangular sandbody model	26
2.7 Aspect ratio affects the connectivity performances	27
2.8 Illustration of universal curves for finite rectangular sandbody model	29
2.9 The universal curves with different ω will have different locations on the X axis.....	29
2.10 Orientation degree of sandbodies will affect connectivity performance.....	33
2.11 Graphical description of two typical orientated sandbody cases	34
2.12 Graphical description of effective-rectangular sandbody transformation....	35
2.13 VBA program of “backward” mode for effective-square sandbody dimension estimation.....	39
3.1 Breakthrough time between Well A and Well B depends on sandbody connectivity and well spacing r of the whole well pattern....	42
3.2 Comparison of breakthrough time estimation from different methods.....	44

FIGURE	Page
3.3	Illustration of breakthrough time distribution for different interwell distances (r values) calculated from King <i>et al.</i> 's (2002) equation 45
3.4	Illustration of interwell estimation result 47
3.5	Illustration for connected sand fraction as a function of well spacing (King, 1990) 48
3.6	The procedure to estimate p_{sand} and P (Nurafza <i>et al.</i> , 2006a)..... 51
3.7	The net sand area map to estimate p_{sand} and P 52
3.8	Graphical description of small domain around one sand 53
3.9	Scheme of different regions 54
3.10	Probability tree for the connectivity probability estimation of A and B 56
3.11	Possible locations of B when A is in the edge region 57
3.12	Illustration of Monte Carlo simulation 61
3.13	Comparison examples of different estimations from different methods 62
4.1	Graphic description of Well A and Well B 63
4.2	Graphic description for the procedure to transform the deferent weight interval model to a uniform weight interval model 65
5.1	Location of the study area in Monument Butte field 68
5.2	Base-map of study area 69
5.3	Net sand overlay sand count map of D1 interval 71
5.4	Net sand overlay sand count map of D2 interval 72
5.5	Net sand overlay sand count map of D3 interval 73
5.6	Estimation of effective-square sandbody dimension of the D1 interval 74
5.7	Interwell connectivity probability estimation of D1 interval 75
5.8	Comparison of different estimates for D1 interval in dimensionless scale 76
5.9	Comparison of different estimates for D1 interval in actual scale 76

FIGURE		Page
5.10	Estimation of effective-square sandbody dimension of D2 interval	77
5.11	Interwell connectivity probability estimation of D2 interval	78
5.12	Comparison of different estimates of D2 interval in dimensionless scale	79
5.13	Comparison of different estimates of D2 interval in actual scale	80
5.14	Interwell connectivity probability estimation of D3 interval	82
5.15	Comparison of different estimates of D3 interval in dimensionless scale	83
5.16	Comparison of different estimates of D3 interval in actual scale	84
5.17	Comparison of estimations from different method for a multilayer reservoir	86

LIST OF TABLES

TABLE	Page	
2.1	Universal exponents β, ν and threshold p_c values for 2D square sandbody model.....	22
2.2	Aspect ratio effect	28
3.1	Summary of exponents and constants	41
5.1	Percolation parameter estimations of D3 interval	81
5.2	Net sand average thickness of D1, D2, and D3 intervals.....	85
5.3	Water saturation of D1, D2, and D3 intervals.....	85
C.1	Reservoir Properties Summary of D1 Interval.....	101
C.2	Reservoir Properties Summary of D2 Interval.....	102
C.3	Reservoir Properties Summary of D3 Interval.....	103

CHAPTER I

INTRODUCTION

1.1 State of problem

Sandstone reservoirs are the result of long and frequently complex histories of geological evolution. The combined processes of deposition, burial, compaction, diagenesis, and structural deformation make interwell connectivity difficult to predict. Uncertainty about the sandbody distribution affects prediction of hydrocarbon flow in reservoirs and, in particular, interwell connectivity.

A conventional workflow based on reservoir simulation for interwell connectivity estimation (Figure 1.1) might include the following steps:

- Build detailed geological models of the reservoir according to the available data.
- Distribute flow properties often based on the geological model to get reservoir models showing the uncertainties.
- Upscale each reservoir model and then simulate fluid flow.
- Perform history matching to check reservoir model quality.
- Decide whether the reservoir model is suitable or not based on history match.
- Combine all results from each reservoir model to determine interwell connectivity based on fluid flow simulation analysis.

This thesis follows the style and format of *Petrophysics*.

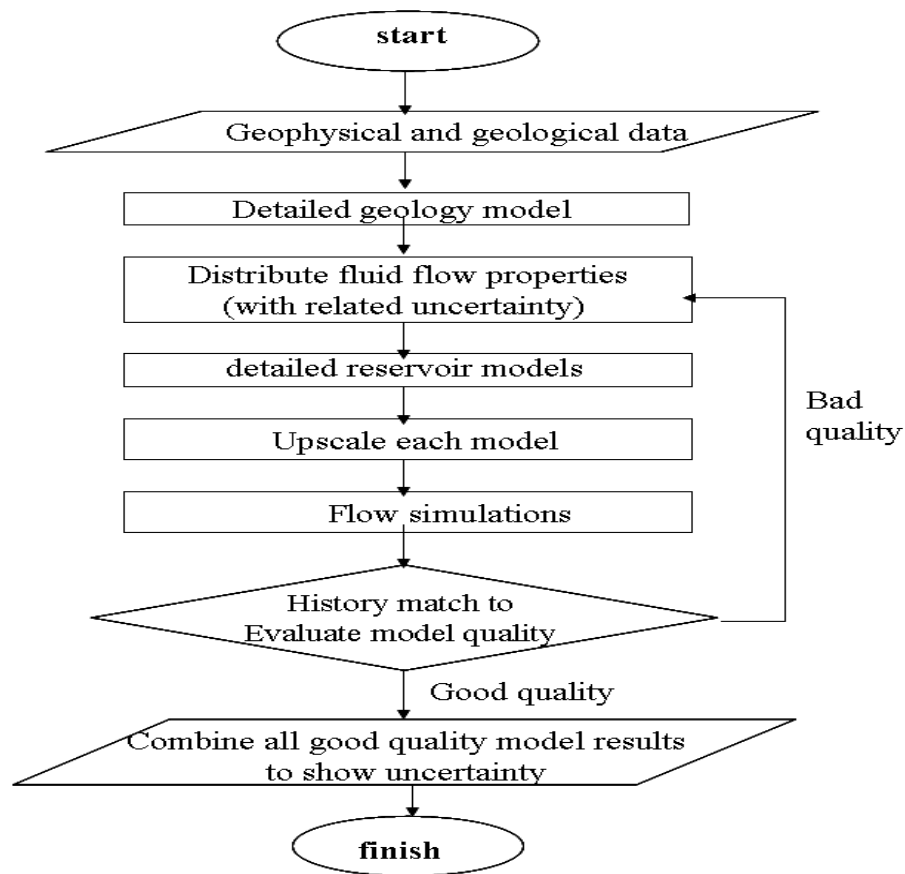


FIG. 1.1 The conventional workflow for interwell connectivity estimation by reservoir simulation.

The disadvantages of estimating interwell connectivity from reservoir simulation are clear.

- It requires several months to build reservoir models and simulate performance.
- It requires many kinds of field data, each with its associated uncertainties.
- It combines deterministic results to show the uncertainty range of interwell connectivity. Since the result will depend on how many reservoir models have been used, the combination of limited deterministic results may not be the “true”

statistical result with an appropriate standard deviation. Statistical results may need hundreds simulations to eliminate extreme realizations effects.

Using percolation phenomena, which are based on extensive statistical simulations, engineers can predict interwell connectivity very quickly. Since the percolation model has interesting universal characteristics that have been studied for decades, percolation theory can be used to estimate interwell connectivity performance very quickly. Compared to conventional interwell connectivity estimation methods, this technique will give a single, rapid, statistical estimate of connectivity with related standard deviation.

1.2 What is percolation?

Imagine we have a conductive lattice with two electrodes on opposite sides. If we connect the electrodes, a light is switched on. We will randomly assign numbers “1” and “0” to the sites of this lattice (Figure 1.2a). The sites with number “1” are conductors and the sites with “0” are insulators. We define occupied probability p to be the ratio of the number of “1” sites to the total number of sites. We will do this experiments many times. For every experiment, we will assign one more “1” than the last experiment, which also means we increase the occupied probability p value every time. Different colors are used to represent different connected conductor clusters. Nothing happen when either $p = 0.4$ or $p = 0.5$ (Figures 1.2b and c). When p is increased to 0.6, the light is switched on (Figure 1.2d). This happens when a percolation cluster of conductors spans across from the left side to the right side. The value $p = 0.6$ appears to be a critical value for our experiment.

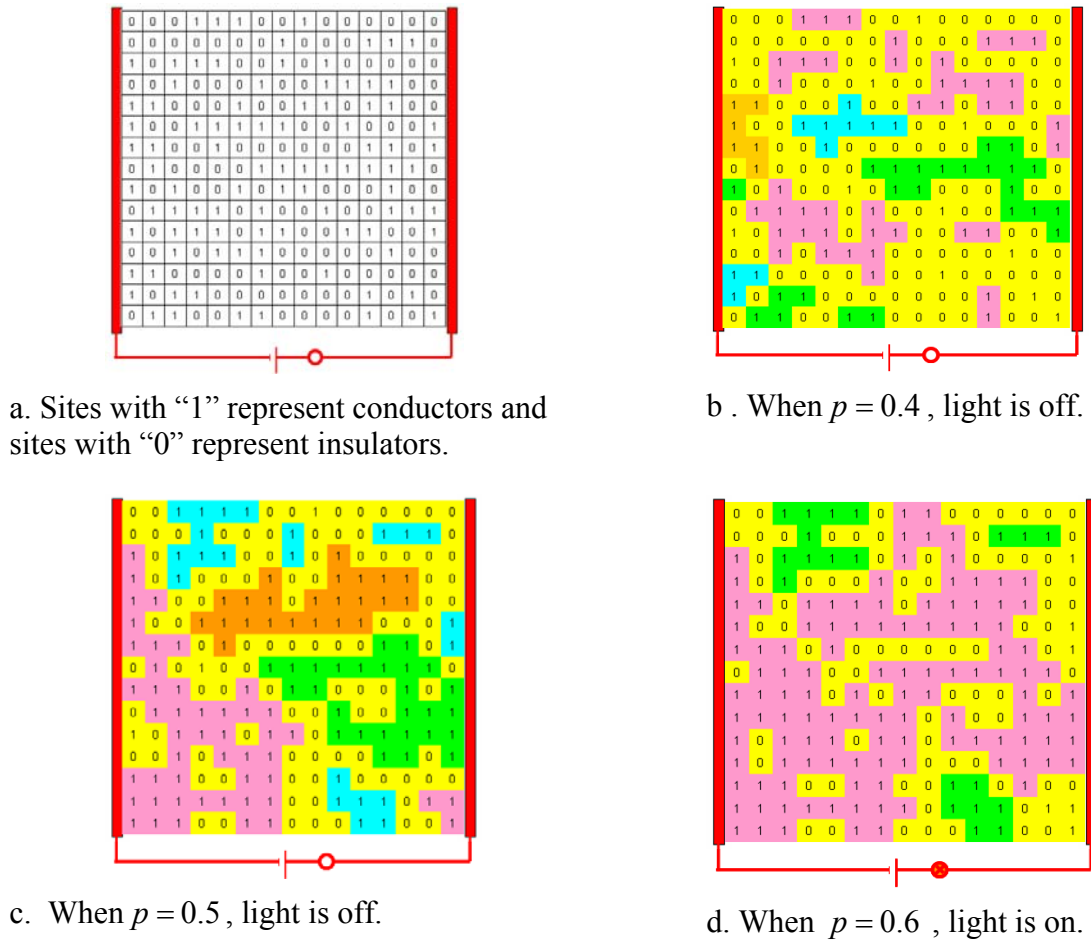
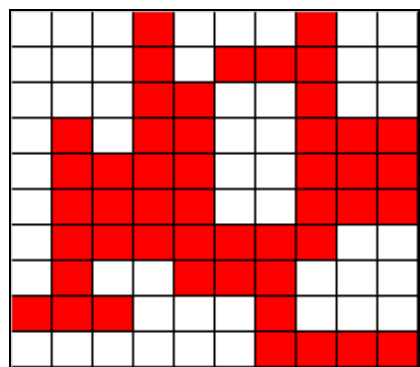


FIG. 1.2 One example to show percolation phenomena.

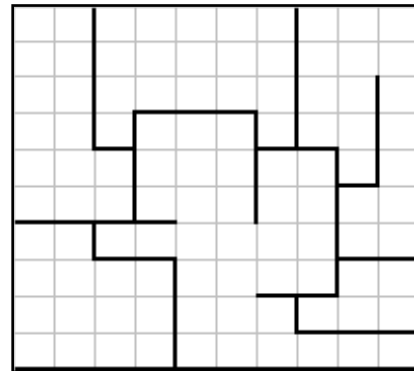
When a connected cluster touches both electrodes, the light is switched on. Otherwise, the light is off. If we do this experiment enough times, the interesting thing is we will find the probability p to switch on the light to be almost a fixed value, which is termed as threshold value p_c . Simulations have shown that the p_c value depends on the dimension, type, shape, and kind of lattice.

This is a simple example to show the percolation phenomena. The model to simulate this kind of phenomenon can be called the *percolation model*. The percolation model (King, 1990) is a simple probabilistic model that can be used to simulate connectivity and transport phenomena in geometrically complex systems and can provide insight into critical phenomena in statistical mechanics.

Two different kind of percolation models (Stauffer and Aharony, 1985) are used to study percolation phenomena. The first model is a site percolation model, which is based on the sites connectivity study of the lattice (Figure 1.3a). The second is a bond percolation model, which is based on the edge connectivity study of the lattice (Figure 1.3b).



a. Site percolation model

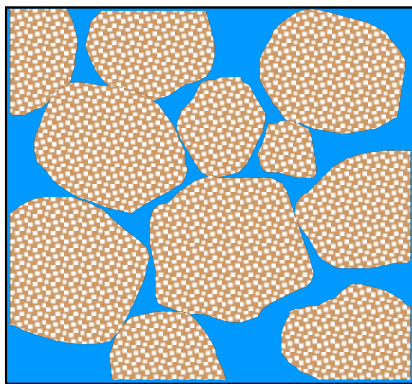


b. Bond percolation model

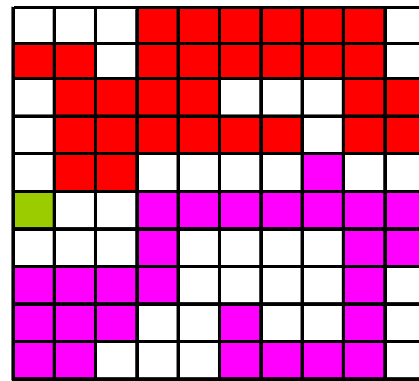
FIG. 1.3 Basic percolation models.

Bond percolation was studied historically first, but now most research is based on site percolation. The site percolation model can be an idealized model to represent the hydrocarbon distribution in porous media. If every void space of a porous medium has one

p probability to be occupied by oil, the connectivity performance of connected spaces will show percolation characterization (Figure 1.4). The connectivity performance in such a discrete percolation model is very interesting to petrophysics study and can be used to study water displacement processes.



a. Porous media with void pores



b. Each site represents one void pore of porous media.

FIG. 1.4 Site percolation model of porous media.

Considering the overlapping structure of sandbody distribution, hydrocarbons can flow from one sandbody to another. Therefore, we can use a continuum percolation model to represent the sandbody connectivity. The continuum percolation model extends the discrete sites geometry model to an overlapped sites geometry model. Current research techniques for the study of continuum percolation attempt to approximate the continuum model with a discrete one. Many results of continuum model are analogues of discrete results only with some different parametric values (Grimmett, 1999).

In the continuum percolation model, the sandbodies are randomly distributed in the reservoir instead of discrete. The sandbodies are not limited to points on a fixed lattice and can be located anywhere in the studied space. The sandbodies can have any shape; they can be squares, rectangles, discs, or ellipses in 2D or cubes, spheres, rods, or ellipsoids in 3D (King, 1990). In this study, we will always use continuum percolation to model overlapping sandbodies.

1.3 Literature review

Since interwell connectivity is often highly important for industry and the reservoir simulation method is quite timing consuming, alternative methods have been developed for field application. Since production and injection data are usually measured every month in the field, current methods include those based on production and injection rate data to estimate interwell connectivity performance. To my knowledge, no interwell connectivity method based on percolation theory has been published, although this theory has been applied to other reservoir engineering problems. The following literature review includes the important results of previous interwell estimation studies and a historical review of percolation studies.

1.3.1 Interwell connectivity study

Yousef *et al.* (2006) briefly reviewed the history of interwell estimation study based on production and injection data analysis. Based on his work, I will discuss more detail about the important published results here.

Using Spearman rank correlations to study injector/producer well pairs, Heffer *et al.* (1995) showed that the collusion is the correlations between injector rates and producer rate can reflect reservoir communication. They suggested the rate correlation between wells could be explained partially by geomechanics.

Jansen and Kelkar (1997) applied the wavelet transformation to decompose the production data into a combination of frequency and smoothed components. Production data are nonstationary in the presence of effect of well control operations, reservoir depletion, near-wellbore damage, and influence from nearby wells. Wavelet transformation can break the production data into its frequency components yet retain its related time information. Since wavelet transformation can treat nonstationary data, it can yield a more reliable correlation between injector/producer well pairs.

Panda and Chopra (1998) used a different approach to determine injector/producer interaction. They trained an artificial neural network to estimate the interwell interaction between different well pairs and applied the approach to numerical simulation of one waterflood project. They showed that a lack of ability to represent physical processes limited neural network application.

Soeriawinata and Kelkar (1999) described one statistical approach based on Spearman rank analysis. They introduced contradictive and destructive interference using a superposition concept. They stated that the superposition of injectors would affect the producer response significantly. This method can identify strong connectivity and potential barriers in the field.

Albertoni and Lake (2002) developed one technique to qualify communication between wells using multivariate linear regression (MLR) and balanced multivariate linear regression (BMLR). This technique is useful to determine permeability trends and the pressure of permeability barriers and it can be used to estimate the total production from given injection rate. The technique is limited to liquid (oil and water) data and does not include gas rate analysis. Applying this technique applied to one waterflood project in Argentina showed some agreement with known geological features.

Yousef *et al.* (2005) modified Albertoni and Lake's (2002) method to evaluate the communication between vertical wells from fluctuations in production and injection rates. They extended the application to a more complex model that includes capacitance (compressibility) and resistive (transmissibility) effects. For analysis, they determined two coefficients to better qualify the interwell connectivity. One parameter, λ , quantifies the connectivity and another parameter, τ , quantifies the fluid storage in the interwell region. The advantages of this method are the applicability to the fields where the wells are frequently shut in and the flow rates include primary production. This method also can incorporate the BHP values if available. Yousef *et al.* (2006) described a diagnostic tool based on the capacitance model to enhance the detection of preferential transmissibility trends and the presence of flow barriers.

1.3.2 Percolation study

In 1957, Broadbent and Hammersley (Grimmett, 1999) introduced the term *percolation process* to model the random flow of a fluid through a medium. Russo,

Seymour and Welsh conducted fundamental research about percolation study, but the problem for 2D was finally solved by Kerstin

During the 1980s, Aizenman, Barsky and Menshikov extended Kestin's theorem to all dimensions for $p < p_c$ (Grimmett, 1999). When $p > p_c$, the key question about the relationship characteristics between p and P was solved by Grimmett and Marstrand following the work of Barsky, Grimmett, and Newman (Grimmett, 1999). The critical case, when p is near or equal to the critical probability p_c , remains largely unresolved by mathematicians. Current research about this case is mainly based on physical simulation.

Physical simulations showed the p_c value depends on the kind and dimension of the lattice. The percolation threshold p_c for the continuum model depends on the shape of objects. A similar universal curve applies to the continuum percolation model with similar exponents for power law $P \propto (p - p_c)^\beta$ (Stauffer and Aharony, 1985).

During the 1990s, many papers described percolation applications for the reservoir engineering problems of fracture systems (Gale *et al.*, 2005; Masihi *et al.*, 2006a and 2006b), waterflood models (Barrufet *et al.*, 1994), permeability distribution estimation (King, 1990; Albert, 1992; Salomao, 1997), and sandbody connectivity estimation (King, 1990; Nurafza *et al.*, 2006a and 2006b).

Andrade *et al.* (2000) reported on their results for the relationship between percolation parameters and connectivity performance of different sites, using random polymer media research. King *et al.* (2002) extended Andrade *et al.*'s (2000) results to estimate the connectivity of sands as well as breakthrough times for a pattern of numerous

wells with dimensionless well spacing. Nurafza *et al.* (2006a and 2006b) showed further results for the effects of sandbody aspect ratio, orientation degree, and system size that have been used for fracture connectivity estimation.

Until now, no research has specially investigated how to estimate interwell connectivity based on percolation theory. Perhaps the most closely related work was by King (1990) and King *et al.* (2002). King (1990) first discussed percolation applications in reservoir characterization, showing that percolation models could simulate the connectivity characteristic of sandbody distributions. Since the sandbody connectivity characteristic will affect the interwell connectivity, percolation theory may be applied to estimate interwell connectivity. King *et al.* (2002) described how to use percolation theory to estimate breakthrough time distributions. Using King *et al.*'s (2002) process and considering sandbody distributions with different geometries, as discussed in Nurafza *et al.* (2006a and 2006b), we developed a method to estimate interwell connectivity

1.4 Research procedure

Monument Butte field, located in the Uinta Basin of northeast Utah, is a low-permeability, high-heterogeneity reservoir containing significant volumes of oil. A DOE Class 1 waterflood demonstration project in Monument Butte Unit, started in 1992, shows this reservoir needs further unconventional methods to improve production (Deo *et al.*, 1994). Newfield Exploration Company is funding studies to compare different technologies for production improvement. My research is one of these studies, and it will focus on the use of percolation theory to estimate interwell connectivity.

Percolation theory was chosen to evaluate sandbody connectivity because it has been found to reproduce reservoir behavior at model scales. In addition, this theory enables us to evaluate the uncertainty of our connectivity predictions.

Actual sandbodies have very complex distributions, with different aspect ratios and orientations. We need to understand how aspect ratio and orientation degree will affect percolation-based connectivity estimates. For percolation analysis, Masihi *et al.* (2006) showed actual sandbody geometries can be represented by sandbodies with different aspect ratios, orientation degrees and boundary effects. Nurafza *et al.* (2006a and 2006b) further proposed that these effects can be represented by effective-square-shape sandbody distribution using simple mathematical transformations. These results suggest that we can study effective-square sandbody models first and then incorporate boundary effects, aspect ratio effects, and orientation degree effects to refine the model to better reflect the actual sand geometries.

From the assumption that actual sandbody distributions can be modeled as square sandbodies, we developed an interwell connectivity estimation method based on percolation. We evaluated the results by comparing them with those from Monte Carlo simulation and a simple geometric model, which was suggested by Jensen during personal communication in 2007.

All dimensionless sandbody lengths are scaled with respect to the typical sandbody size in King *et al.*'s (2002) process. Since it is difficult to identify separate sandbody dimensions accurately, we used the universal property of percolation to estimate the mean and standard deviation of sandbody dimensions instead of finding the "typical" sandbody

dimension. Finally, we successfully removed the impractical aspects of King *et al.*'s (2002) process for field application. In addition, we proposed a practical way to apply our model for multilayered reservoirs.

1.5 Objective of this study

- a. Identify and categorize important factors or issues of percolation, including the following:
 - a. sandbody occupied probability, p_{sand} , which has same meaning with net-to-gross ratio
 - b. percolation cluster probability, P , which has same meaning with connected sand fraction of all sands in the study reservoir
 - c. boundary effect
 - d. aspect ratio
 - e. orientation degree
 - f. well spacing
 - g. sandbody effective-dimension
- b. Develop a method to determine p_{sand} and P from Monument Butte maps using a universal curve of percolation theory instead of using separate sandbody parameters, as is done in King *et al.*'s (2002) process.
- c. Develop an interwell connectivity estimation process using our results of sandbody occupied probability p_{sand} and percolation cluster probability P . This work, based

on sensitivity analysis of the effective-square sandbody model, will include well spacing and critical percolation parameters.

- d. Use Monte Carlo simulation to evaluate whether the estimation results from our new model are reasonable or not.
- e. Introduce the following three considerations into the new effective-square sandbody model to simulate real, underground sandbody distribution:
 - a. effects of sandbody aspect ratio
 - b. orientation degree
 - c. multilayer reservoirs
- f. Implement the procedures in VBA and Mathematica programs so that field operators can input parameters from zone maps to make their own analyses.

1.6 Outline of this thesis

The thesis consists of five chapters. This chapter presents the motivation of this thesis, general introduction of percolation, and a literature review of interwell connectivity estimation and percolation studies. Chapter II is a detailed discussion of percolation theory background for interwell estimation. Chapter III discusses the analysis procedures and proposed methods for thin intervals, which can be approximated by a 2D system. Chapter IV presents a multilayer estimation method for a 3D reservoir. Chapter V describes the application for Monument Butte field and the results that we obtained. Chapter VI presents a summary and conclusions, and Chapter VII proposes possibilities for future work.

CHAPTER II

PERCOLATION MODEL ANALYSIS

2.1 Relevance of percolation model to interwell connectivity

Interwell connectivity in this study is defined as the chance that two wells will penetrate the same sand cluster at a given well spacing. The connectivity performance between well pairs is one critical parameter for well pattern design. Uncertainty about the sandbody distribution affects prediction of hydrocarbon flow in the reservoir and, in particular, interwell connectivity.

Sandbodies underground are mixed with good quality sandbodies and poor quality sandbodies. Good quality sandbodies means sandbodies with high porosity and permeability. Better quality sandbodies can store more hydrocarbons in void pores, and water can displace the hydrocarbons through the connected pores that serve as flow paths from injection wells to production wells. The ratio of good quality sandbodies to total sandbodies is one important concern for connectivity performance, which has the same meaning as occupied probability p in percolation theory.

The conductivity of the sandbody cluster affects the interwell connectivity behavior. The conductivity can be represented by the ratio of connected good quality sandbodies to all the good quality sandbodies. Having more good quality sandbodies in the connected cluster means more effective sandbodies will contribute to the fluid flow. Therefore, this ratio is another important consideration for interwell connectivity

performance. This ratio has same meaning as percolation cluster probability P of percolation theory.

2.2 Infinite square sandbody model

The basic model in this study is the infinite square sandbody model. Infinite means reservoir is large enough that the boundary effect can be ignored. Square sands with length l are distributed randomly in one reservoir. The center points of sands are distributed independently and the sands are allowed to overlap each other. The overlapped area will not be counted twice (Figure 2.1).

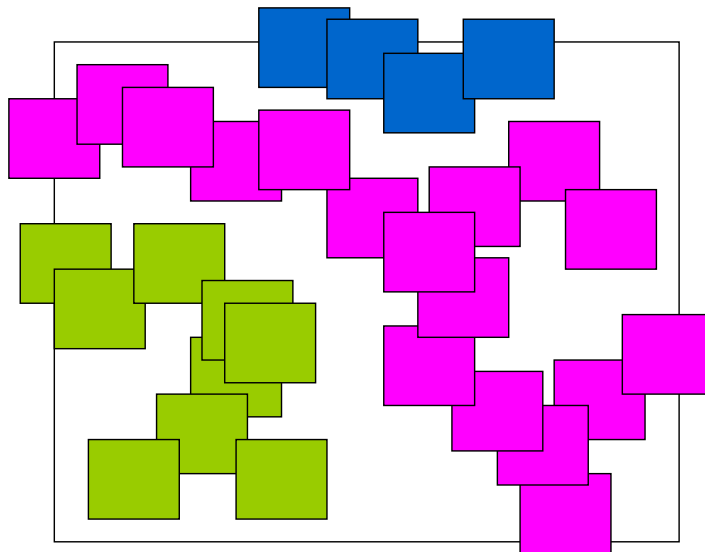


FIG. 2.1 Infinite square sandbody model.
(Different colors represent different connected clusters).

We will use one interesting example to describe how to use this kind of model to study the interwell connectivity. Suppose that we use one square area to represent a

reservoir (Figure 2.2a), with one injector well located along the left boundary and one producer located along the right boundary. Compared to the sandbody dimension, this reservoir is very big and so the left boundary is far away from right boundary, which means the boundary effect can be ignored. This is one approximation of an infinite reservoir. Square sandbodies are randomly distributed in this reservoir area. We define p_{sand} as the sandbody occupied probability, which is the ratio of sand area to the entire reservoir area. When a percolation cluster is present between these two wells, the two wells are connected. That means there is at least one path through the sand that connects the two wells. $P_{\infty}(p_{\text{sand}})$ is the percolation cluster probability of this infinite model, which represents the probability of one sandbody pixel belonging to the percolating sandbody cluster and will depend only on p_{sand} .

No connectivity is present between the injector and the producer when $p_{\text{sand}} = 0.45$ or $p_{\text{sand}} = 0.65$ (Figure 2.2b and c). However, if we throw one more sandbody into this reservoir, giving $p_{\text{sand}} = 0.69$, both wells become connected (Figure 2.2d). Not all clusters form a part of the connecting cluster (Figure 2.2e); we can see only the biggest percolation cluster connects the two opposite boundaries (Figure 2.2f). This is the interesting property for the percolation phenomenon. In this simulation, when $p_{\text{sand}} < 0.69$, no percolation cluster exists; when $p_{\text{sand}} = 0.69$, a percolation cluster is present. The value $p_{\text{sand}} = 0.69$ appears to be a critical value for our percolation model.

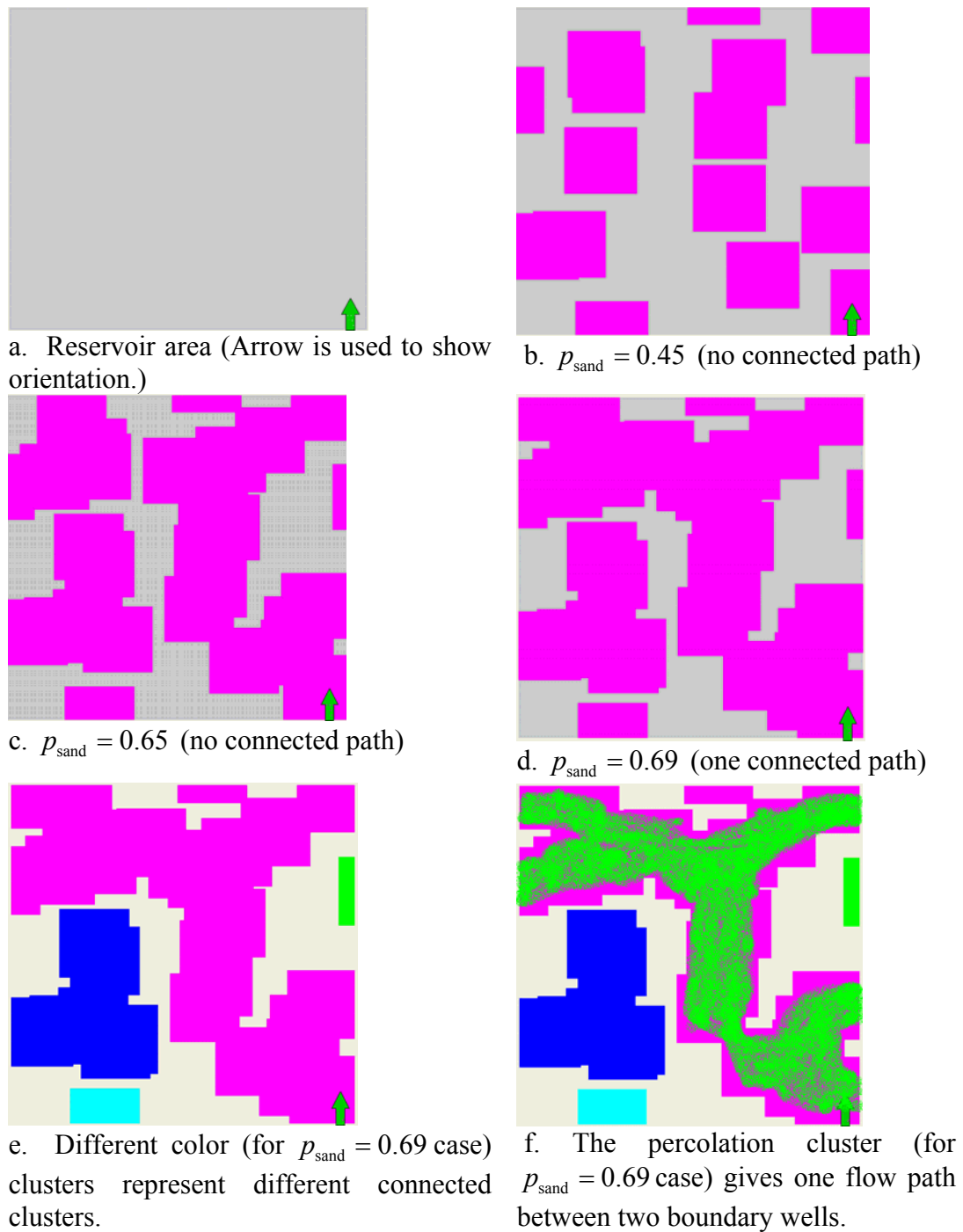


FIG. 2.2 Square sandbody distribution simulation with one injector located at left boundary and one producer located at right boundary. When $p_{\text{sand}} < 0.69$, no connected cluster appears between two opposite boundary wells. When $p_{\text{sand}} = 0.69$, one connected cluster appears between two opposite boundary wells.

If we do this simulation enough times for an infinite reservoir, the probability of getting a connected cluster across the system will increase very quickly when $p_{\text{sand}} \geq 0.6674$. However, if $p_{\text{sand}} < 0.6674$, the probability of getting a connected cluster is almost zero. We can define $p_{\text{sand}} = 0.6674$ as the percolation threshold p_c for this system. p_c is one fixed value for the infinite square sandbody model. This also means that, when $p_{\text{sand}} \geq p_c$, the connectivity performance (represented by the percolation cluster probability P) between two boundary wells will increase very quickly by a power law $P_{\infty}(p_{\text{sand}}) \propto (p_{\text{sand}} - p_c)^{\beta}$, where β is a critical universal exponent (Stauffer and Aharony, 1985). When $p_{\text{sand}} < p_c$, however, the connectivity probability of these two boundary wells will almost be zero (Figure 2.3).

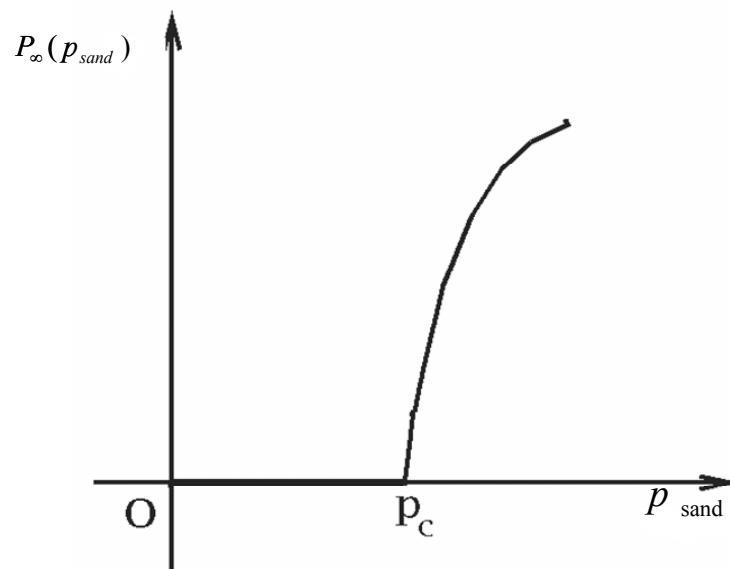


FIG. 2.3 Universal curve for percolation phenomenon (Modified from Gimmet, 1999).

2.3 Boundary effect analysis

Let us consider one reservoir having finite size, which means the boundary cannot be ignored. In this model, square sands with length l are distributed randomly in one finite square reservoir with area A . The reservoir (or system) dimensionless length is defined as

$L = \frac{\sqrt{A}}{l}$ ($L \gg 1$). p_{sand} , with the same meaning as in the infinite system, is the sandbody

occupancy probability, which is the ratio of sand area to the entire reservoir area.

$P_{\infty}(p_{\text{sand}})$ is replaced by $P(p_{\text{sand}}, L)$, the percolation cluster probability of the finite model,

which represents the ratio of connected sand area to sand area. $P(p_{\text{sand}}, L)$ depends on p_{sand} and L values.

Now, we have three parameters to study, including reservoir dimensionless length L , sandbody occupied probability p_{sand} , and percolation cluster probability $P(p_{\text{sand}}, L)$.

Different realizations with different L or different p_{sand} will give different percolation cluster probabilities $P(p_{\text{sand}}, L)$. If we plot $P(p_{\text{sand}}, L)$ against p_{sand} for one given L value, we can get a scatter of points. From this kind of plot, we can determine the mean value of $P(p_{\text{sand}}, L)$ and its related error bars $\Delta(p_{\text{sand}}, L)$ (Figure 2.4) (Mashihi, 2006a).

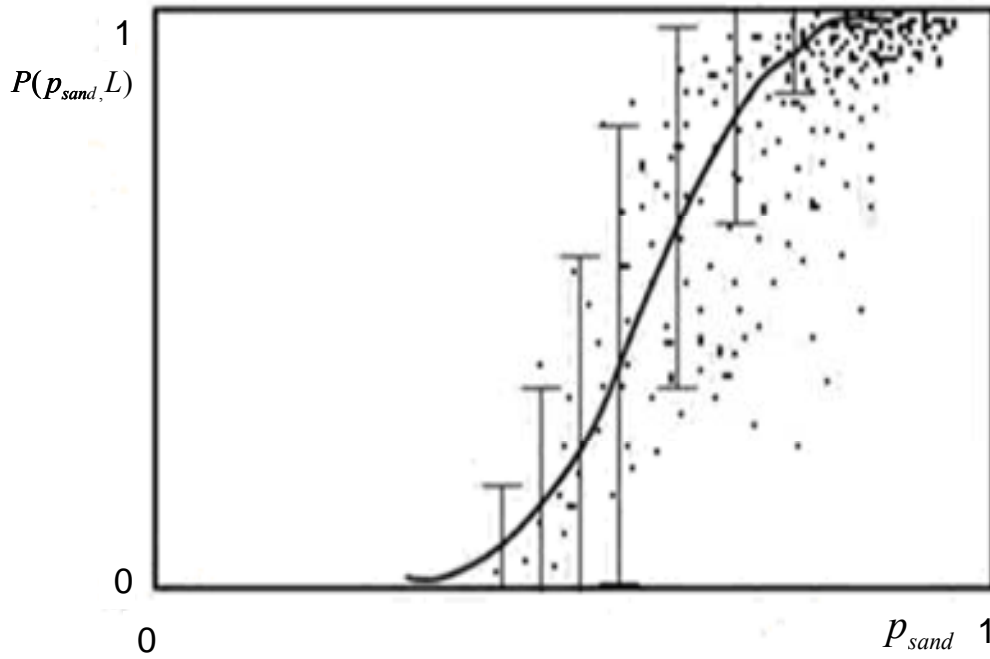


FIG. 2.4 Scatter points of $P(p_{\text{sand}}, L)$ against p_{sand} for a given L along with the average curve and error bars.(Modified from Mashihi, 2006a).

For all L values, we can always get similar curves. From Stauffer and Aharony (1985), we know the finite universal scaling law for the connectivity in the overlapping sandbodies could be written as

$$P(p_{\text{sand}}, L) = L^{-\beta/\nu} \mathfrak{F}_L \left[(p_{\text{sand}} - p_c) L^{1/\nu} \right] \dots\dots\dots (2.1)$$

$$\Delta(p_{\text{sand}}, L) = L^{-\beta/\nu} \mathfrak{R} \left[(p_{\text{sand}} - p_c) L^{1/\nu} \right] \dots\dots\dots (2.2)$$

where

$\mathfrak{F}[x]$ is the universal mean connectivity function

$\mathfrak{R}[x]$ is the universal standard deviation connectivity function

β, ν are universal exponents

p_{sand} is sandbody occupied probability

$P(p_{sand}, L)$ is percolation cluster probability

$\Delta(p_{sand}, L)$ is the relative uncertainty range

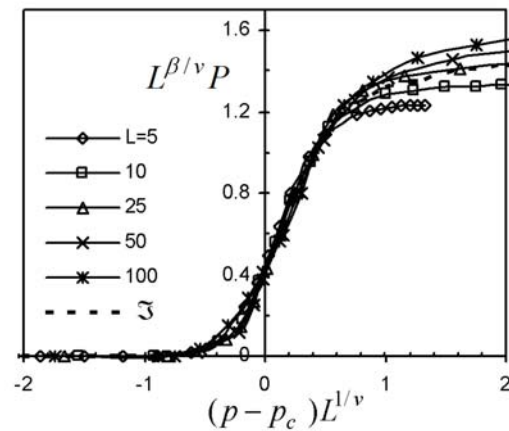
“Universal” here means that the functions and the exponents are independent of the size of the system and only depend on the system dimension. The percolation threshold p_c depends on the shape of the sandbody and system dimension.

Nurafza *et al.* (2006a) showed current best estimates for β, ν , and p_c of a 2D finite square sandbody model (Table 2.1).

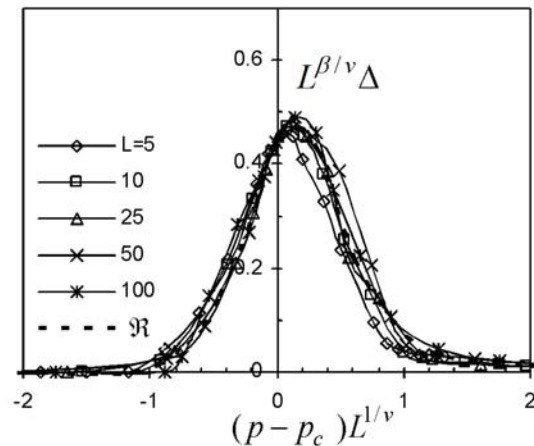
TABLE 2.1 Universal exponents β, ν and threshold p_c values for 2D square sandbody model.

ν	1.62 ± 0.07
p_c	0.6674 ± 0.1
β	0.14 ± 0.01

Using these parameter values, Nurafza *et al.* (2006a) described two universal curves for a finite system. One curve is for the mean connectivity function $\mathfrak{S}_L[x]$ of $L^{\beta/\nu}P$ against $(p - p_c)L^{1/\nu}$ (Figure 2.5a), and the other curve is for the standard deviation connectivity function $\mathfrak{R}_L[x]$ of $L^{\beta/\nu}\Delta$ against $(p - p_c)L^{1/\nu}$ in (Figure 2.5b). As expected from Stauffer and Aharony's (1985) results, the curves for different L values lie almost on top of each other.



a. Universal curve for the mean connectivity function $\mathfrak{S}_L[x]$.



b. Universal curve for the standard deviation connectivity function $\mathfrak{R}_L[x]$.

FIG. 2.5 Universal curves for finite square sandbody model (Nurafza *et al.*, 2006a).

The finite square sandbody model has two universal curves. One universal curve is for the mean connectivity function $\mathfrak{S}_L[x]$ and the other is for the standard deviation connectivity function $\mathfrak{R}_L[x]$. Each universal curve has three variables; one is with p_{sand} , $P(p_{\text{sand}}, L)$ and L , and the other is with p_{sand} , $P(p_{\text{sand}}, L)$ and Δ . If we know separate sandbody dimension L and p_{sand} , we can get the value of $P(p_{\text{sand}}, L)$ and Δ . Inversely, if we know $P(p_{\text{sand}}, L)$ and p_{sand} , we can get the value of L and Δ .

Since L is included on both the X-axis and the Y-axis, we need use one regression function of Figure 2.5a to calculate L value from p_{sand} and $P(p_{\text{sand}}, L)$. The regression function has the following form:

$$y = a \frac{1}{\sqrt{2\pi}} e^{-\frac{(bx+c)^2}{2}} + d \dots\dots\dots (2.3)$$

where

$$x = (p - p_c)L^{1/v}$$

$$y = L^{\beta/v} P$$

$$\beta = 0.14 \setminus$$

$$v = 1.62$$

$$p_c = 0.6674$$

a, b, c and d are the coefficient to be regressed.

The best estimations for constants a, b, c , and d are:

$$a = 1.362472077$$

$$b = 2.691135819$$

$$c = -0.452517301$$

$$d = 0.006404353$$

2.4 Rectangular effect analysis

Real sandbodies will have more complex shapes than square. Nurafza *et al.* (2006b) studied the finite rectangular sandbody distribution first. Their results showed the rectangular sandbody model has universal curves similar to the square sandbody model.

Rectangular sandbodies with length l_x and width l_y are distributed independently and uniformly in one rectangular reservoir with area $A = x \times y$ (Figure 2.6). In this model, we have different dimensionless system lengths $L_i, i \in \{x, y\}$ and aspect ratios

$\omega_i, i \in \{x, y\}$. $L_x = x/l_x$ is the dimensionless system length of the horizontal direction

and $L_y = y/l_y$ is the dimensionless length of the vertical direction. The aspect ratio for the

horizontal direction is defined as $\omega_x = L_x/L_y$ and for the vertical direction is defined

as $\omega_y = L_y/L_x$.

As already defined for the finite square sandbody model, sandbody occupied probability p_{sand} is the ratio of sand area to the entire reservoir area. $P(p_{\text{sand}}, L)$ is replaced

by $P_i(p_{\text{sand}}, L_i, \omega_i)$, the percolation cluster probability for i direction, which represents the probability of a sandbody belonging to the percolating sandbody cluster in this model.

$P_i(p_{\text{sand}}, L_i, \omega_i)$ depends on p_{sand} , L_i accounting for boundary effect and ω_i accounting for orientation effect. $P_i(p_{\text{sand}}, L_i, \omega_i)$ is different for different directions when $\omega_i \neq 1$.

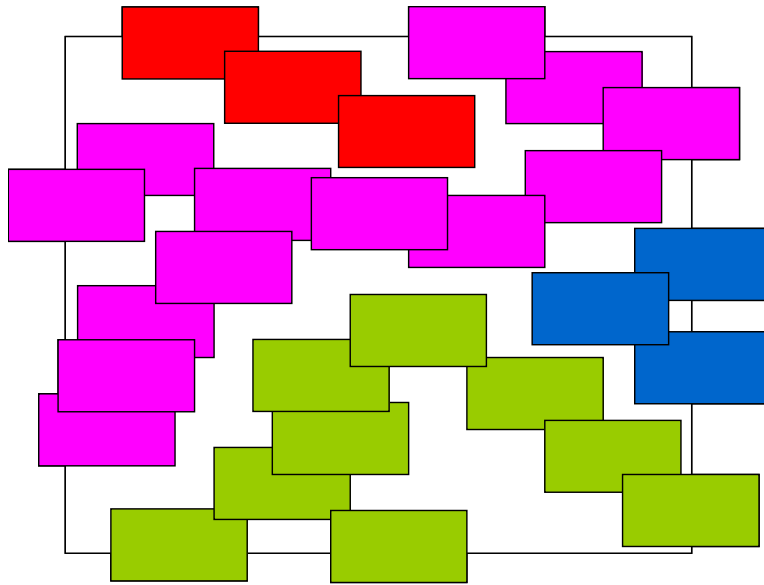
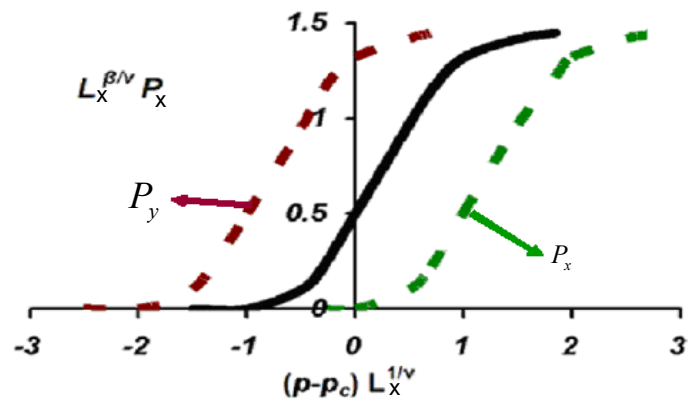


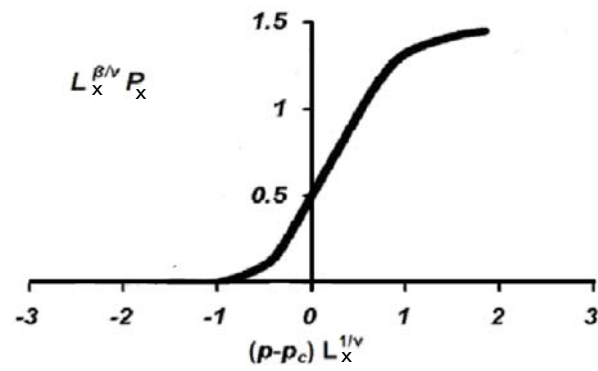
FIG. 2.6 Rectangular sandbody model.
One horizontal percolation cluster across the reservoir,
but no percolation cluster for the vertical direction.

Two kinds of universal curves represent the mean connectivity function, one for the horizontal direction and the other for the vertical direction. We use P_x as the percolation cluster probability for the horizontal direction and P_y for the vertical direction.

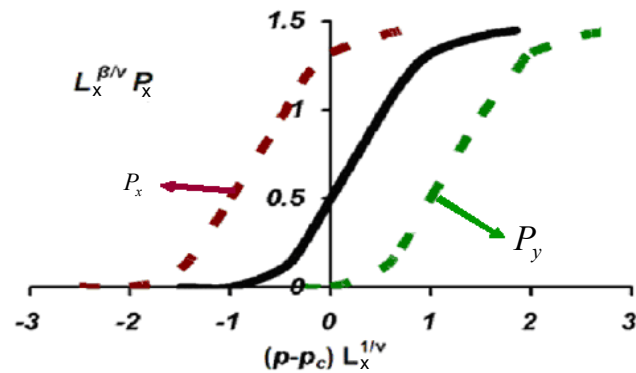
King (1990) suggests that the universal curves based on P_x and P_y have the same increasing trend as the universal curve of the infinite square sandbody model (Figure 2.5). When $\omega > 1$, the universal curve for P_x is depressed and for P_y , it is elevated (Figure 2.7a). When $\omega = 1$, this is identical to the square sandbody model and the two universal curves are coincident (Figure 2.7b). When $\omega < 1$, the universal curve for P_x is elevated and for P_y is depressed (Figure 2.7c).



a. $\omega > 1$



b. $\omega = 1$ (Square sandbody model)



c. $\omega < 1$

FIG. 2.7 Aspect ratio affects the connectivity performances (Modified from Nurafza *et al.*, 2006a).

The aspect ratio effects can be summarized in one table (Table 2.2):

TABLE 2.2 Aspect ratio effect (after Nurafza *et al.*, 2006a).

		Connectivity Performance
$\omega = 1$	$L_x = L_y$ (square sandbody model)	Same for x and y direction.
$\omega > 1$	$L_x > L_y$	Easier for x direction.
$\omega < 1$	$L_x < L_y$	Easier for y direction.
Note: When $L_x \rightarrow \infty$ and $L_y \rightarrow \infty$, then aspect ratio ω must be irrelevant because no boundary effect available (Stauffer and Aharony, 1985).		

Since $\omega_y = \frac{1}{\omega_x}$, the connectivity performance for the horizontal and vertical directions is the same for their respective ω . We only need to discuss the connectivity performance of one direction. The following discussion is based on the horizontal direction.

Using a constant of proportionality,

$$\Lambda_x = c \left(\omega_x^{1/v} - 1 \right) \dots\dots\dots (2.4)$$

where $c \approx 0.41$ (Nurafza *et al.*, 2006b). (We suggest $c \approx 0.041$ instead of $c \approx 0.41$; we will discuss later.)

King (1990) described the universal functions considering the aspect ratio effect:

$$P(p, L_x, \omega) = L_x^{-\beta/v} \Im[(p - p_c)L_x^{1/v} - \Lambda_x] \dots\dots\dots (2.5)$$

$$\Delta(p, L_x, \omega) = \omega^{1/2} L_x^{-\beta/v} \Re[(p - p_c)L_x^{1/v} - \Lambda_x] \dots\dots\dots (2.6)$$

When $\omega = 1$ and hence $\Lambda_x(\omega = 1) = 0$, Eqs. 2.5 and 2.6 are the universal functions for the finite square sandbody model (Eqs. 2.1 and 2.2). Illustrations of these two universal curves are showed in Figure 2.8.

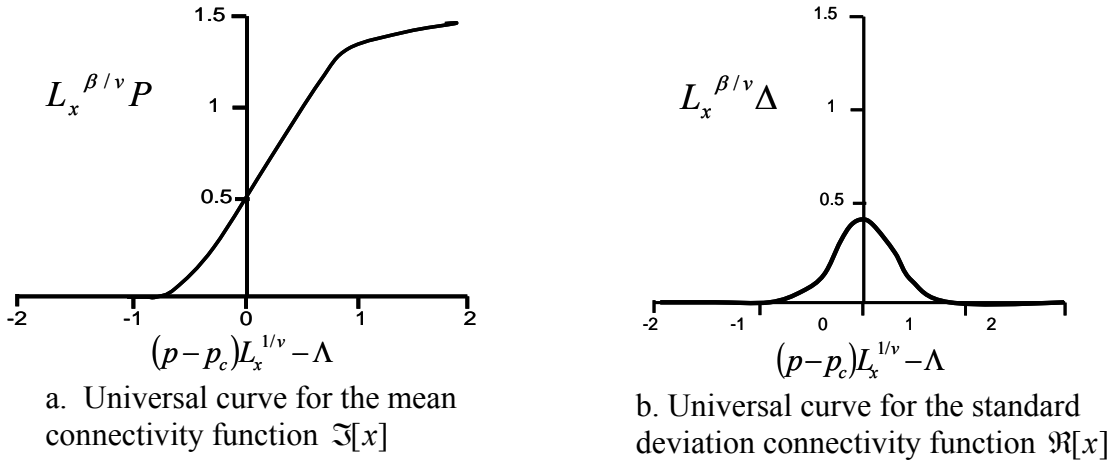


FIG. 2.8 Illustration of universal curves for finite rectangular sandbody model (Nurafza *et al.*, 2006b).

For different ω_i values, Λ_i is different. The universal curves will move a distance Λ_i along the X-axis from the original universal curves of $\omega = 1$ (Figure 2.9).

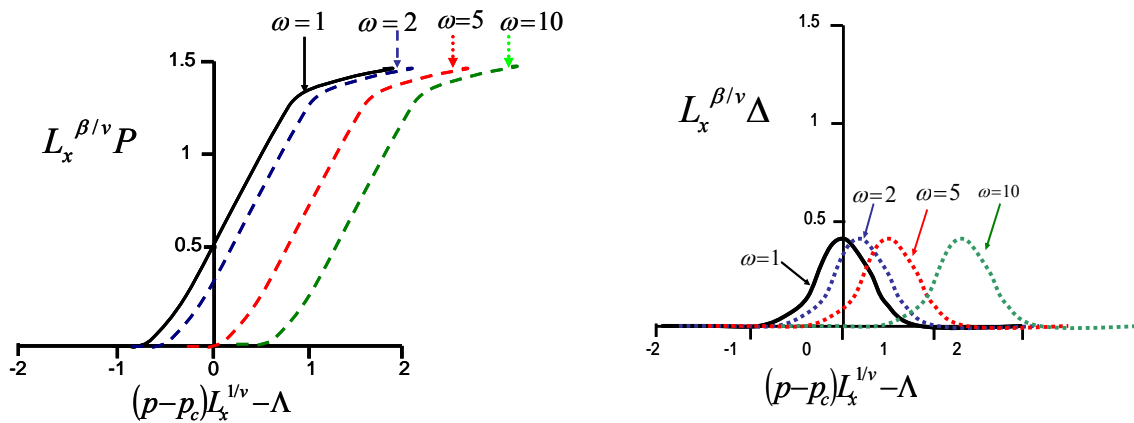


FIG. 2.9 The universal curves with different ω will have different locations on the X axis.

The regression function Eq. 2.3 will change to Eq. 2.4 with parameter values unchanged:

$$y = a \frac{1}{\sqrt{2\pi}} e^{-\frac{(bx+c)^2}{2}} + d \dots\dots\dots (2.4)$$

Where

$$x = (p - p_c)L_x^{1/v} - \Lambda$$

$$y = L_y^{1/v} P$$

$$\Lambda = c(\omega_x^{1/v} - 1)$$

The reason for our suggestion to use $c \approx 0.041$ instead $c \approx 0.41$ can be shown by one example. For one finite rectangular sandbody model, suppose that we know $p_{\text{sand}} = 0.75$, $L_x = 10$ and $L_y = 2$. Thus, $\omega_x = L_x/L_y = 5$. Based on the regressed function Eq. 2.4, we can get the following results:

Case 1: When $c \approx 0.41$, $(p - p_c)L_x^{1/v} - \Lambda = -0.35$. The P value is almost zero from Eq. 2.4. $p_{\text{sand}} = 0.75$ is a high value for an actual reservoir, which means many sands are distributed in this reservoir. It is unreasonable that P is almost zero, which means nearly no sand connected.

Case 2: When $c \approx 0.041$, $(p - p_c)L_x^{1/v} - \Lambda = 0.094$. The estimated P value is 0.65, which means 65% of total sands will be connected from one boundary to its opposite boundary. This is more reasonable than Case 1. In addition, the area A_s of the effective-square sandbody and the area A_r of the rectangular sandbody should be the same (Nurafza

et al., 2006b). The L of the effective-square sandbody model from Eq. 2.4 is 4.38. Therefore, $A_s = L^2 = 4.38^2 = 19.2$ and $A_r = L_x \times L_y = 20$, which means $A_s \approx A_r$.

Therefore, the rectangular sandbody model with $p_{\text{sand}} = 0.75$, $L_x = 10$ and $\omega = 5$, and one square sandbody model with $p_{\text{sand}} = 0.75$ and $L \approx 4.24$ has same connectivity performance $P = 0.33$. This square sandbody model is the effective-square sandbody model for the original rectangular sandbody model.

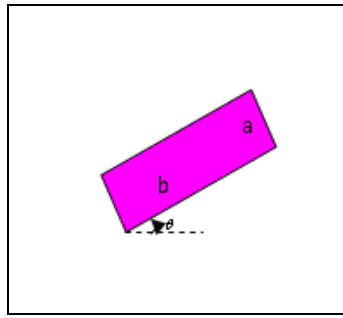
From the discussion above, we know the rectangular and square sandbody models have similar universal curves. For the same p_{sand} , and P_i values, we can get one L_i of i direction in the finite rectangular sandbody model (for a given ω_i value) and one L for the finite square sandbody model (where $\omega_i = 1$). This also means using p_{sand} , L_i and ω_i in the finite rectangular sandbody model or using p_{sand} and L in the square sandbody model will have the same P value for the i direction. These two models show the same connectivity performance for the i direction. Therefore, the original rectangular sandbody model can be replaced by its effective-square sandbody model with connectivity performance unchanged ($P_i(p_{\text{sand}}, L_i, \omega_i) = P(p_{\text{sand}}, L)$).

2.5 Orientation degree effect analysis

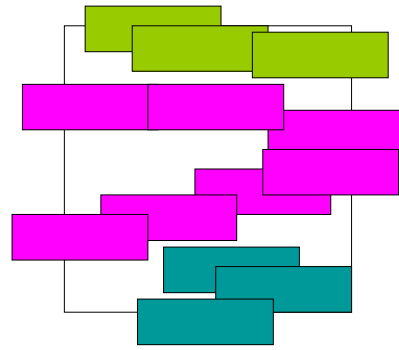
In reality, the sandbodies cannot be aligned in one direction. The depositional system and its sedimentation environment will affect the orientation of the sands. The orientation will affect the connectivity performance also.

For example, rectangular sandbodies are distributed randomly in one finite reservoir (Figure 2.8a). The sandbody occupied probability p_{sand} still is the ratio of sand area to the entire reservoir area. $P(p_{\text{sand}}, L)$ is replaced by $P(p_{\text{sand}}, L, \theta)$, the percolation cluster probability, which represents the ratio of connected area to sand area. L is the reservoir dimensionless length of the effective-square sandbody model. The orientation angle θ is the degree between the longer size direction of the sandbody and the study direction. $P(p_{\text{sand}}, L, \theta)$ depends on p_{sand} , L , and θ .

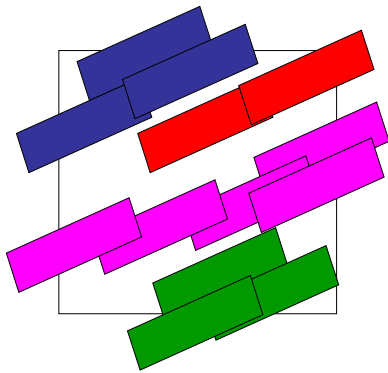
For example, we randomly distribute rectangular sandbodies $b \times a$ with fixed orientation degree θ (Figure 2.10a) in one reservoir. The study direction is horizontal. When $\theta = 0^\circ$, there is one percolation cluster for the horizontal direction, which includes seven sands (Figure 2.10b). When $\theta = 30^\circ$, there is one percolation cluster for the horizontal direction, which includes five sands (Figure 2.10c). When $\theta = 45^\circ$, there is no percolation cluster for either direction (Figure 2.10d). When $\theta = 60^\circ$, there is one percolation clusters for the vertical direction, including four sands (Figure 2.10e). No percolation cluster is available for the horizontal direction. When $\theta = 90^\circ$, there are two percolation clusters for the vertical direction including nine sands (Figure 2.10f). The percolation cluster probability P_x for the horizontal direction decreases and the percolation cluster probability P_y for the vertical direction increases when orientation degree θ increases from 0° to 90° . When the rectangular sandbody is longer and thinner, the value of orientation degree will affect the connectivity performances much more.



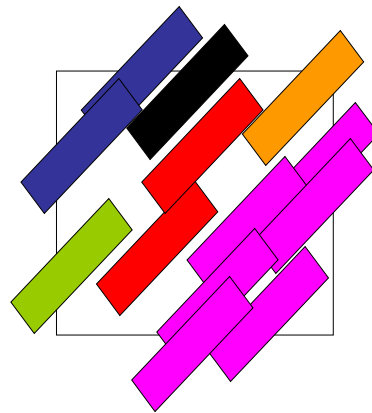
a. Rectangular sandbody sample



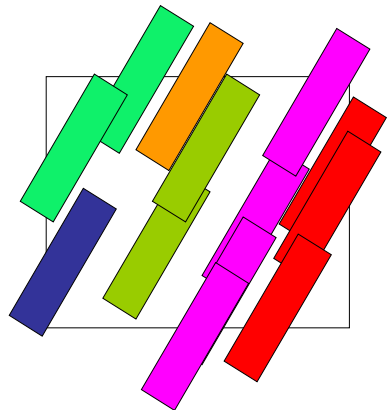
b. $\theta = 0^\circ$ There is 1 percolation cluster in the horizontal direction including 7 sands.



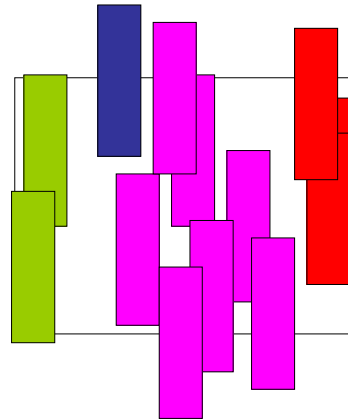
c. $\theta = 30^\circ$ There is 1 percolation cluster in the horizontal direction including 5 sands.



d. $\theta = 45^\circ$ There is no percolation cluster in either direction.



e. $\theta = 60^\circ$ There is 1 percolation cluster in the vertical direction including 4 sands.



f. $\theta = 90^\circ$ There are 2 percolation clusters in the vertical direction including 9 sands.

FIG. 2.10 Orientation degree of sandbodies will affect connectivity performance.

We consider two possible oriented sandbody cases separately. In the first case, all sands have a fixed orientation degree θ (Figure 2.11a). In the other case, the orientation degree θ distribution of sands is a uniform distribution ($\theta_{\min} \leq \theta \leq \theta_{\max}$) (Figure 2.11b).

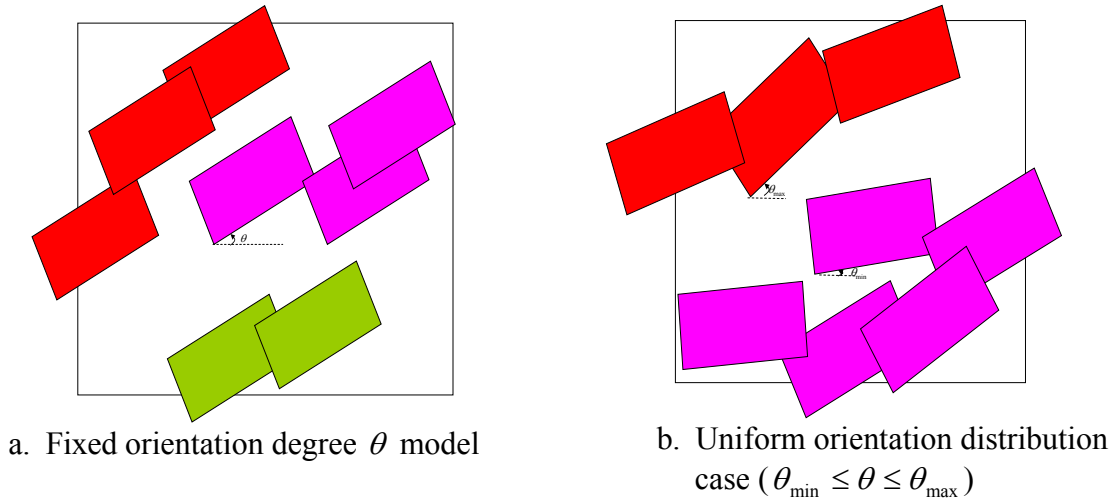
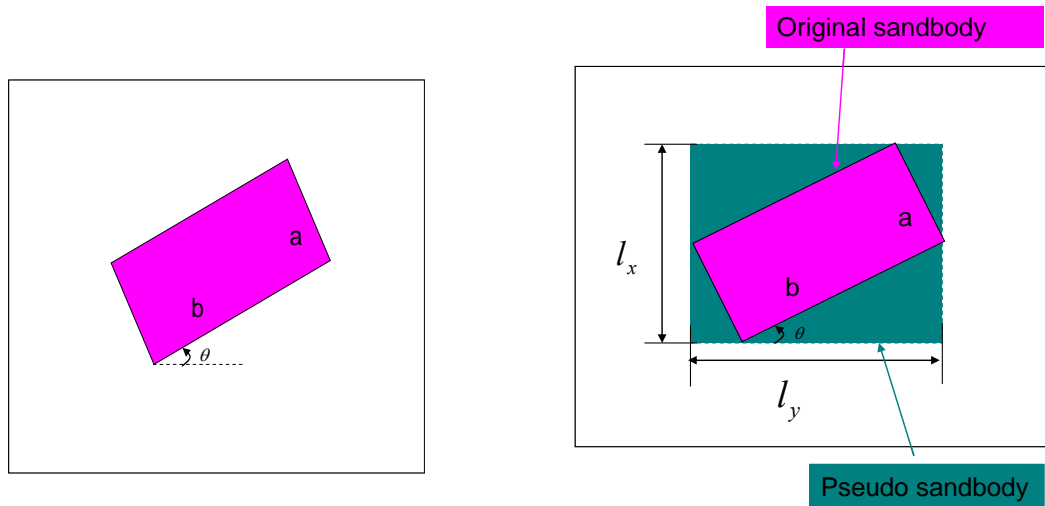


FIG. 2.11 Graphical description of two typical orientated sandbody cases.

Fixed orientation degree θ case:

The connectivity performance for this case can be replaced by one effective-rectangular sandbody model (Nurafza *et al.*, 2006b) (Figure 2.12). For X direction, the effective length of the effective-rectangular sandbody is $l_x = a \cos \theta + b \sin |\theta|$. For the Y direction, the effective length is $l_y = a \sin |\theta| + b \cos \theta$. Then, the original oriented sandbodies are transformed to effective-rectangular sandbodies aligned to the study direction. The connectivity performance remains same before and after the transformation.



a. Sandbody with fixed orientation degree θ

b. Effective-rectangular sandbody aligned along with study direction

FIG. 2.12 Graphical description of effective-rectangular sandbody transformation (Modified from Nurafza *et al.*, 2006b).

Uniform orientation distribution $\theta_{\min} \leq \theta \leq \theta_{\max}$ model:

For the case of degree of orientation, we use variables in the $\theta_{\min} \leq \theta \leq \theta_{\max}$ range (Figure 2.9b); the orientation distribution is assumed uniform, *i.e.* $U[\theta_{\min}, \theta_{\max}]$. The dimension of effective-rectangular sandbodies is the arithmetic average of effective size of the study direction for all sandbodies (Nurafza *et al.*, 2006b). The effective length of effective-rectangular sandbody is calculated as:

$$l_x = \frac{\sum_{\theta_i = \theta_{\min}}^{\theta_{\max}} a \cos \theta + b \sin |\theta|}{n} \dots \dots \dots (2.7)$$

$$l_y = \frac{\sum_{\theta_i = \theta_{\min}}^{\theta_{\max}} a \sin |\theta| + b \cos \theta}{n} \dots \dots \dots (2.8)$$

Using simple mathematics calculations, oriented sandbodies can be replaced by effective-rectangular sandbodies with effective length l_i for the i direction. The effective-rectangular sandbody model has the same connectivity behavior as the original model. Therefore, we can transform the orientation effect to an aspect ratio effect based on the results of Nurafza *et al.* (2006b).

2.6 Discussion

Based on the results of Nurafza *et al.* (2006), we can conclude that oriented sandbodies can be replaced by the effective-rectangular sandbody (discussed in Section 2.5) and rectangular sandbody model can be studied in terms of the effective-square sandbody (discussed in Section 2.4) using simple mathematic calculations.

Therefore, the effective-square sandbody model is the basic and most important model. By using the effective-square sandbody model, we can estimate the connectivity behavior of the original model with different aspect ratios and orientations. As discussed in Section 2.3, we can use two general processes to estimate unknown parameter values from other known parameter values for the transformed effective-square sandbody model.

If we know sandbody occupied probability p_{sand} and reservoir dimensionless size L , we can estimate percolation cluster probability P using Eq. 2.3. This process is straightforward and can be called a “forward mode” method.

Another way is to use p_{sand} and P to calculate reservoir dimensionless length L using Eq. 2.3 first. After we get L , we can input it to the universal curve of the standard deviation connectivity function $\mathfrak{R}_L[x]$ (Figure 2.4b) to get the standard deviation Δ . Then

backward inputting $P(1+\Delta)$ and $P(1-\Delta)$ into Eq. 2.3, we can get L_{\min} and L_{\max} . Then, we get the L uncertainty range, which is $L_{\min} < L < L_{\max}$. This process can be called a “backward mode” method.

We implemented this process in a spreadsheet by VBA to estimate the uncertainty range of L . Engineers and managers can input parameters to make their own analyses (Figure 2.12 and Code attached in Appendix A).

The interface of VBA program for “backward mode” method is showed in Figure 2.13, which includes figures of universal curves called Fig.1 and Fig. 2. The detail workflow to use this program is described as following:

(1) Input p_{sand} , P and the reservoir dimension into the program to get the X-axis value of universal curves.

(2) Follow the message given by the program to find the Y-axis from Fig. 2 to estimate the standard deviation Δ .

(3) Check the immediate results in the interface with the universal curves. If the immediate values of the X-axis and Y-axis can match the universal curves in Fig. 1 and Fig. 2, the L estimation in the OUTPUT section is L_{mean} , go to Step 4 directly. Otherwise, go back to Step 2 again to input a new Y-axis value from Fig. 2 with more figures, such as 0.401 instead 0.40. The reason for this step is to eliminate the solution fluctuation problem, which may lead to unreasonable results.

(4) Input $P(1+\Delta)$ and $P(1-\Delta)$ respectively to estimate L_{\max} and L_{\min} . The sandbody dimension can be estimated form the L value by definition.

p_{sand} and L are the input parameters for the interwell estimation method, which we will discuss in detail in Chapter III. For Monument field, it is difficult to estimate the individual sandbody dimension from geology analysis and so it is difficult to estimate L from the “forward mode” method. We will discuss in more detail how to apply the “backward mode” method in Chapter V.

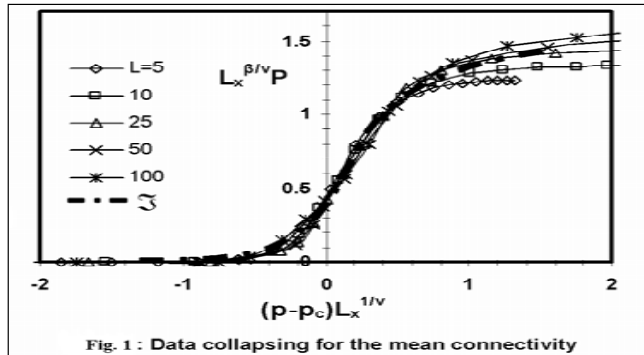


Fig. 1 : Data collapsing for the mean connectivity

Regression function for Fig. 1

$$y = a * \text{Nor}(bx+c) + d$$

a	1.362472077
b	2.691135819
c	-0.452517301
d	0.006404353

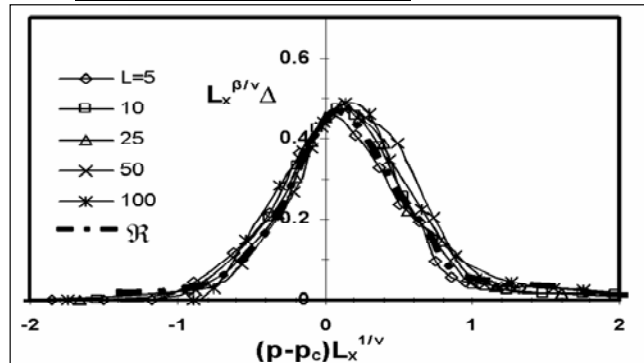


Fig. 2 : Data collapsing for standard deviation in connectivity

2D interwell connectivity probability forecast using percolation theory (with square sandbody assumption)

INPUT:

Reservoir length (in one direction), l=	8210	ft
Net gross ratio p=	0.62085	fraction
Connected net sand fraction, P=	0.30000	fraction

INTERMEDIATE RESULT

Figure 1:

x axis value	-0.096
y axis value	0.332

Figure 2:

x axis value	-0.096
y axis value	0.403

OUTPUT

Standard deviation Δ =	36.43	%
Dimensionless reservoir length L=	3.213 +/-	1.170
Range of effective sandbody size, l=	1873 ~	4020 ft
Mean value of effective sandbody size, l=	2555	ft

RUN

FIG. 2.13 VBA program of “backward” mode for effective-square sandbody dimension estimation

CHAPTER III

INTERWELL CONNECTIVITY ESTIMATION ANALYSIS

This chapter presents the development of an interwell connectivity estimation method based on King *et al.*'s (2002) work. King *et al.* (2002) proposed a method for predicting the distribution of breakthrough arrival times in a network. By integrating possible breakthrough times, we can estimate the connectivity.

In this chapter, we also develop a practical process to calculate the parameters L and p_{sand} from net sand map. Finally, we describe a two non-percolation methods for estimating interwell connectivity for comparison with the percolation-based approach. One method is a simple geometrical method that is only applicable in the case of very small well spacings. The other method uses Monte Carlo simulation to simulate the sandbody and well pair distributions in the reservoir. The results of comparisons of these methods will be covered in Chapter V.

3.1 King *et al.*'s (2002) process for breakthrough time estimation

Andrade *et al.* (2000) studied the flow of fluid in porous media of 2D and 3D systems. Their research is based on a bond percolation model of one lattice. They modeled the flow front with tracer particles driven by a pressure difference between two fixed sites spaced by distance r . Considering the dimensionless system size L and the occupied probability p , they investigated the distribution function of minimum travel time between these two sites. Based on published results and previous research, they proposed the following relationship:

$$P(t_{\min}|r, L, p) \sim \frac{1}{r^d} \left(\frac{t_{\min}}{r^d} \right)^{-g} f_1 \left(\frac{t_{\min}}{r^d} \right) f_2 \left(\frac{t_{\min}}{L^d} \right) f_3 \left(\frac{t_{\min}}{\xi^d} \right) \dots \dots \dots (3.1)$$

$$f_1(y) = e^{-a y^{-\phi}} \dots \dots \dots (3.2)$$

$$f_2(y) = e^{-b y^{-\psi}} \dots \dots \dots (3.3)$$

$$f_3(y) = e^{-c y} \dots \dots \dots (3.4)$$

where

L	dimensionless system size
r	geometric distance between sites
$\xi \sim p - p_c ^{-\nu}$	correlated length between sites
p	occupied probability
p_c	percolation threshold value
t_{\min}	minimum traveling time
g	exponent for geometric spacing effect
d	fractal dimension
ν, ϕ, ψ	exponents
a, b, c	constants

Andrade *et al.* (2000) suggested that the scaling forms for 2D and 3D are the same except for their different critical exponents. Based on extensive simulation, they summarized their best estimates for the parameters in Eqs. 3.1 to 3.4 in Table 3.1.

TABLE 3.1 Summary of exponents and constants (Andrade *et al.*, 2000)
[The notation N/A means not applicable since no theoretical value exists, while the notation (+/-) indicates above or below p_c .

For 2D system, $p_c \approx 0.6674$; for 3D system, $p_c \approx 0.2788$.]

	2D		3D	
	Simulation	Theory	Simulation	Theory
d	1.33 ± 0.05	N/A	1.45 ± 0.1	N/A
g	2.0 ± 0.1	N/A	2.1 ± 0.1	N/A
a	1.1	N/A	2.5	N/A
ϕ	3.0	3.0	1.6	2.0
b	5.0	N/A	2.3	N/A
ψ	3.0	N/A	2.0	N/A
c	1.6(-), 2.6(+)	N/A	2.9(-)	N/A

We should note that the c parameter for 3D has no value when $p > p_c = 0.2788$, and so Andrade *et al.*'s (2000) results are only suitable for $p < 0.2788$ in 3D system and for all p in 2D system. Since the range $p < 0.2788$ in 3D system is too small for practical application, this research only concentrates the 2D application of Andrade *et al.*'s (2000) results.

King *et al.* (2002) extended Andrade *et al.*'s (2000) results to estimate breakthrough time for a pattern of numerous wells with dimensionless well spacing r (Figure 3.1).

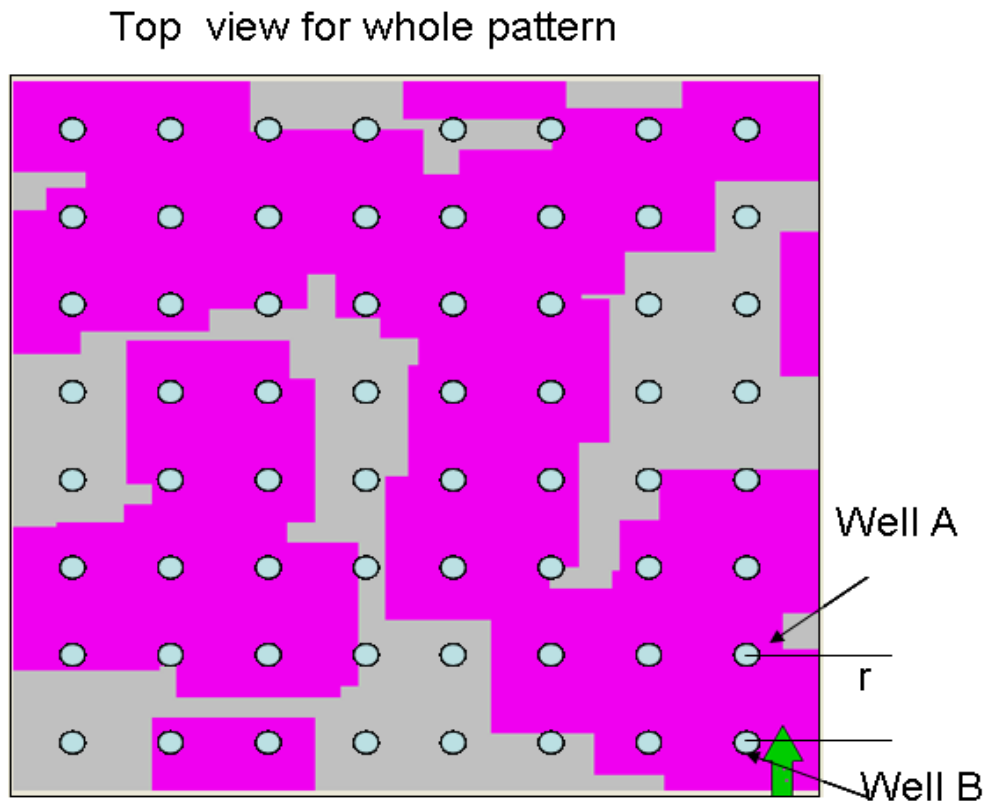


FIG. 3.1 Breakthrough time between Well A and Well B depends on sandbody connectivity and well spacing r of the whole well pattern.

King *et al.* (2002) modified Andrade *et al.*'s. (2000) equation with reservoir terms:

$$P(t_{br}|r, L, p_{sand}) \sim \frac{1}{r^d} \left(\frac{t_{br}}{r^d} \right)^{-g} f_1 \left(\frac{t_{br}}{r^d} \right) f_2 \left(\frac{t_{br}}{L^d} \right) f_3 \left(\frac{t_{br}}{\xi^d} \right) \dots \dots \dots (3.5)$$

where

L	dimensionless reservoir size
r	well spacing
$\xi = p_{sand} - p_c ^{-\nu}$	correlated length between two wells
p_{sand}	sandbody occupied probability
p_c	percolation threshold value $p_c \approx 0.6674$ for 2D continuum sandbody model
t_{br}	breakthrough time
g	exponent for well spacing effect
d	2D fractal dimension
ν, ϕ, ψ	exponents
a, b, c	constants

King *et al.* (2002) also explained the significance of functions f_1, f_2 and f_3 . The first expression, f_1 , is a function for the shortest path length between two wells in a percolating cluster. The second expression, f_2 , is used to show the boundary effect of a real field system. In a finite system, there is a maximum streamline length that is limited by the reservoir boundary. The third expression, f_3 , is used to show the percolation threshold effect. When the sandbody occupied probability p_{sand} value is far from p_c , the system has fewer sandbody clusters to be included in the main flow path, which is the main contributor to the fluid flow. This also means that, of the sand available, a greater proportion will be included in the branches of the main flow path, where they make only a small contribution to fluid flow. All these will affect the fluid flow path from injector to producer.

The breakthrough time distribution conditionally depends on reservoir size L , sandbody occupied probability p_{sand} and well spacing r . We should note all these parameters are dimensionless values, which means all L and r values are scaled to the typical sandbody dimension and breakthrough times are scaled by the traveling time of fluid flow through the typical sandbody.

King *et al.* (2002) applied this process to an ideal reservoir and compared the results to those from reservoir simulation (Figure 3.2).

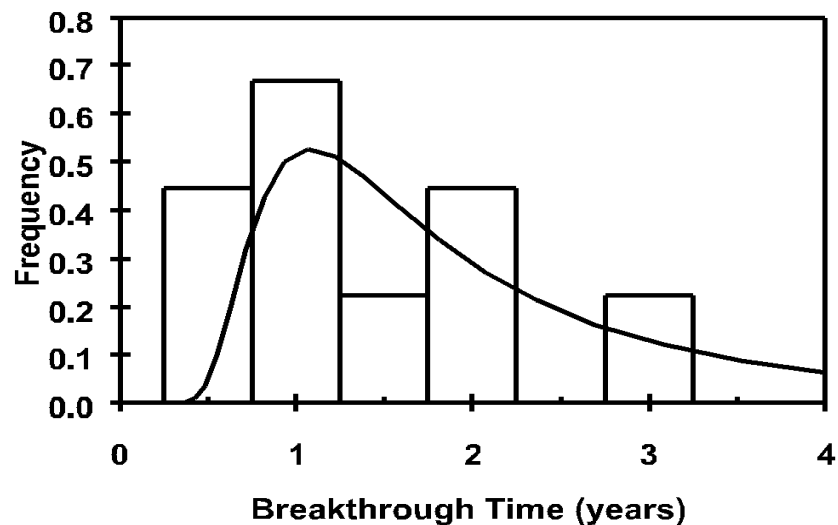


FIG. 3.2 Comparison of breakthrough time estimation from different methods. Histogram is the reservoir simulation result and smooth curve is the percolation estimation result. (King *et al.*, 2002)

King *et al.* (2002) suggested the agreement is good enough for engineering applications. The most important point is that this breakthrough time estimate took only a few seconds of CPU time. Compared to the low efficiency of conventional reservoir simulation methods, this is a very useful tool to make engineering and management decisions.

3.2 Interwell estimation method based on King *et al.*'s (2002) process

3.2.1 Derivation of interwell connectivity estimation method

In this study, interwell connectivity depends only on reservoir static properties. Since breakthrough time distributions are affected by interwell connectivity, one way to estimate the interwell connectivity probability would be to apply King *et al.*'s (2002) process. However, breakthrough time distributions are also affected by characteristics other than interwell connectivity. Thus, for example, a connectivity assessment from King *et al.*'s (2002) process would change according to the mobility ratio. For a given p_{sand} and L value, we can calculate the breakthrough time distribution for different dimensionless r values from King *et al.*'s (2002) equation (Figure 3.3).

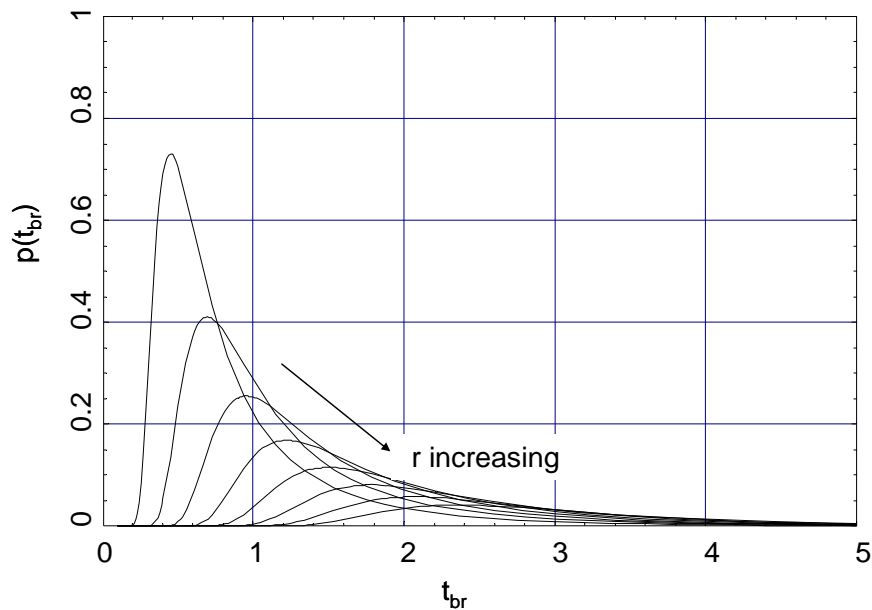


FIG. 3.3 Illustration of breakthrough time distribution for different interwell distances (r values) calculated from King *et al.*'s (2002) equation.

The breakthrough time t_{br} is a dimensionless parameter, which is the ratio of the actual breakthrough time to the traveling time for fluid flow through a typical sand. For $0 < t_{br} < \infty$, the integration of t_{br} has same meaning as the probability of two wells being connected:

$$\begin{aligned}
 &P(Cwp = 1|r, L, p_{sand}) \\
 &= \int_0^\infty \frac{1}{r^d} \left(\frac{t_{br}}{r^d}\right)^{-g} f_1\left(\frac{t_{br}}{r^d}\right) f_2\left(\frac{t_{br}}{L^d}\right) f_3\left(\frac{t_{br}}{\xi^d}\right) dt_{br} \dots\dots\dots (3.6)
 \end{aligned}$$

where Cwp is an indicator variable to determine whether the well pair is connected. When $Cwp=1$, the well pair is connected; when $Cwp=0$, the well pair is disconnected.

For engineering application, it is more reasonable to only consider t_{br} from 0 to t_{max} , which means that two wells are considered to be disconnected when the breakthrough time is too long. In this study, we choose $t_{max} = 100$. When two wells are separated by more than 100 typical sandbodies and so the dimensionless breakthrough time $t_{br} > 100$, they are disconnected. Therefore, Eq. 3.6 becomes:

$$\begin{aligned}
 &P(Cwp = 1|r, L, p_{sand}) \\
 &= \int_0^{100} \frac{1}{r^d} \left(\frac{t_{br}}{r^d}\right)^{-g} f_1\left(\frac{t_{br}}{r^d}\right) f_2\left(\frac{t_{br}}{L^d}\right) f_3\left(\frac{t_{br}}{\xi^d}\right) dt_{br} \dots\dots\dots (3.7)
 \end{aligned}$$

Inputting the functions f_1 , f_2 and f_3 into Eq. 3.7, we obtain:

$$\begin{aligned}
 &P(Cwp = 1|r, L, p_{sand}) \\
 &= \int_0^{100} \frac{1}{r^d} \left(\frac{t_{br}}{r^d}\right)^{-g} e^{\left(-a\left(\frac{t_{br}}{r^d}\right)^{-\phi}\right)} e^{\left(-b\left(\frac{t_{br}}{L^d}\right)^{-\psi}\right)} e^{\left(-c\left(\frac{t_{br}}{|p_{sand} - p_c|^{-dv}}\right)\right)} dt_{br} \dots\dots\dots (3.8)
 \end{aligned}$$

All parameters have the same meaning as in Eq. 3.5. In Eq. 3.8, the only unknown variable is the interwell distance r to estimate the well pair connectivity. By numerical integration, we see the relationship between r and interwell connectivity probability p (Figure 3.4). The error bars in Figure 3.4 account for the uncertainty of estimated reservoir dimensionless size $L_{\min} \leq L \leq L_{\max}$.

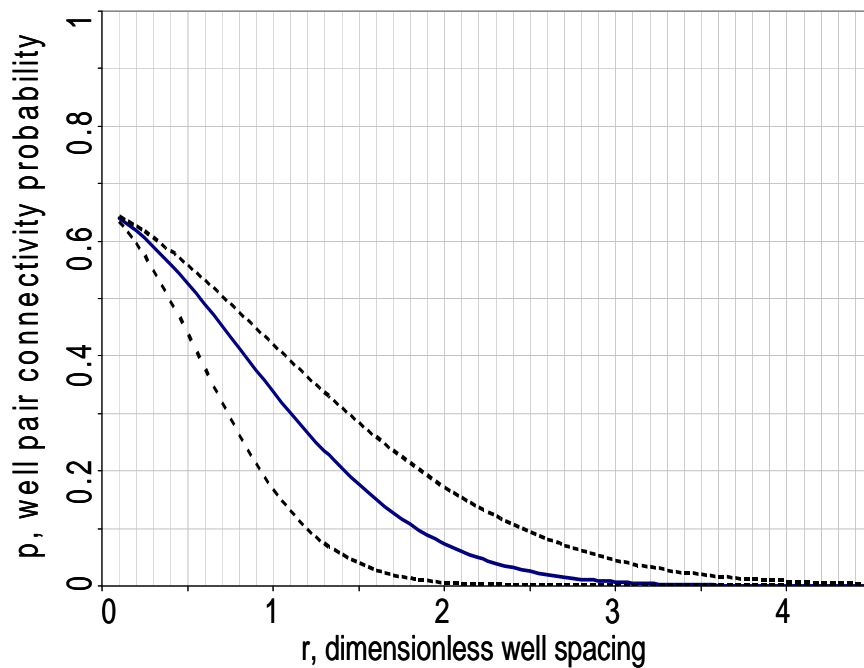


FIG. 3.4 Illustration of interwell estimation result.

We implemented our method for estimating interwell connectivity in a Mathematica program. Engineers and managers can input p_{sand} and L parameters to make their own analyses (Appendix. B). When r is smaller than 0.01, Mathematica fails. However, further analysis can give us the probability of interwell connection. King

(1990) described the relationship between connected sand fraction and well spacing for different p_{sand} values (Figure 3.5).

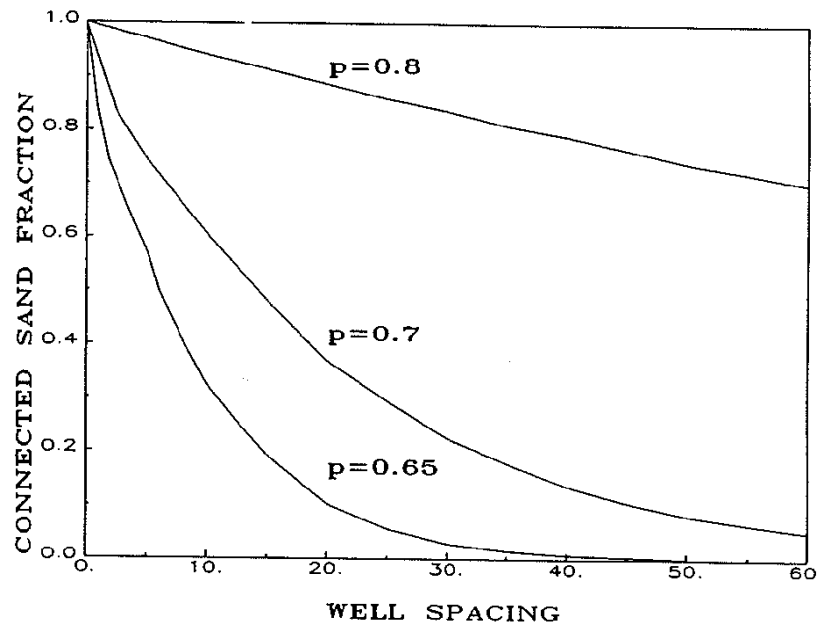


FIG. 3.5 Illustration for connected sand fraction as a function of well spacing (King, 1990)

King (1990) suggested that the connected sand fraction could represent the connectivity between well pairs. Thus, the connectivity probability for well pairs with very small well spacing will always approach unity since the connected sand fraction is one when well spacing is equal to zero (Figure 3.5). From probability analysis, however, this analysis overlooks the effect of the net-to-gross ratio p_{sand} . When the well spacing of a well pair approaches zero, these two wells are at almost the same location and so the interwell connectivity probability for these two wells must approach the sand occupied probability p_{sand} .

In Section 3.3, we use a simple geometric model to show the interwell connectivity probability is p_{sand} when r approaches zero. Since parameter g in Eq. 3.8 is the exponent for the well spacing effect, we can change its value every time to make the connectivity probability p equal to p_{sand} when the well spacing r approaches zero.

Therefore, the user can input the p_{sand} and L parameters into the Mathematica program first. Then Mathematica program will output one relationship curve. The user should change parameter g values several times to make the connectivity probability of zero well spacing to be p_{sand} .

So far, we have derived a method to estimate interwell connectivity based on King *et al.*'s (2002) process. Below, we propose a geometrical model (Section 3.3) and a Monte Carlo simulation process (Section 3.4) to evaluate the estimates from this percolation method..

3.2.2 Generation of input parameters L and p_{sand}

To estimate the dimensionless reservoir size L value, King *et al.* (2002) suggested using $L_{\text{min}} = \min\{L_x, L_y, L_z\}$. This suggestion is based on simulation results rather than theory. King *et al.*'s (2002) process used $p_c = 0.6674$, which is the 2D continuum percolation threshold. Therefore, while L is estimated from 3D considerations, the p_c value is from 2D. In addition, Andrade *et al.*'s (2000) results are only suitable for 2D application, as we have discussed in Section 3.2.1. Thus, it appears that L needs to be estimated from the 2D characteristics of the reservoir.

For very thin intervals, we can assume that all sands have the same thickness as the interval thickness. Based on this approximation, the 3D interval problem can be treated as a 2D problem. As King *et al.* (2002) suggested, now we can estimate $L_{\min} = \min\{L_x, L_y\}$, if we can get a separate sandbody dimension using the “forward mode” method. Another way is to use the “backward mode” method to estimate the effective-square sandbody L directly. The practical way is to use a net sand map, which shows all net sands areas in one plan-view map. Based on our previous discussion, this interwell estimation method is suitable to thin intervals and we do not need to worry about the different dimension problem any further.

To estimate the dimensionless reservoir size p_{sand} value, Nurafza *et al.* (2006a) suggested using very detailed permeability cross-section maps. Assuming the mode permeability value to be the cutoff, the sandbodies with permeability lower than the cutoff are set to be “bad” sandbodies and the sandbodies with permeability above than that are set to be “good” sandbodies. The “good” designation means this sandbody is permeable, while the “bad” designation implies a nonpermeable one, and the sandbody occupied probability p_{sand} is the ratio of the total “good” sand area to the whole sand area. This workflow is initially used to estimate sandbody connectivity, so percolation cluster probability P is estimated in their workflow also. P is estimated by the ratio of connected “good” sandbodies to all “good” sandbodies.

The detailed workflow is shown below (Figure 3.6).

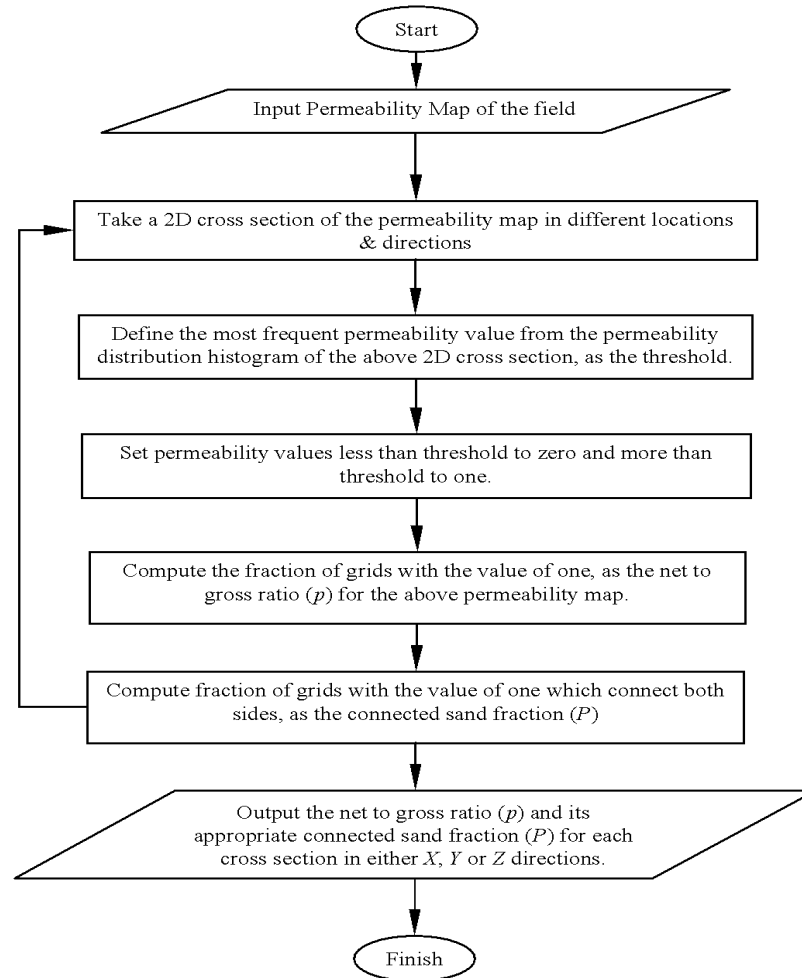


FIG. 3.6 The procedure to estimate p_{sand} and P (Nurafza *et al.*, 2006a)

In this study, we do not have enough permeability data to produce a detailed permeability map. We used porosity data, which maybe more abundant in most fields, to define “good” sand or “bad” sand. The porosity cutoff used to identify “good” sand or “bad” sand can be chosen according to field experience. All sands having ability to store hydrocarbons and be fluid flow paths should be defined as “good” sands.

Using the chosen porosity cutoff, we can get the net sand map. From the net sand map, we need to find one square study region that has a percolation cluster in the studied direction and separate sandbodies. We can call this region the “best representative area,”

which includes enough information to represent the connectivity performance of the entire reservoir. King (1990) suggested the length of the representative area should be greater than five times the typical sandbody size.

This best representative area may contain several separate sandbody clusters and one sandbody percolation cluster in the study direction. The ratio of the sandbodies' area to the area of the entire square reservoir region is the sandbody occupied probability p_{sand} . The ratio of the area of sandbody percolation cluster to the total sandbodies area is percolation cluster probability P .

For example, Figure 3.7 shows one percolation cluster with area A and three separate sandbodies with areas B_1 , B_2 and B_3 in the study reservoir with area T . we

calculate p_{sand} as $p_{sand} = \frac{A_s}{A_r} = \frac{A+B_1+B_2+B_3}{T}$ and P as $P = \frac{A_{pl}}{A_s} = \frac{A}{A+B_1+B_2+B_3}$.

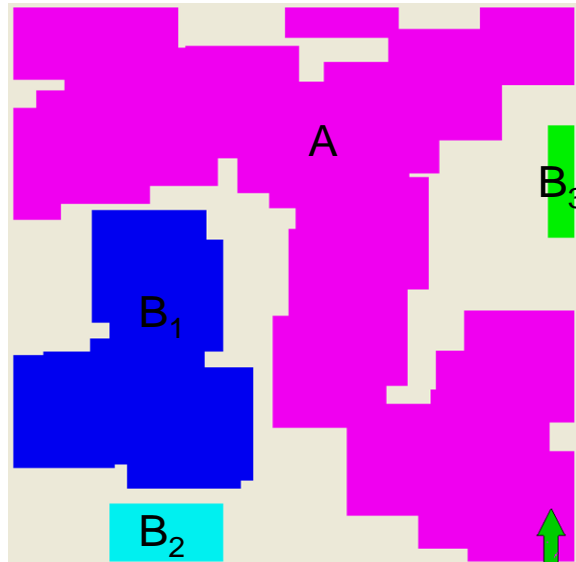


FIG. 3.7 The net sand area map to estimate p_{sand} and P .

For multilayer reservoir applications, we can estimate the interwell connectivity for individual intervals first. Then, using the multilayer application method (discussed in Section 3.5), we can estimate the connectivity probability for this multilayer reservoir.

3.3 Simple geometric model analysis

We describe here a method to estimate the connectivity probability when well spacing r approaches zero, which was proposed by Jensen during personal communication in 2007.

Let us consider only one small area around one sand in a square sandbody model (Figure 3.8). The square sand dimension is W . Points A and B represent two nearby wells and are spaced by w_0 , which represents the well spacing. Thus, the dimensionless well spacing r is $\frac{w_0}{W}$. The problem we try to solve is the connectivity probability of well pair A and B when r is small.

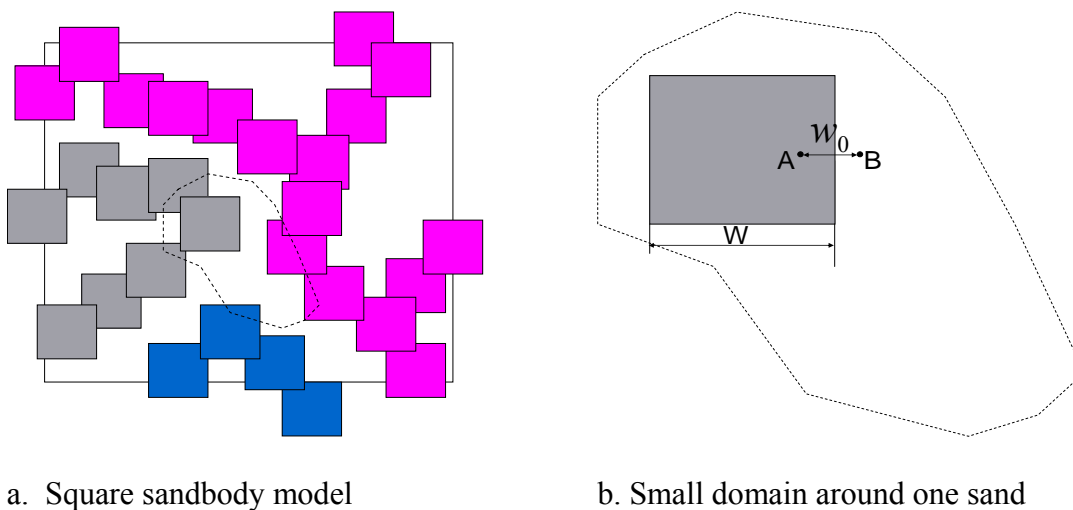


FIG. 3.8 Graphical description of small domain around one sand.

To calculate the connected probability, we separate the sand by two regions (Figure 3.9). One is the interior (blue) region at the center of the sand with dimension $W - 2w_0$, and the grey region is edge region. From Figure 3.9, we know $0 \leq w_0 \leq 0.5W$.

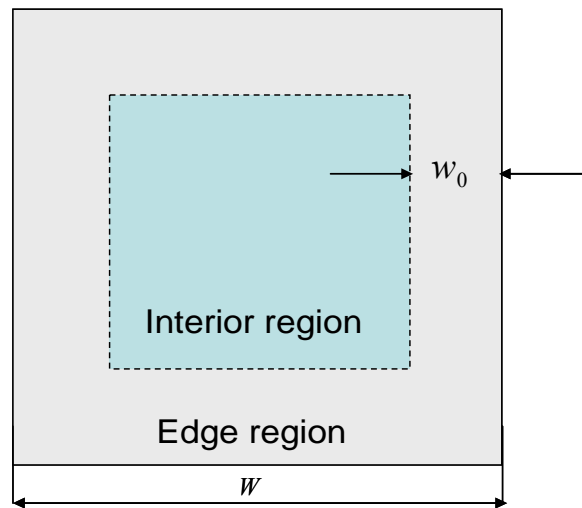


FIG. 3.9 Scheme of different regions.

If the reservoir size is very big, the probability for point A to be in this sand can be approximated by the net-to-gross ratio N . With Well A in sand, Well B can be at several locations inside the sand or outside the sand. Changing the location of B changes the probability for A and B being connected. Using a probability tree, we can investigate all the possible connected cases to estimate the connected probability of A and B (Figure 3.10).

The probability of A and B being connected can be calculated as follows:

$$\begin{aligned}
 &P(\text{wells } A \text{ and } B \text{ are connected}) \\
 &= P(\text{Branch } A) + P(\text{Branch } B) + P(\text{Branch } C) \\
 &= P(A \text{ is in interior region}) \cap P(B \text{ is in sand}) \\
 &\quad \dots \\
 &+ P(A \text{ is in edge region}) \cap P(B \text{ is in sand}) \\
 &+ P(A \text{ is in edge region}) \cap P(B \text{ is not in this sand}) \\
 &\quad \cap P(B \text{ is in an adjacent sand}) \\
 &\quad \cap P(\text{Adjacent sand is connected to central sand}) \dots\dots\dots (3.9)
 \end{aligned}$$

For Branch A:

The probability is calculated as:

$$\begin{aligned}
 &P(A \text{ is in interior region}) \cap P(B \text{ is in sand}) \\
 &= P(A \text{ is in interior region}) \times P(B \text{ is in sand} | A \text{ is in interior region}) \dots\dots\dots (3.10)
 \end{aligned}$$

Since,

$$P(A \text{ is in interior region}) = N \frac{\text{Area of interior region}}{\text{Area of entire sand}} = N \frac{(W - 2w_0)^2}{W^2} \dots\dots\dots (3.11)$$

Because space between A and B is w_0 and the space between the interior region boundary and the entire region boundary is w_0 , point B must be in the sand.

$$P(B \text{ is in sand} | A \text{ is in interior region}) = 1 \dots\dots\dots (3.12)$$

Inputting Eq. 3.11 and 3.12 into Eq. 3.10, we get:

$$P(\text{Branch } A) = N \frac{(W - 2w_0)^2}{W^2} \dots\dots\dots (3.13)$$

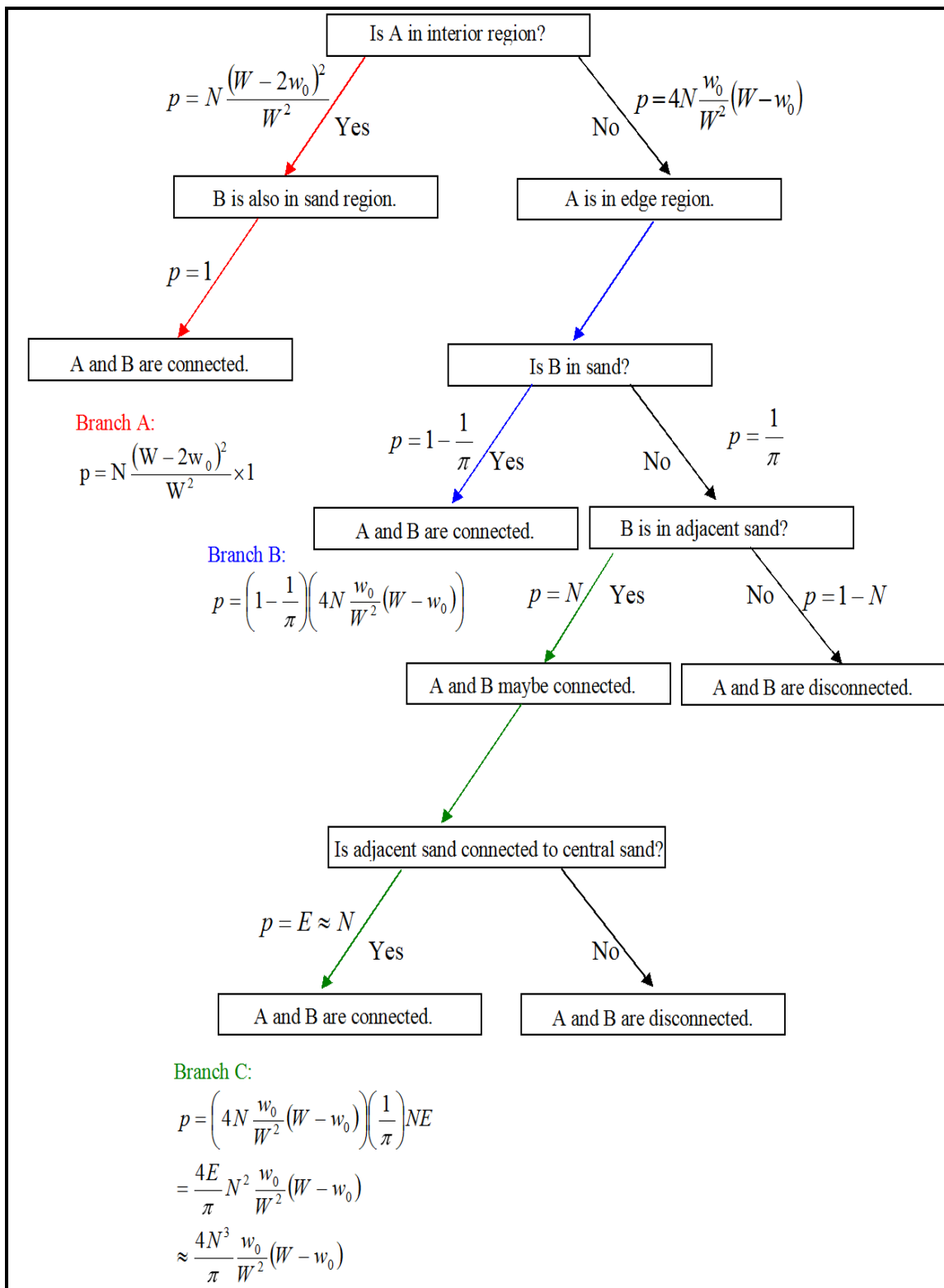


FIG. 3.10 Probability tree for the connectivity probability estimation of A and B.

For Branch B:

The probability is calculated as:

$$\begin{aligned}
 &P(A \text{ is in edge region}) \cap P(B \text{ is in sand}) \\
 &= P(A \text{ is in edge region}) \times P(B \text{ is in sand} | A \text{ is in edge region}) \dots\dots\dots (3.14)
 \end{aligned}$$

Since,

$$P(A \text{ is in edge region}) = N \frac{\text{Area of edge region}}{\text{Area of entire sand}} \approx \frac{4Nw_0(W - w_0)}{W^2} \dots\dots\dots (3.15)$$

For $P(B \text{ is sand} | A \text{ is in edge region})$, it is identical to solve the question:

If A is in the edge region, what is the probability of case B is also in sand?

B can be anywhere on a circle of radius w_0 with center at A (Figure 3.10).

If B is at the position b' , it is out of the sand.

If B is at the position b'' , it is in the sand.

If B is at the position b''' , it is in the sand.

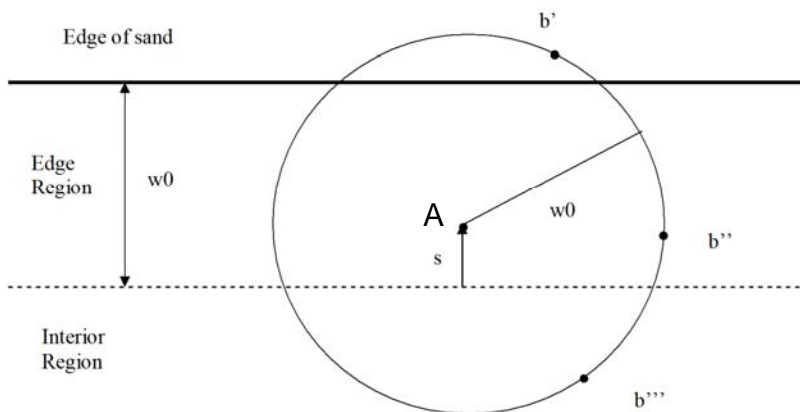


FIG. 3.11 Possible locations of B when A is in the edge region.

From Figure 3.11, we know the probability that B is in the sand when A is s distance from the edge/interior boundary is given by:

$$P(B \text{ is in sand} | A \text{ is in edge region}) = 1 - \frac{\text{Arc cos}(1 - \frac{s}{w_0})}{\pi} \dots\dots\dots (3.16)$$

For all possible positions for A in edge region from $s = 0$ to $s = w_0$:

$$\begin{aligned} P(B \text{ is in sand} | A \text{ is in edge region}) &= \int_{s=0}^{s=w_0} \left[1 - \frac{\text{Arc cos}(1 - \frac{s}{w_0})}{\pi} \right] \frac{ds}{w_0} \\ &= \int_0^1 \left[1 - \frac{\text{Arc cos}(1-u)}{\pi} \right] du \\ &= 1 - \frac{1}{\pi} \dots\dots\dots (3.17) \end{aligned}$$

Inputting Eq. 3.16 and 3.18 into Eq. 3.15, we can get:

$$P(\text{Branch B}) = \left(1 - \frac{1}{\pi} \right) \left[4N \frac{w_0}{W^2} (W - w_0) \right] \dots\dots\dots (3.18)$$

For Branch C:

The probability is calculated as:

$$P(A \text{ is in edge region}) \cap P(B \text{ is not in this sand}) \cap$$

$$P(B \text{ is in an adjacent sand}) \cap P(\text{Adjacent sand is connected to central sand})$$

$$= P(A \text{ is in edge region}) \cap P(B \text{ is not in this sand} | A \text{ is in edge region})$$

$$\cap P(B \text{ is in an adjacent sand} | A \text{ is in edge region and } B \text{ is not in this sand})$$

$$\cap P(\text{Adjacent sand is connected to central sand}) \dots\dots\dots (3.19)$$

Since

$$P(A \text{ is in edge region}) = 4N \frac{w_0}{W^2} (W - w_0) \dots\dots\dots (3.20)$$

$$P(B \text{ is not in this sand} | A \text{ is in edge region}) = 1 - \left(1 - \frac{1}{\pi}\right) = \frac{1}{\pi} \dots\dots\dots (3.21)$$

$$\begin{aligned} &P(B \text{ is in an adjacent sand} | A \text{ is in edge region and } B \text{ is not in this sand}) \\ &= N \times \frac{1}{\pi} \times 4N \frac{w_0}{W^2} (W - w_0) \dots\dots\dots (3.22) \end{aligned}$$

Since well spacing w_0 is very small compared to sand dimension W , the efficient factor E of adjacent sand being connected to the center sand can be approximated by net-to-gross ratio N. Therefore,

$$P(\text{Adjacent sand is connected to central sand}) \approx N \dots\dots\dots (3.23)$$

Inputting Eqs. 3.21, 3.22, 3.23, and 3.24 into Eq. 3.20, we can get:

$$P(\text{Branch C}) \approx \frac{4N^3}{\pi} \frac{w_0}{W^2} (W - w_0) \dots\dots\dots (3.24)$$

Therefore, the connected probability of A and B is:

$$\begin{aligned} &P(\text{the probability of } A \text{ and } B \text{ being connected}) \\ &= P(\text{Branch A}) + P(\text{Branch B}) + P(\text{Branch C}) \\ &= N \frac{(W - 2w_0)^2}{W^2} + \left(1 - \frac{1}{\pi}\right) \left[4N \frac{w_0}{W^2} (W - w_0)\right] + \frac{4N^3}{\pi} \frac{w_0}{W^2} (W - w_0) \end{aligned}$$

$$\begin{aligned}
&= N \left[1 + 4 \left(\frac{w_0}{W} \right)^2 - 4 \left(\frac{w_0}{W} \right) \right] + \left(1 - \frac{1}{\pi} \right) \left\{ 4N \left(\frac{w_0}{W} \right) \left[1 - \left(\frac{w_0}{W} \right) \right] + \frac{4}{\pi} N^3 \left(\frac{w_0}{W} \right) \left[1 - \left(\frac{w_0}{W} \right) \right] \right\} \\
&= N \left[1 + 4 \left(\frac{w_0}{W} \right)^2 - 4 \left(\frac{w_0}{W} \right) \right] + \left[\left(1 - \frac{1}{\pi} \right) N + \frac{N^3}{\pi} \right] \left\{ 4 \left(\frac{w_0}{W} \right) \left[1 - \left(\frac{w_0}{W} \right) \right] \right\} \\
&= N(1 + 4r^2 - 4r) + \left[\left(1 - \frac{1}{\pi} \right) N + \frac{N^3}{\pi} \right] [4r(1-r)] \dots\dots\dots (3.25)
\end{aligned}$$

From Eq. 3.25, we know the probability for A and B being connected is net-to-gross ratio N when r approaches to zero. Since $0 \leq w_0 \leq 0.5W$, this method will be suitable for interwell connectivity probability estimation of r in the range of $0 \leq r \leq 0.5$. Field application for data as discussed in Chapter V showed this method could get good results for $0 \leq r \leq 0.3$.

3.4 Monte Carlo simulation

Monte Carlo simulation is especially useful in studying systems with a large number of modeling phenomena with significant uncertainty in inputs, such as percolation phenomenon (Stauffer and Aharony, 1985). We applied the Monte Carlo simulation method to evaluate our interwell connectivity methods.

In Monte Carlo simulation, we randomly distribute square sandbodies with sandbody occupied probability p_{sand} as well as line segments with length r in one reservoir with dimensionless length L . When one line segment is in the same connected sandbody cluster, the two wells represented by the line end points are connected (Figure 3.12). We can do this simulation many times to get the interwell connectivity behavior

for well pairs with different well spacing r and then compare with the estimation results from our new method.

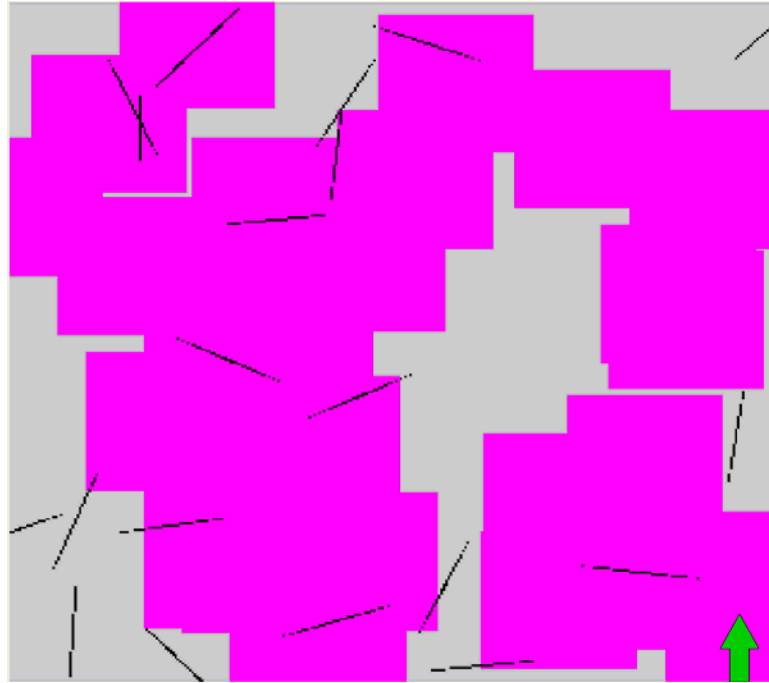


FIG. 3.12 Illustration of Monte Carlo simulation.

The comparison of estimates from the new percolation method, the simple geometrical method, and Monte Carlo simulation can be used to evaluate our method. Comparison of the results shows that our approach is sufficiently accurate and reasonable. Figure 3.13 is one typical comparison for the D1 interval in Monument Butte field. The error bar of estimates from the percolation method symbolizes the related uncertainty of sandbody dimension. The simple geometrical model only estimates the connectivity probability for a range $0 \leq r \leq 0.3$. Using Monte Carlo simulation, we simulated the random distribution of sandbody and well pairs many times, collected the connectivity probability data for different well spacing r and then joined all the data

points to show the relationship between dimensionless well spacing r and connectivity probability p . Drawing all these estimates in one figure as Figure 3.13 shows the differences among these approaches and the estimation quality of our new method. A detailed discussion appears in Chapter V.

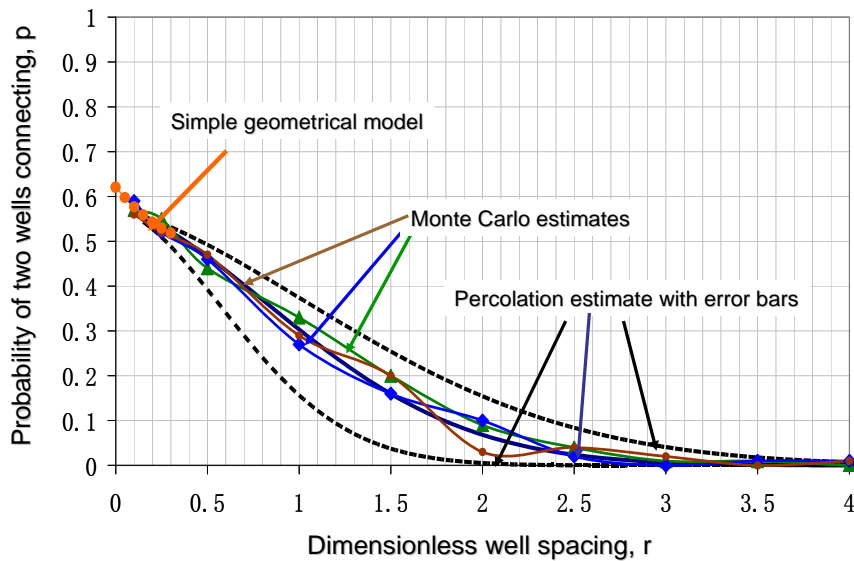


FIG. 3.13 Comparison examples of different estimations from different methods.

CHAPTER IV

MULTILAYER ESTIMATION METHOD

Most reservoirs are multilayer, so we propose one method to extend the new percolation method to estimate the connectivity performance of multilayer reservoirs.

Let us consider Well A and Well B, which are spaced by dimensionless well spacing r (Figure 4.1). Based our method, we can calculate the interwell connectivity probability p_i for the i^{th} individual interval and combine the p_i s to give a probability that the two wells are connected by one or more intervals. However, many cases entail an added complication. Each interval can also have a “value”, D , which can affect whether or not it is important for this interval to be included in the connectivity assessment. D may represent different properties for different fields, such as OOIP, initial water saturation S_{wi} , interval thickness h , etc. The problem is how to estimate the interwell connectivity for a final decision if Wells A and B perforate several intervals at the same time (Figure 3.13).

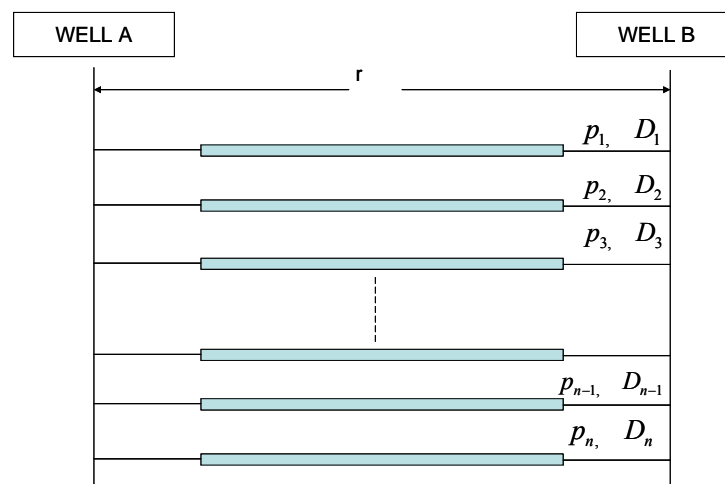


FIG. 4.1 Graphic description of Well A and Well B.

If the decision values D for different intervals are same, the interwell connectivity is straightforward from reliability theory.

$$\begin{aligned}
 p &= 1 - \overline{p} \\
 &= 1 - \prod_{i=1}^n \overline{p}_i \\
 &= 1 - \prod_{i=1}^n (1 - p_i) \dots\dots\dots (4.1)
 \end{aligned}$$

This can be called a “uniform” weight model.

If different intervals have different D values, then the importance of different intervals for the final decision is different. Such a model is called a different-weight model. We need to incorporate both D and p to get one weighted connectivity probability for our final decision.

For example, Well A and Well B with spacing r perforate three intervals at the same time. The probability for A and B being connected at the i^{th} interval is p_i [$i \in \{1,2,3\}$]. Assume for an example that the interval thickness is the associated decision value $D_i = h_i$ [$i \in \{1,2,3\}$, $h_1 = l$, $h_2 = 2l$ and $h_3 = 3l$]. The interval with higher h_i will have higher weight for the final decision. By separating the interval with h_2 to two intervals and the interval with h_3 to three intervals, we successfully transform the original reservoir to one uniform weight interval reservoir (Figure 4.2).

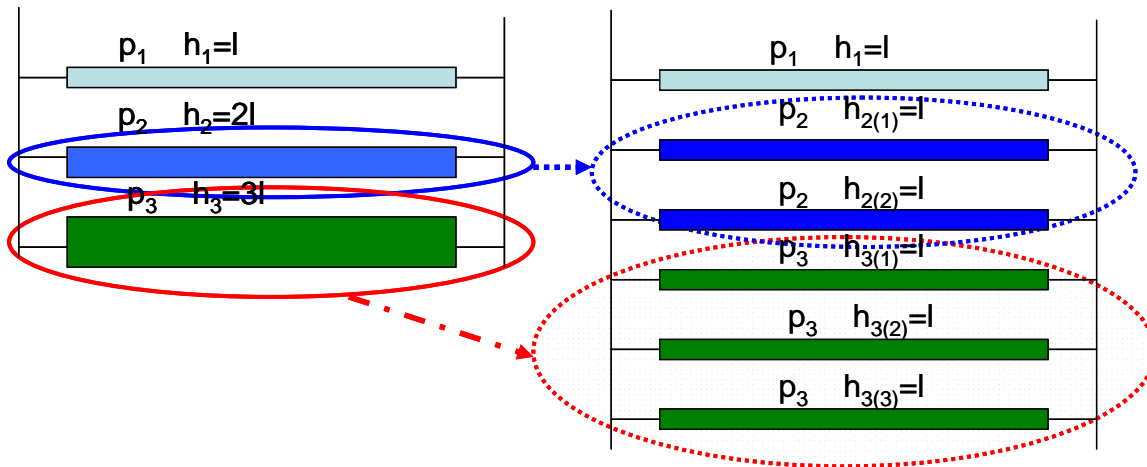


FIG. 4.2 Graphic description for the procedure to transform the deferent weight interval model to a uniform weight interval model.

Then, we can estimate the interwell connectivity probability based on the uniform weight model as follows:

$$\begin{aligned}
 p[h] &= 1 - (1 - p_1)(1 - p_2)(1 - p_2)(1 - p_3)(1 - p_3)(1 - p_3) \\
 &= 1 - (1 - p_1)(1 - p_2)^2(1 - p_3)^3 \dots\dots\dots (4.2)
 \end{aligned}$$

Generally, the weighted connectivity probability $p[h]$ depends on the h value of different intervals and can be calculated as:

$$p[h] = 1 - \prod_{i=1}^n (1 - p_i)^{\frac{h_i}{h_{\min}}} \dots\dots\dots (4.3)$$

This kind of method can be called a “positive” weight estimation method. In this method, an interval with higher decision factor D value has a higher weight for the final decision.

Now consider another case where the initial water saturation is the associated decision parameter, *i.e.* $D = S_w$. The intervals with higher S_w will have lower weight

for the final decision. The interval with maximum value S_w has lowest weight for the final decision. Similarly, the connected probability for this case can be calculated as:

$$p[S_w] = 1 - \prod_{i=1}^n (1 - p_i)^{\frac{S_{wi}}{S_{w\max}}} \dots\dots\dots (4.4)$$

This kind of method can be called a “negative” weight estimation method. In this method, the interval with the higher decision factor D value has a lower weight for the final result.

When h and S_w are two decision parameters for one multilayer reservoir, then the connected probability for the final decision is one uncertainty range:

$$p[S_w] \leq p[h, S_w] \leq p[h] \dots\dots\dots (4.5)$$

Generally, engineers and managers can consider several decision parameters. First, they need to choose a “positive” weight or a “negative” weight method for each decision parameter and then calculate the weighted connected probability results for each decision parameter. The connectivity probability estimated for the different-weight model is one range between maximum weight result and minimum weight result. If the value of decision parameters is same for all intervals, the result from different-weight model is same as the result from a “uniform” weight model.

CHAPTER V

APPLICATION AND RESULTS

In this chapter, we applied our new interwell connectivity estimation method to Monument Butte field. Then we compared the estimations from our new method, Monte Carlo simulation, and the simple geometrical model. The comparison showed our method could get plausible results very quickly for $25\% \leq p_{\text{sand}} \leq 80\%$. We also successfully applied the multilayer estimation method for this field.

5.1 Description of field data

The study area lies within the Wells Draw - Travis Units of Monument Butte field (Figure 5.1). The selected study area is 1,362 acres and encompasses 35 wells (17 water injectors and 18 oil producers) having an average well spacing of 1,320 ft (Figure 5.2). For this area, we studied the Douglas Creek D1, D2, and D3 intervals to gain a better understanding of the sandstone connectivity. Following the approach described in the previous chapter, we obtained the connectivity estimates for the three intervals in this study area. Assuming these estimates are representative of the entire field, we can predict the interwell connectivity performance throughout the reservoir.

Selected Study Area

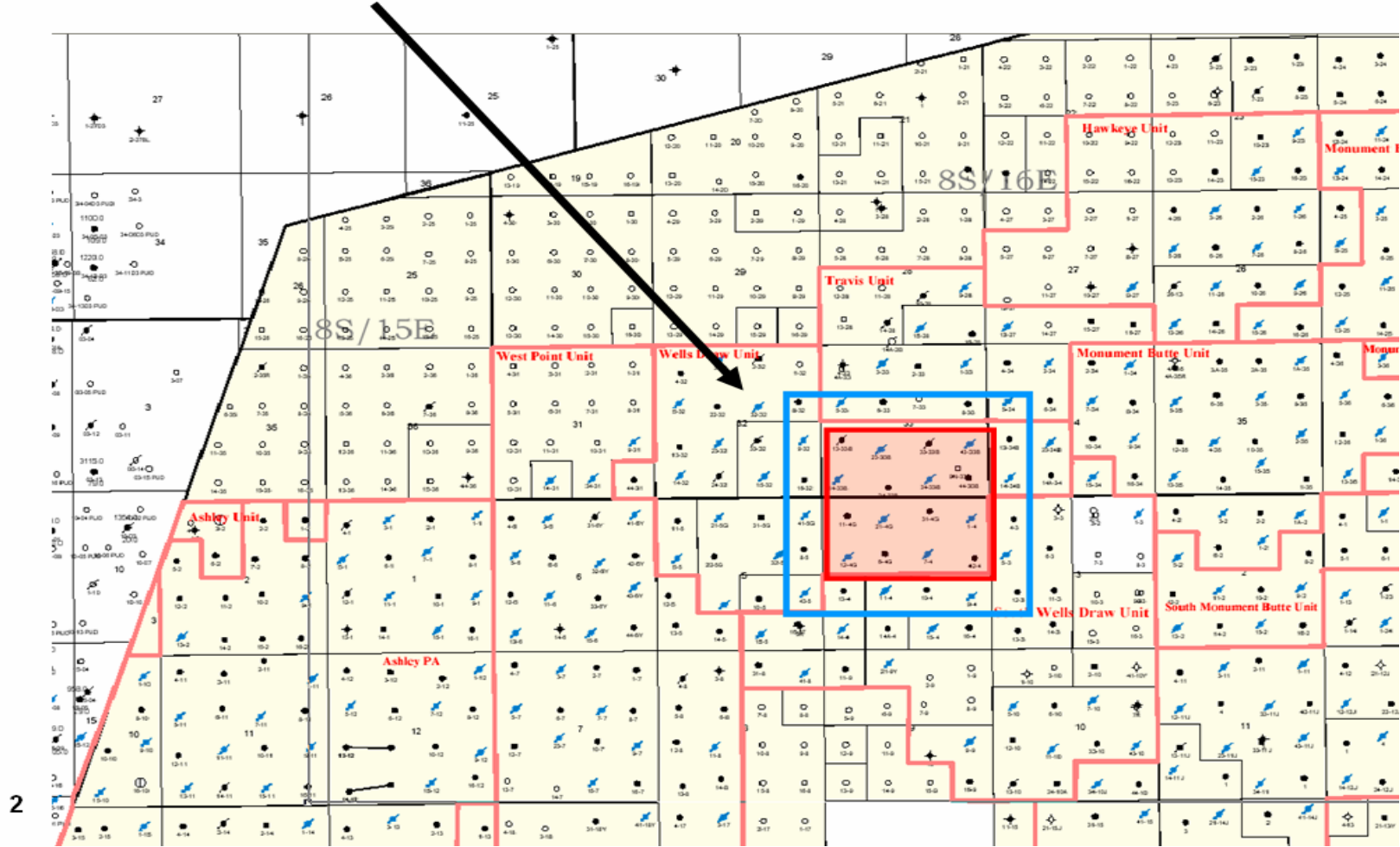


FIG. 5.1 Location of the study area in Monument Butte field.

$X_{DIST} = 2350 \text{ m}$
 $Y_{DIST} = 2346 \text{ m}$
 Area = 5.51 km^2
 (1362.31 acres)

 No. of wells = 35
 Water injectors = 17
 Oil producers = 18
 Avg. spacing = 1320 ft

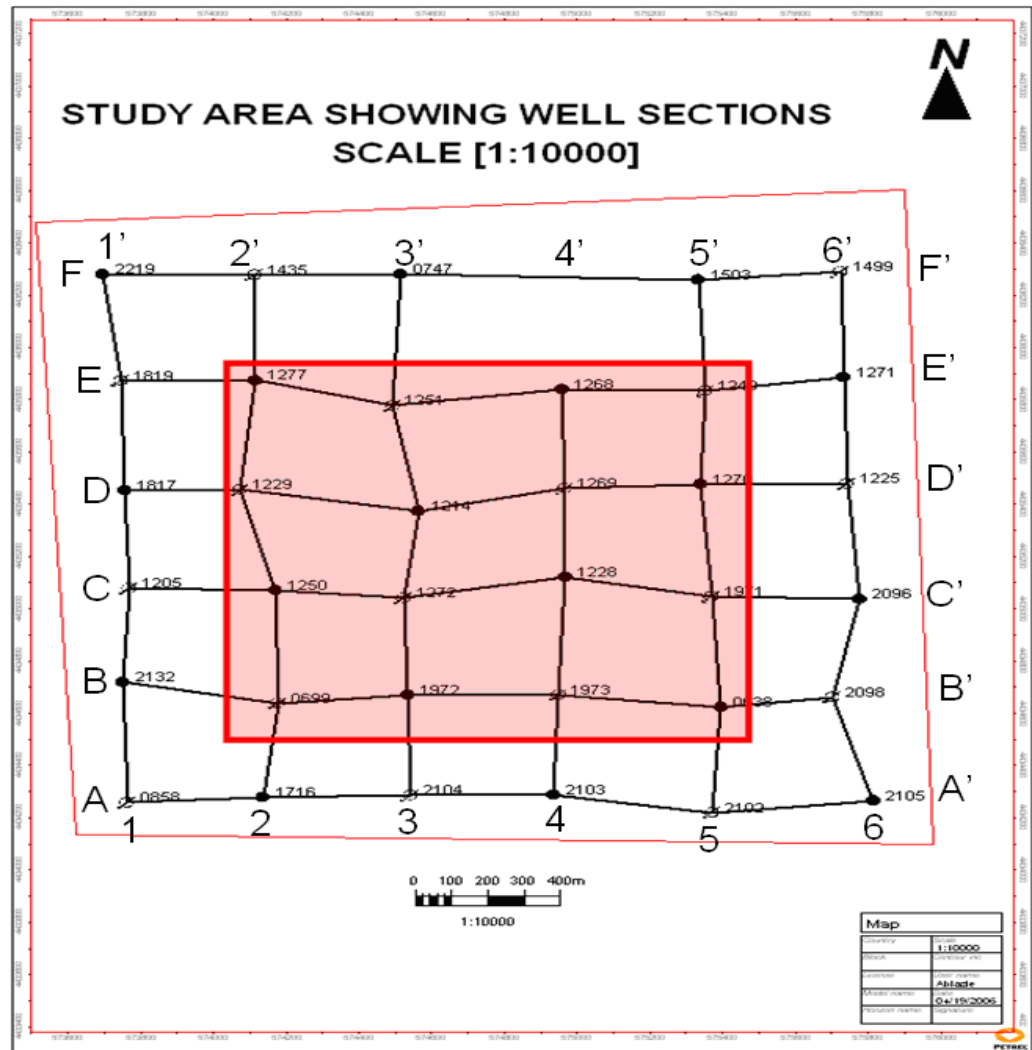


FIG. 5.2 Base-map of study area.

In a separate study, gamma ray logs were used for lithology identification and correlation, and porosity logs were used to identify the reservoir quality sandstones within these intervals. Following initial data quality checks, a porosity cutoff of 10% was used to identify reservoir sandstones.

Evaluations of the D1, D2, and D3 intervals yielded net sand overlay sand count maps (Figures 5.3, 5.4, and 5.5) and reservoir properties summary tables (Tables C.1, C.2 and C.3). The areas of individual sandbody clusters are shown in the zone maps, which can be used to calculate sandbody occupied probability p_{sand} and percolation cluster probability P .

Sandbody distribution interpretation also has uncertainty arising from the sandbody distribution uncertainty and different interpretation methods. The connected sandbody cluster interpreted in the net sand map should include many separate sand areas that have not been identified. The branch of the connected cluster has a high possibility to be separated sands. Inversely, the backbone of the connected cluster has a high likelihood to be the percolation sandbody cluster. Similarly, the sands with higher thickness values are more likely to be included in the backbone. Therefore, the net sand thickness information can be used to identify the sandbody percolation cluster. One cutoff value can be chosen from geology analysis and the thickness distribution information, such as the mode value of net sand thickness distribution. We assume the sand with thickness bigger than this cutoff is included in the percolation cluster. Otherwise, this sand belongs to separate sandbodies.

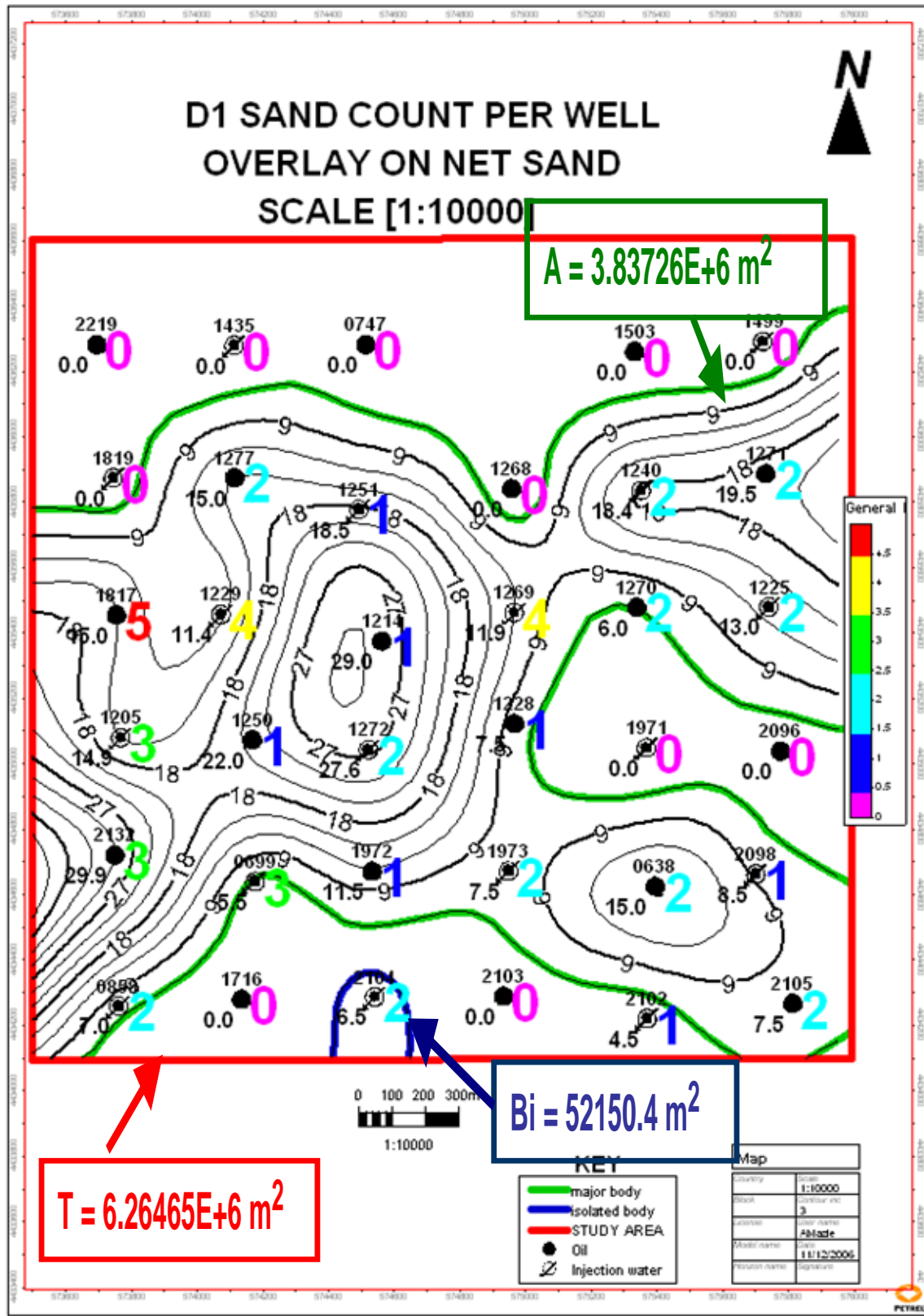


FIG. 5.3 Net sand overlay sand count map of D1 interval.

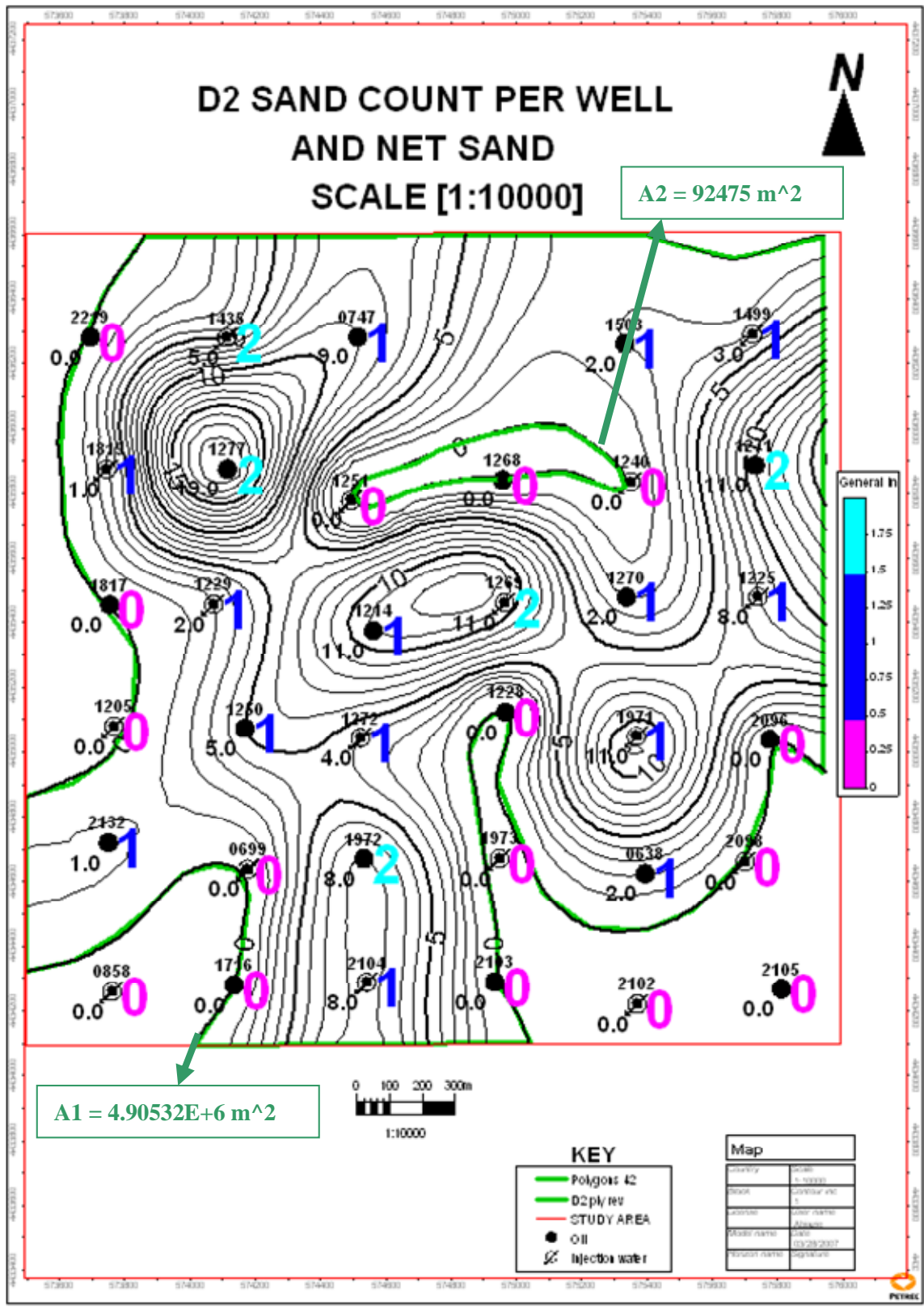


FIG. 5.4 Net sand overlay sand count map of D2 interval.

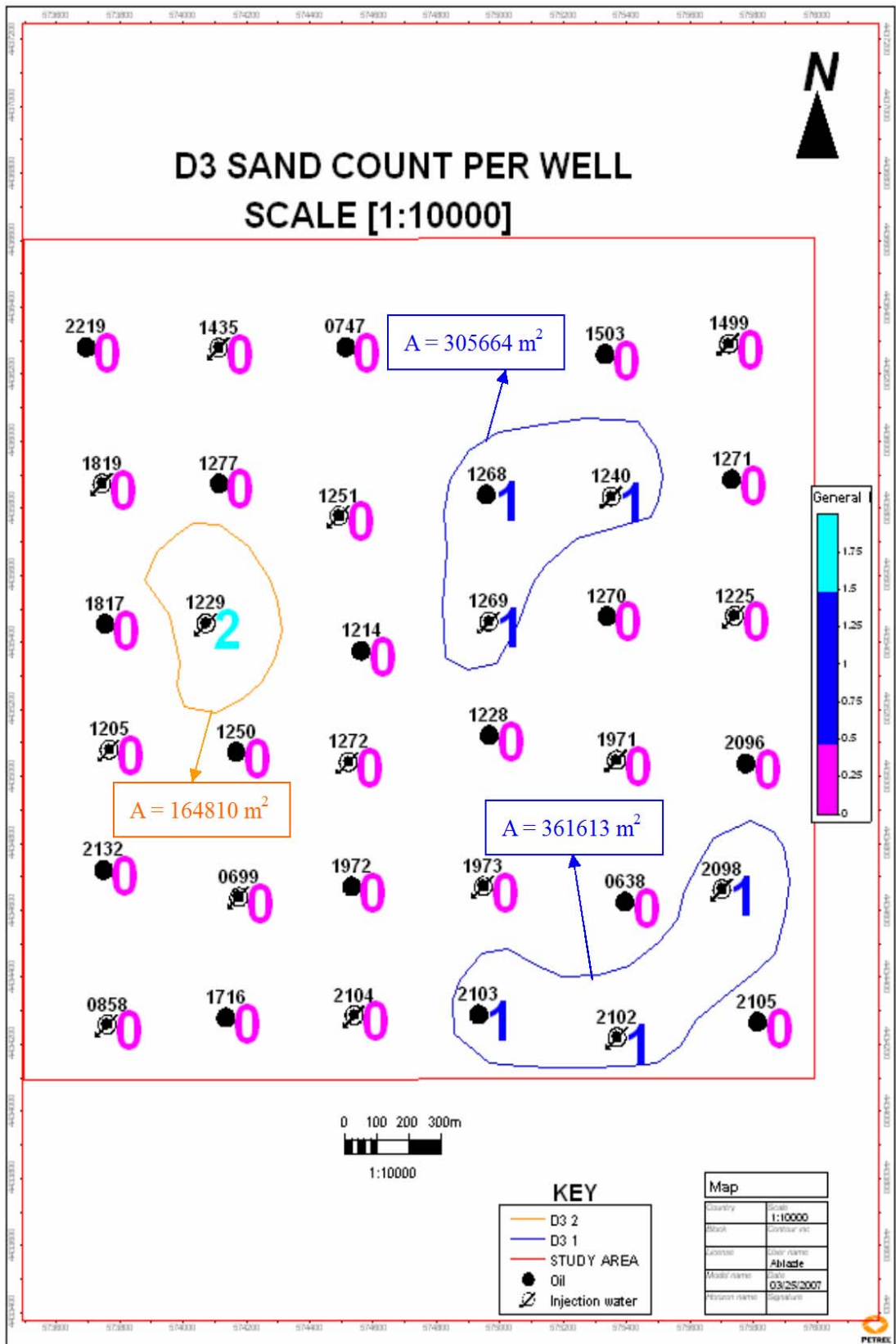


FIG. 5.5 Net sand overlay sand count map of D3 interval.

5.2 Analysis and results

5.2.1 D1 interval

In the D1 zone map (Figure 5.3), we can find one sandbody percolation cluster and one separate sandbody cluster. The net sand thickness in this interval ranges from 4.5 to 30 ft (Table C.1). The mode value of thickness distribution is about 12 ft. According to the discussion in Section 5.1, this value also is the cutoff to separate the sandbody percolation cluster from the biggest connected sandbody cluster. We can use the “backward” mode to estimate effective-square sandbody dimension (Figure 5.6).

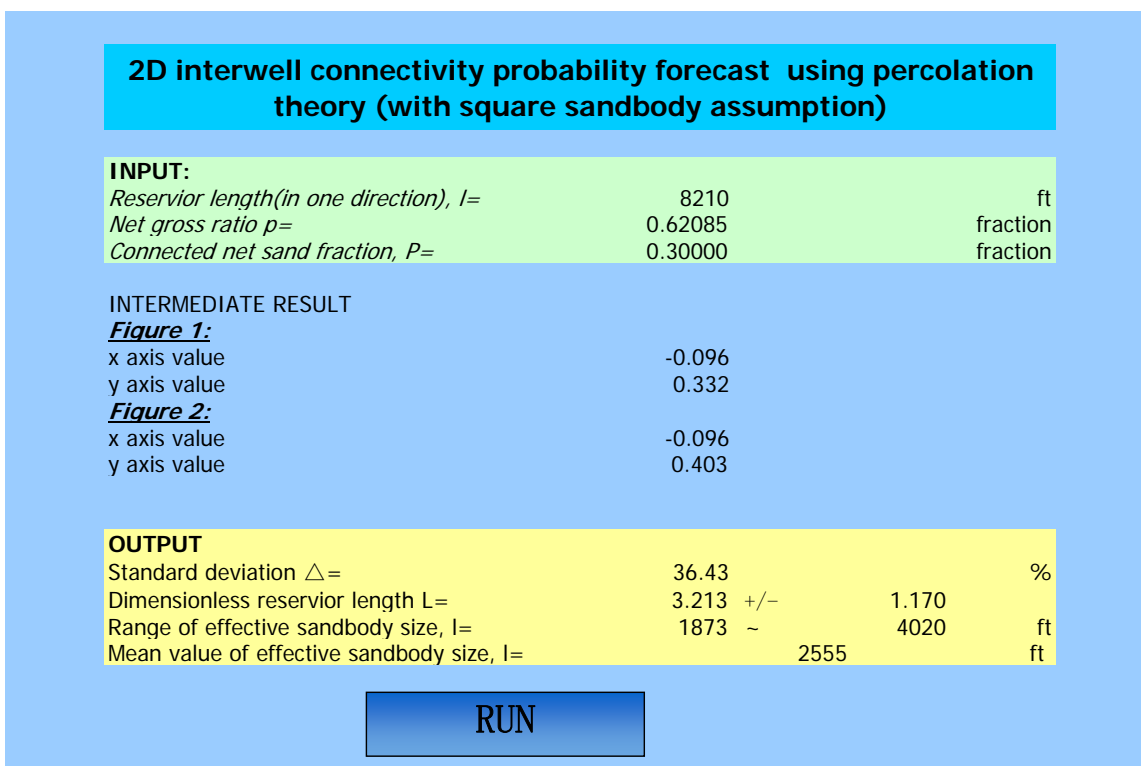


FIG. 5.6 Estimation of effective-square sandbody dimension of the D1 interval.

The average well spacing is 1,320 ft. The mean value of effective-square sandbody dimensions is 2,555 ft and the range is 1,873 to 4,020 ft. Therefore, the

estimated effective-square sandbody dimension is about 1.4 to 3.0 times the average well spacing. This is a reasonable value. The standard deviation Δ is 36.43%. The reason for this value is big may due to the study area is not big enough. As we have discussed in Section 3.2.2, the best representative area should be big enough to include enough information to represent the connectivity performance of entire reservoir. The least value of L suggested by King (1990) is $L = 5$. The L of the D1 interval is 3.213, which is less than the suggested value.

Inputting $L_{\text{mean}} = 3.2$, $L_{\text{max}} = 4.35$, $L_{\text{min}} = 2.05$ and $p_{\text{sand}} = 0.62$ into our Mathematica program which is based on Eq. 3.8 (Appendix B), we can get the estimated probability of connection for the D1 interval (Figure 5.7). The data points on the center dashed line (Figure 5.7) are the numerical interpretation results for L_{mean} . The data points along the upper dashed line and the lower dashed line are for L_{max} and L_{min} , respectively. Therefore, the space between the upper dashed line and the lower dashed line can be interpreted as the error bar of the connectivity probability estimation, which indicates the uncertainty of estimated reservoir dimensionless size $L_{\text{min}} \leq L \leq L_{\text{max}}$.

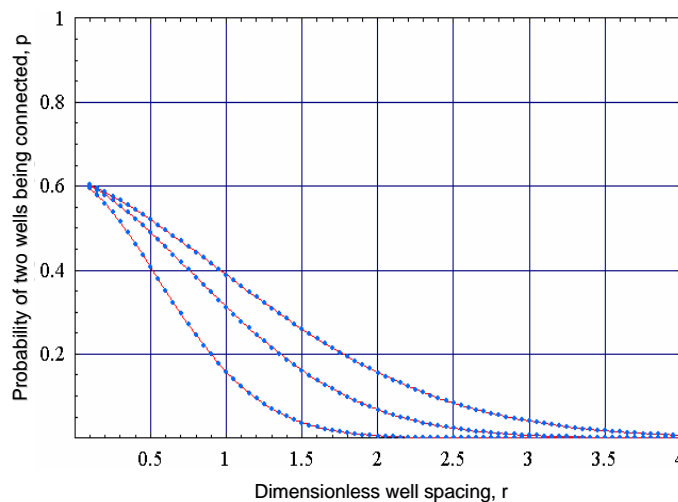


FIG. 5.7 Interwell connectivity probability estimation of D1 interval.

We compared the estimates from our percolation method, Monte Carlo simulation and the simple geometrical model for the D1, assuming that the backward mode gave an appropriate range of sandbody sizes. The estimates from different methods overlap each other and so the agreement among these methods is good (Figures 5.8 and 5.9).

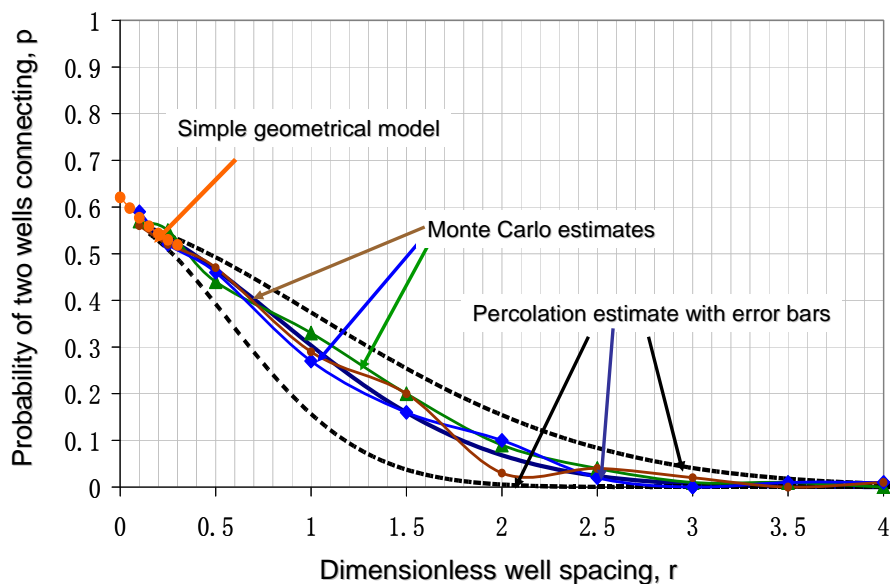


FIG. 5.8 Comparison of different estimates for D1 interval in dimensionless scale.

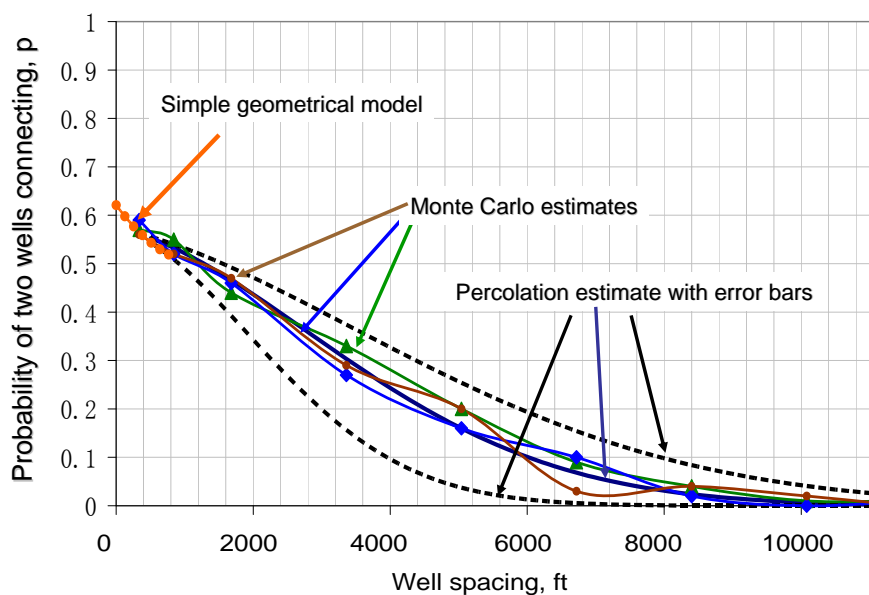


FIG. 5.9 Comparison of different estimates for D1 interval in actual scale.

5.2.2 D2 interval

The D2 is rather different from the D1. In the D2 zone map (Figure 5.4), we can find one percolation cluster but cannot find any separate sandbodies. The net sand thickness ranges from 0.98 to 18.5 ft (Table C.2). We chose the mode value of thickness distribution, 2 ft, as the cut off to separate the sandbody percolation cluster from the biggest connected sandbody cluster. Then, we used the “backward” mode to estimate the effective-square sandbody dimension (Figure 5.10).

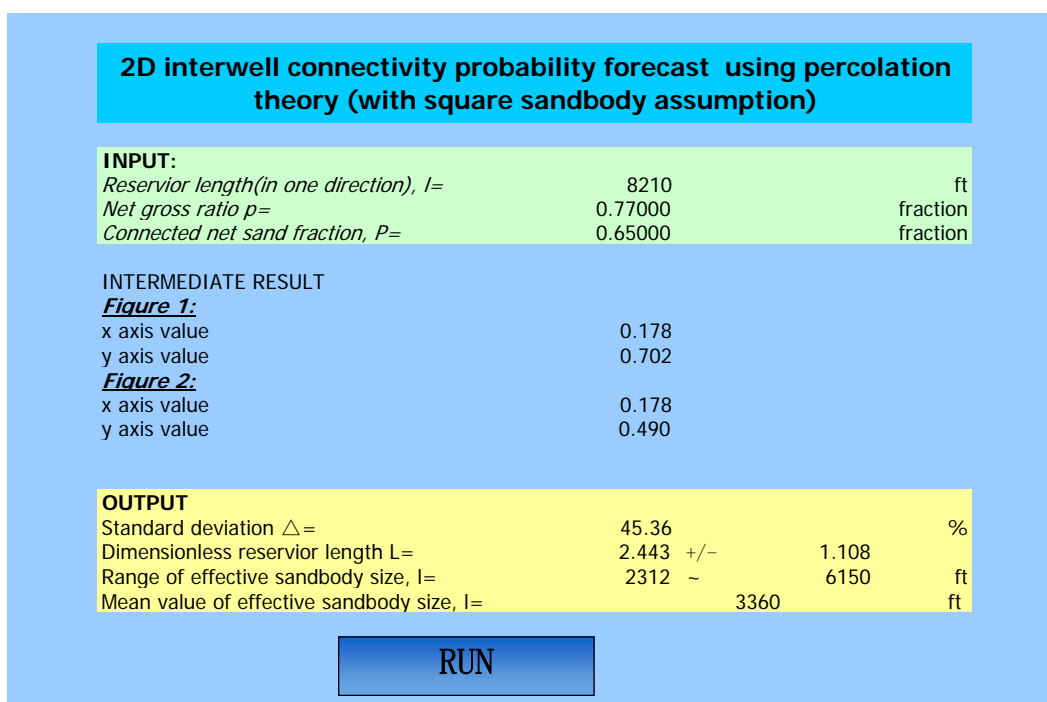


FIG. 5.10 Estimation of effective-square sandbody dimension of D2 interval.

The average well spacing is 1,320 ft. The mean value of the effective-square sandbody dimension is 3,360 ft and the range is 2312 to 6150 ft. Therefore, the estimated effective-square sandbody dimension is about 1.8 to 5.1 times the average well spacing.

This appears reasonable. In addition, the standard deviation Δ for D2 is bigger than the value for D1, which mean there is more uncertainty for the D2 interval. The mean value of L for D2 interval is 2.443, which is less than the value 3.213 for D1. As we have discussed for the D1 interval, the smaller study area may have led to bigger uncertainty. In further study, we can choose a larger study area to refine our interwell connectivity estimation. For this study, we still assume this area can represent the entire reservoir, although with a big uncertainty range.

Similar to the procedure for the D1 interval, we input the estimated values for $L_{\text{mean}} = 2.44$, $L_{\text{max}} = 3.48$, $L_{\text{min}} = 1.32$ and $p_{\text{sand}} = 0.77$ into our Mathematica program to get the estimated probability of connection for the D2 interval (Figure 5.11).

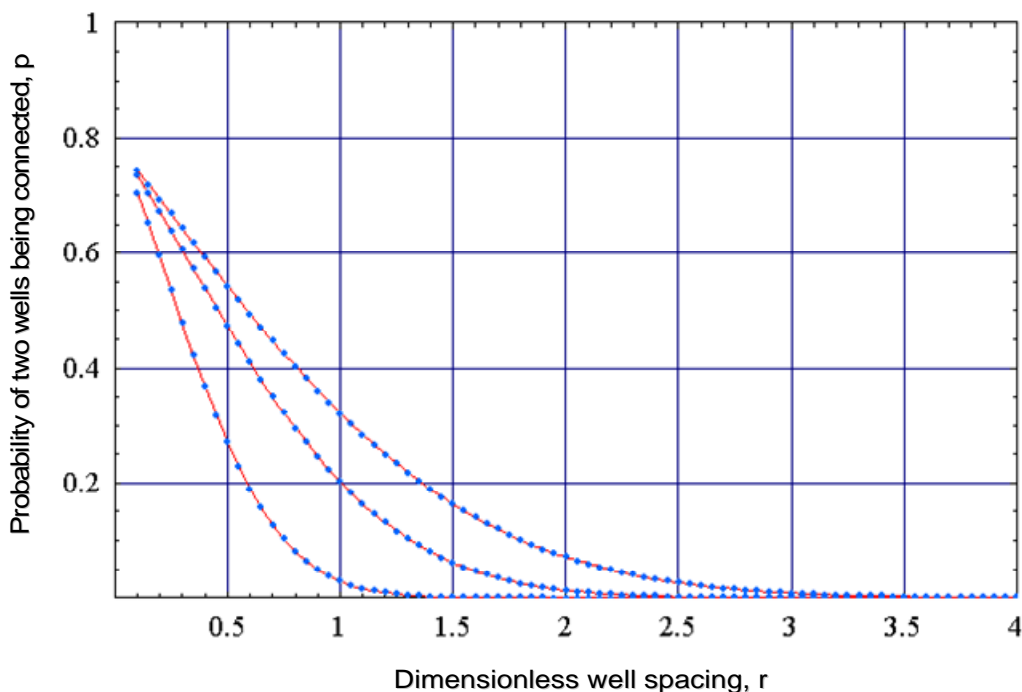


FIG. 5.11 Interwell connectivity probability estimation of D2 interval.

We compared interwell connectivity estimates from our new method, Monte Carlo simulation, and the simple geometrical model (Figures 5.12 and 5.13). Monte Carlo simulation and percolation estimation do not match very well. The mean curve of the Monte Carlo estimates is above the mean curve of percolation estimation and is almost same as the upper dashed curve of percolation estimation. But all data points of Monte Carlo simulation are still within the error bars of the percolation estimate, we suggest this agreement still is good enough for engineering applications.

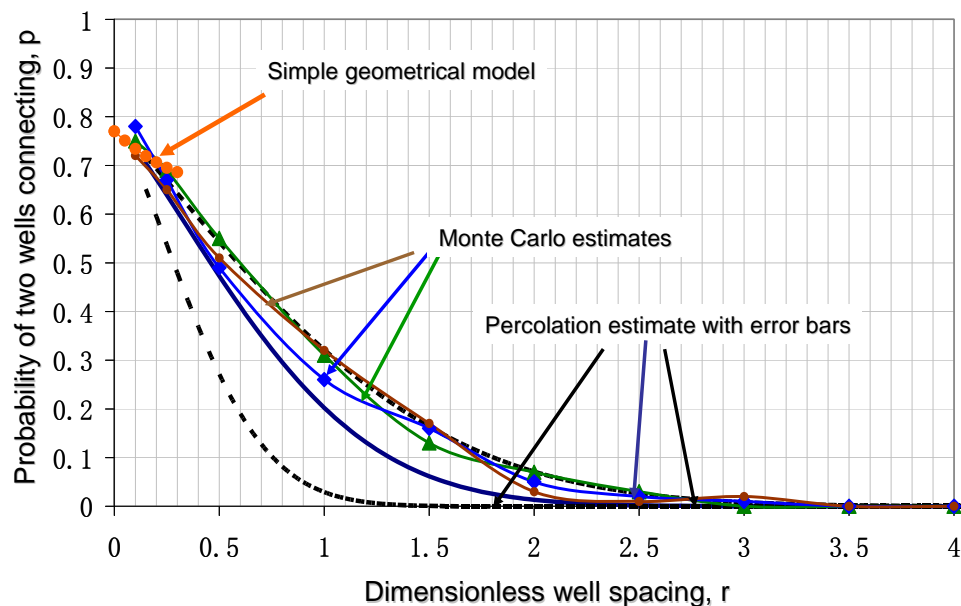


FIG. 5.12 Comparison of different estimates of D2 interval in dimensionless scale.

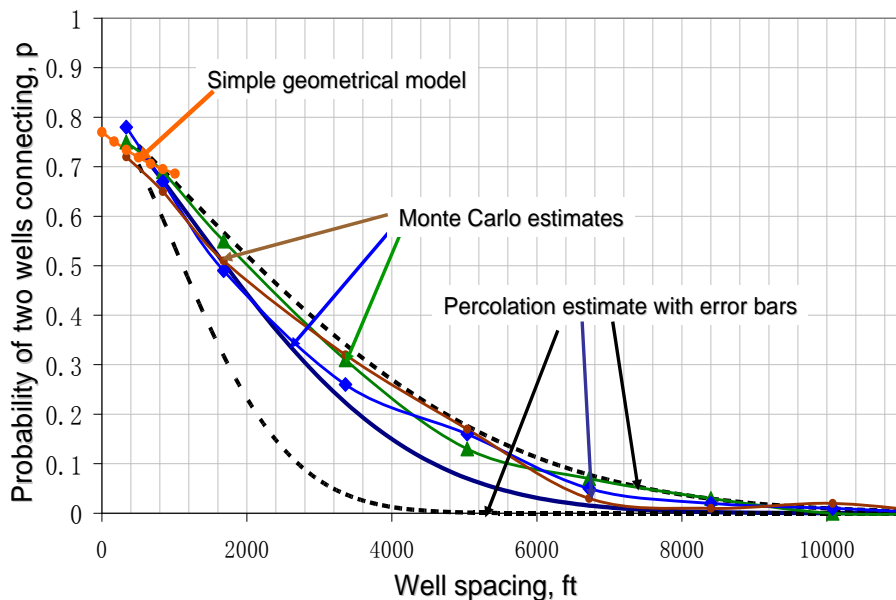


FIG. 5.13 Comparison of different estimates of D2 interval in actual scale.

5.2.3 D3 interval

The D3 interval is available only in seven wells. In the D3 zone map (Figure 5.5), we only can find three isolate sandbodies and no percolation cluster area in this interval. The “backward” mode needs P to estimate the effective-square sandbody dimension. To calculate P , we need know the area of percolation cluster. Therefore, we cannot apply the “backward” mode for the D3 interval. Assuming these three areas are separate sands, we can approximate the reservoir dimensionless length by following method.

Assuming the sand has a square shape, the effective length of every sand object is calculated as:

$$l_i = \sqrt{A_i} \dots\dots\dots (5.1)$$

Where A_i is the area of i^{th} sand and $i \in \{1,2,3\}$.

Then the reservoir dimensionless length is the ratio of the reservoir size to every sand size:

$$L_i = \frac{\sqrt{A_r}}{l_i} \dots\dots\dots (5.2)$$

Where A_r is the reservoir area.

The average L value is calculated as:

$$L_{average} = \frac{\sum_{i=1}^n L_i}{n} \dots\dots\dots (5.3)$$

Where $n=3$ for the D3 interval.

The sandbody occupied probability p_{sand} is calculated by definition:

$$P_{sand} = \frac{\sum_{i=1}^n A_i}{A_r} \dots\dots\dots (5.4)$$

The results are summarized as in Table 5.1:

TABLE 5.1 Percolation parameter estimations of D3 interval.

Sand	A_i, m^2	l_e, ft	L_i	$L_{average}$	P_{sand}
1	305664	1813	4.527	4.952	0.133
2	361613	1972	4.162		
3	164810	1332	6.166		

The mean value of the effective-square sandbody dimension is $l = \frac{1,813+1,972+1,332}{3} = 1,705 \text{ ft}$, which is about 1.3 times the average well spacing of 1,320 ft. Therefore, this approximation value of the effective-square sandbody is reasonable.

Inputting estimated effective-square sandbody dimensions $L_{\text{mean}} = 4.95$, $L_{\text{min}} = 4.16$, $L_{\text{max}} = 6.17$, and $p_{\text{sand}} = 0.133$ into our Mathematica program, the best interwell estimation we got for D3 is Figure 5.14.

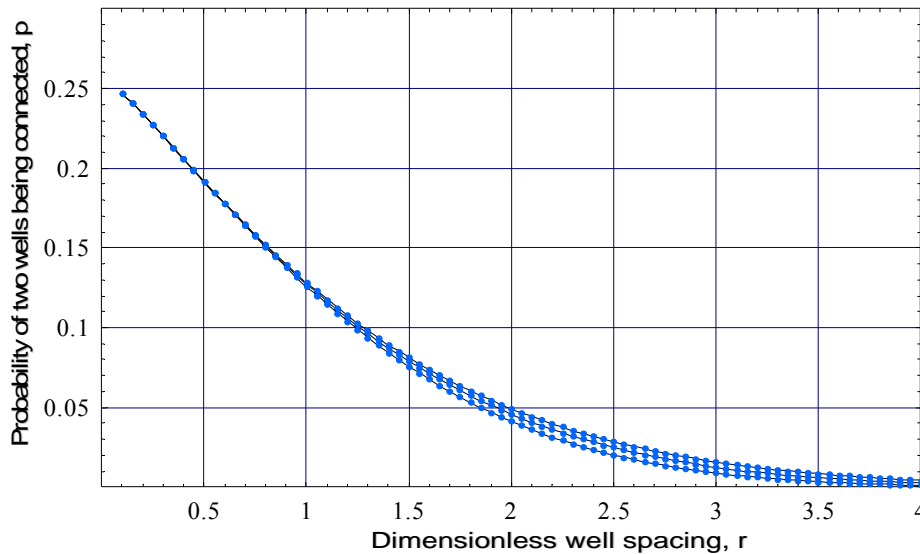


FIG. 5.14 Interwell connectivity probability estimation of D3 interval.

From the simple geometrical model discussion, we know the connectivity probability is p_{sand} when well spacing r approaches zero. For the D3 interval, we cannot make the connectivity probability be $p_{\text{sand}} = 0.133$ for zero well spacing r in our Mathematica program. The lowest connectivity probability we can get is 25%. Therefore, above estimation result is not right.

The reason may be that the exponent values of Eq. 3.8 cannot be applied for the systems far away from p_c . As we have discussed in Section 1.4.2, current research on percolation theory is mainly from Monte Carlo simulation, which may not cover the entire range of possible occupation probability values. We do not have enough theoretical

background to understand the way to improve the estimation value of these parameters in the current study.

We need to use other two methods to estimate the interwell connectivity performance of the D3 interval. We compared the estimates from Monte Carlo simulation and the simple geometrical model (Figures 5.15 and 5.16). The agreement between these two methods is good for the range $0.1 \leq r \leq 0.4$. From our Chapter III discussion, we know that the simple geometrical model application range is $0 \leq r \leq 0.5$. In Monte Carlo simulation, it is difficult to simulate interwell connectivity for well pair with very small r . We suggest using the simple geometrical model when $0 \leq r \leq 0.3$ and using the mean curve of Monte Carlo estimations when $r > 0.3$ to estimate the interwell connectivity performance of the D3 interval.

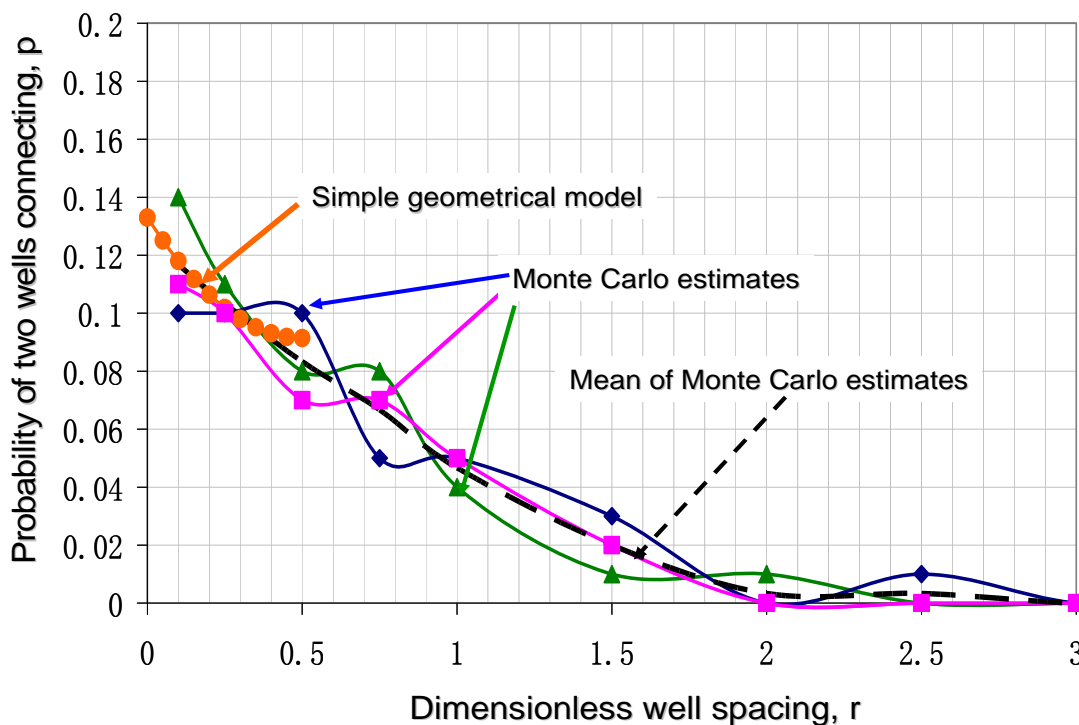


FIG. 5.15 Comparison of different estimates of D3 interval in dimensionless scale.

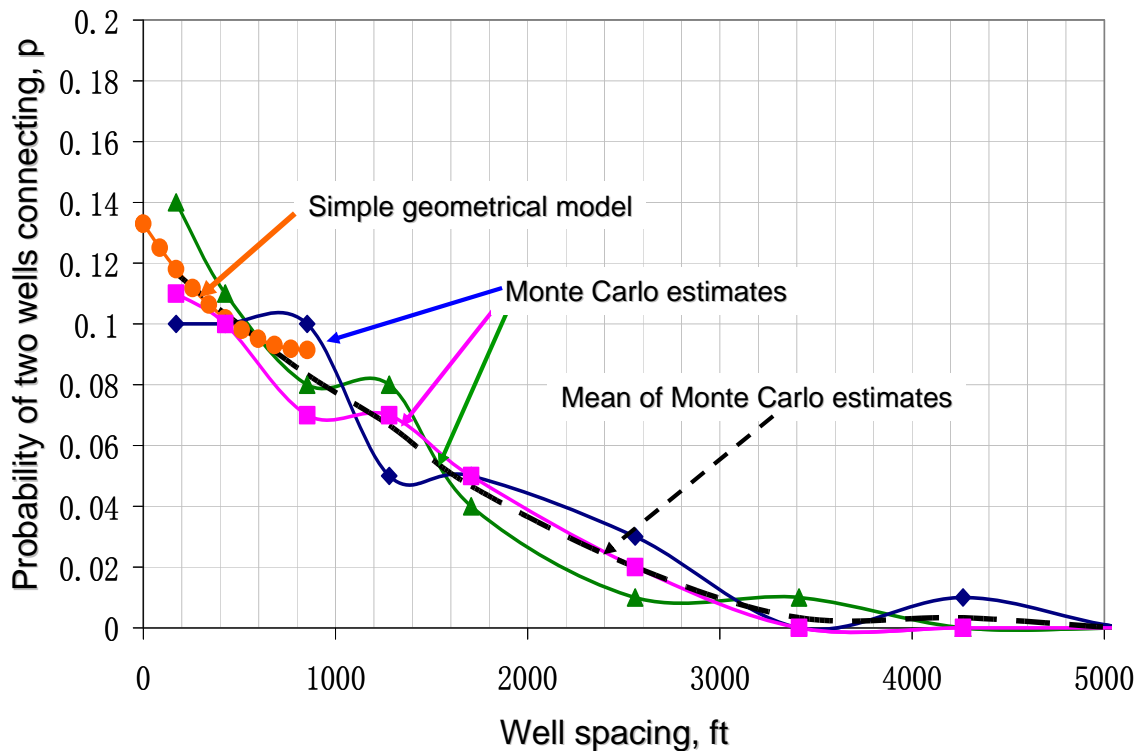


FIG. 5.16 Comparison of different estimates of D3 interval in actual scale.

5.2.4 Multilayer estimation

The Monument Butte field actually consists of many producing horizons. Therefore, we need to be able to predict interwell connectivity for all horizons together as well as individually. Here, we look at the combination of horizons D1, D2, and D3 as an example.

As discussed in Chapter III, we can choose any interesting property as the decision factor D to weight the connectivity of every interval. First, we choose the net sand thickness as the decision factor. The net sand average thicknesses of the D1, D2, and D3 intervals are summarized in Table 5.2.

TABLE 5.2 Net sand average thickness of D1, D2, and D3 intervals.

Interval	Average thickness, ft
D1	14
D2	7
D3	5

The interval with the higher thickness value is more important for the connectivity probability estimate. Therefore, we need to use the “positive” method to estimate the interwell connectivity.

Since many wells are perforated at the D1 interval, then let us consider another case when D1 is almost watered out but D2 and D3 remain highly oil saturated. We can assume that D1, D2 and D3 have different water saturation values after a long production period (Table 5.3).

TABLE 5.3 Water saturation of D1, D2, and D3 intervals
(hypothetical data).

Interval	Water saturation %
D1	85
D2	15
D3	12

The interval with the lower water saturation value is more important for estimating the connectivity probability. Therefore, we need to use the “negative” method to estimate the interwell connectivity.

We compared estimates from the “uniform” weight estimation; the “positive” weight estimation method, which is weighted by thickness; and the “negative” weight estimation method, which is weighted by water saturation (Figure 5.17).

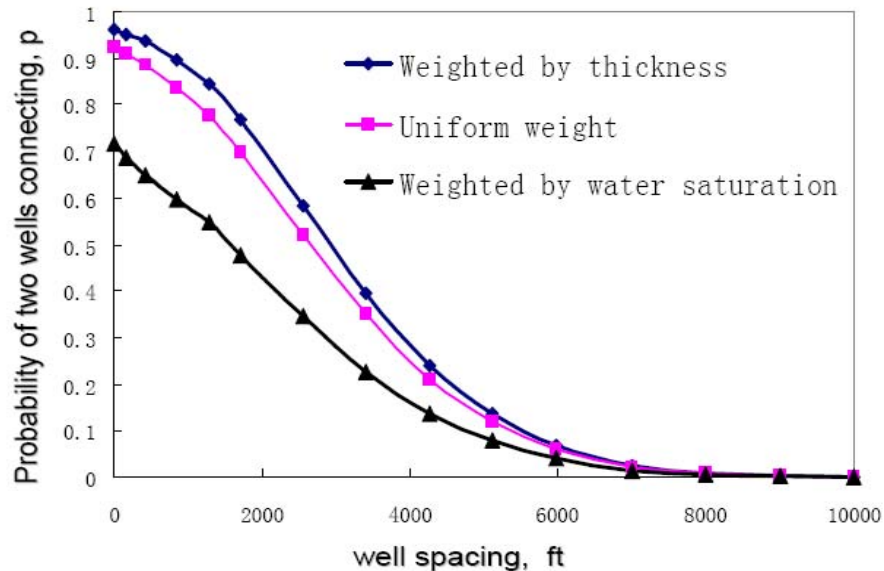


FIG. 5.17 Comparison of estimations from different method for a multilayer reservoir.

If we choose water saturation and interval thickness at the same time to be the decision factors, then the estimated connectivity is the spacing range between the “positive” method and “negative” method as we have discussed in Section 3.5.

We also should note water saturation will change for different production periods and so the weighted connectivity will change for different production time. This is very meaningful for field applications. If some interval breaks through very quickly, its related connectivity probability should also have quickly less weight in the multilayer connectivity. Once the interval is watered out, the interval has no value and the weight

factor of its connectivity probability changes to zero, which means this interval has no contribution for total production.

5.3 Summary and discussion

This chapter described the application of our new percolation method to D1, D2, and D3 intervals in a small study area of the Monument Butte field. We compared estimates from the new method, a simple geometrical model, and Monte Carlo simulation.

The comparison for the D1 interval with $p_{\text{sand}} = 0.62$ shows the agreement is very good. The comparison based on D2 with $p_{\text{sand}} = 0.77$ shows only small differences, which is acceptable for field application. For the D3 interval with $p_{\text{sand}} = 0.133$, the percolation-based method cannot get reasonable results but we still can apply the other two methods to estimate the interwell connectivity.

As we have discussed, this method will be less accurate when the sandbody occupied probability is far below the threshold value of $p_c \approx 0.6674$. Our suggestion is to use the new percolation method only when we find numerous and possibly touching sands in the study region. From the detailed application discussions of the D1 and D2, we know this percolation method can get reasonable estimates for p_{sand} in range of 60% to 80%. For D3 interval, our method fails when $p_{\text{sand}} = 0.13$. All this means our method limited to the application range of p_{sand} around $p_c = 0.6674$. For different L and P values, this application range may be different.

When p_{sand} is far from $p_c = 0.6674$, we suggest using the simple geometrical model when $0 \leq r \leq 0.3$ and using the mean curve of Monte Carlo estimations when

$r > 0.3$ to estimate the interwell connectivity performance as we discussed in Section 5.2.3.

For multilayer application, our method is straightforward to apply. From the chosen decision factors, engineers can do the estimates just by very simple mathematical calculations. The field operators can do their own analyses by choosing different parameters as the decision factors to weight the connectivity of every interval and then get the final estimate for the multilayer reservoir.

CHAPTER VI

CONCLUSIONS

This study showed that percolation theory is a very powerful tool that can be used to simulate the connectivity behavior between well pairs and can be used to estimate the interwell connectivity probability. Using the universal behavior of percolation phenomena, we proposed a new percolation method to estimate the interwell connectivity using simple mathematic calculation without having to perform a large number of numerical realizations for each new reservoir.

The comparison of estimations from our new method, Monte Carlo simulation and the simple geometrical model suggests that the percolation method can get reasonable results for Monument Butte field when p_{sand} in range of 60% to 80%. When the sandbody occupied probability p_{sand} is far from $p_c = 0.6674$, the estimation result may be wrong. We still can use Monte Carlo simulation and the simple geometrical model, however, to estimate the interwell connectivity probability.

Considering different intervals may have different weights, we propose a statistical method to incorporate the interval value D as a decision factor to get a multilayer estimation, which is more meaningful for well pattern design.

All these methods assume sandbodies distributed randomly and independently. If the actual sandbody distribution is very heterogeneous at field scale, the estimates from these methods are less representative or maybe wrong.

The estimation depends on the parameters from the study area we choose. This also means we need choose one “best representative area” to calculate the inputting

parameters p_{sand} and P . The best representative area should be big enough — i.e. L is big enough— to include enough information to represent the connectivity performance of entire reservoir. The smallest value of L suggested by King (1990) is $L = 5$.

In a pilot study of a field, we can use our percolation method to estimate interwell connectivity from a detailed study of one small area. Then, we can extrapolate the estimation results to the entire reservoir. When more data are available, other methods may need months of time to do the estimation again, but the percolation method can get one new estimate in several hours.

CHAPTER VII

RECOMMENDATIONS FOR FURTHER WORK

While the comparisons among our new percolation method, the simple geometrical model, and Monte Carlo simulation are encouraging, our method still exhibits a few limitations.

Sensitivity analysis of different L and P values will be helpful to determine the application range of p_{sand} . For example, more Monte Carlo tests based on the D3 interval might show the method still gives useful results for cases between $p_{sand} = 25\%$ and 40% . Based on this idea, we can find the minimum p_{sand} where the percolation-based method works and propose the application range of p_{sand} between the minimum p_{sand} and 80% for Monument Butte field.

In addition, further study should be made to compare our method with results from other methods, such as estimates from reservoir simulation and production/injection fluctuation rate analysis. These efforts may lead us to find more ways we can refine our method.

Our method is more suitable for reservoirs with thin intervals. Although we have proposed a multilayer estimation method for 3D application, the result from this method is an approximation, assuming no crossflow between different intervals. Extending our method to a 3D system will be more realistic than idealistic, but this will require more fundamental percolation research.

The assumption for this study is that the sandbodies are distributed randomly and independently in the reservoir. It will be more realistic to distribute the sands

conditionally, considering the spatial correlation of the sandbodies. A new study topic is correlated percolation study. Once the study of topic has promising results, we can consider how to incorporate the new research results into our interwell estimation method.

NOMENCLATURE

a	constants
A_{pl}	area of percolation cluster
A_r	area of the region
A_s	area of sands
b	constants
B	area of separate sands
c	constants
d	fractal dimension
D	decision factor; value of interval
E	efficient factor
g	exponents for geometric spacing effect
h	interval thickness
i	index
j	index
l	sandbody dimension
l_x	sandbody dimension in X direction
L_y	sandbody dimension in Y direction
L	dimensionless reservoir length
L_{max}	maximum value of dimensionless reservoir length
L_{mean}	mean value of dimensionless reservoir length
L_{min}	minimum value of dimensionless reservoir length
N	net-to-gross ratio
p	occupied probability
p_c	percolation threshold

p_{sand}	sandbody occupied probability
P	percolation cluster probability
P_{∞}	percolation cluster probability of infinite system
$P(x)$	probability of x
$P(\dots \dots)$	conditional probability
r	dimensionless well spacing
S_w	water saturation
t_{min}	minimum traveling time
t_{br}	breakthrough time
w_0	well spacing with field scale in small domain
W	dimension of sand with field scale in small domain
x	reservoir length in X direction; direction index
y	reservoir length in Y direction; direction index
β	exponents
θ	orientation degree
ν	exponents
ω	aspect ratio
φ	exponents
ψ	exponents
ξ	correlate length
Λ	constant of proportionality
\mathfrak{S}	universal mean connectivity function
\mathfrak{R}	universal standard deviation connectivity function
Δ	standard deviation

REFERENCES

- Albert, F. G., 1992, Stochastic models of reservoir heterogeneity: impact on connectivity and average permeabilities, SPE 24893: Society of Petroleum Engineering, presented at the SPE Annual Technical Conference and Exhibition, 16 p.
- Albertoni, A. and Lake, L. W., 2002, Inferring interwell connectivity only from well-rate fluctuations in waterfloods, SPE 75225: Society of Petroleum Engineering, presented at the SPE/DOE Improved Oil Recovery Symposium, 15 p.
- Andrade, J. S., Buldyrev, S. V., Dokholyan, N. V., Sholmo, H., King, P. R., Gerald, P., and Stanley, H. E., 2000, Flow between two sites in percolation systems, *Physical. review*, Vol. E62, p 8270-8281.
- Barrufet, M. A. and White, R. J., 1994, A waterflood model based upon percolation theory concepts, SPE 27018: Society of Petroleum Engineering, presented at the Latin American Caribbean Petroleum Engineering Conference, 13 p.
- Deo, M. D., Sarkar, A., Nielson, D. L., Lomax, J. D., and Pennington, B. I., 1994, Monument Butte unit case study: demonstration of a successful waterflood in a fluvial deltaic reservoir, SPE 27749: Society of Petroleum Engineering, presented at the SPE/DOE Improved Oil Recovery Symposium, 8 p.
- Gale, J. F. W., Laubach, S. E., and Olson, J., 2005, Using the link between diagenesis and fracturing to accurately predict, characterize, and model fluid-flow in fractured carbonate rocks, SPE 97382: Society of Petroleum Engineering, presented at the SPE Latin American and Caribbean Petroleum Engineering Conference, 15 p.
- Grimmett, G., 1999, *Percolation*, Springer, New York, 440 p.

- Heffer, K. J., Fox, R. J., and McGill, C. A., 1995, Novel techniques show links between reservoir flow directionality, earth stress, fault structure and geomechanical changes in mature waterfloods, SPE 30711: Society of Petroleum Engineering, presented at the SPE Annual Technical Conference and Exhibition, 8 p.
- Jansen, F. E. and Kelkar, M. G, 1997, Application of wavelets to production data in describing inter-well relationships, SPE 38876: Society of Petroleum Engineering, presented at the SPE Annual Technical Conference and Exhibition, 8 p.
- King, P. R, 1990, The connectivity and conductivity of overlapping sandbodies, *North sea oil and gas reservoirs II*, p 352-362.
- King, P. R., Buldyrev, S. V., Dokholyan, N. V., Havlin, S., Lee, Y., Paul, G., Stanley, H. E. and Vandesteeg, N., 2002, Predicting oil recovery using percolation theory, *Physics*, A 306, P 105-107.
- Masihi, M., King, P. R. and Nurafza, P., 2006a, Connectivity of fracture networks: the effects of anisotropy and spatial correlation, CMWR XVI-99, presented at the Computational Methods in Water Resources International Conference, 8 p.
- Masihi, M., King, P. R., and Nurafza, P. R., 2006b, Connectivity prediction in fractured reservoirs with variable fracture size: analysis and validation, SPE 100229: Society of Petroleum Engineering, presented at the SPE Europec/EAGE Annual Conference and Exhibition Vienna, 13 p.
- Nurafza, P. R., King, P. R., and Masihi, M., 2006a, Facies connectivity modeling: analysis and field study, SPE 100333: Society of Petroleum Engineering, presented at the SPE Europec/EAGE Annual Conference and Exhibition, 13 p.

- Nurafza, P. R., King, P. R. and Masihi, M., 2006b, Connectivity modeling of heterogeneous systems: analysis and field study, CMWRXVI-189, presented at the Computational Methods in Water Resources International Conference, 18 p.
- Panda, M. N. and Chopra, A. K., 1998, An integrated approach to estimate well interactions, SPE 39563: Society of Petroleum Engineering, presented at the SPE India Oil and Gas Conference and Exhibition, 14 p.
- Salomao, M. C., 1997, Analysis of flow in spatially correlated systems by applying the percolation theory, SPE 39039: Society of Petroleum Engineering, presented at the Latin American and Caribbean Petroleum Engineering Conference and Exhibition, 9 p.
- Soeriawinata, T. and Kelkar, M., 1999, Reservoir management using production data, SPE 52224: Society of Petroleum Engineering, presented at the SPE MidContinent Operation Symposium, 6 p.
- Stauffer, D. and Aharony, A., 1985, *Introduction to percolation theory*, Taylor and Francis Ltd., London, p 1-56.
- Yousef, A. A., Pablo G., Jensen, J. L., and Lake, L. W., 2005, A capacitance model to infer interwell connectivity from production and injection rate fluctuations, SPE 95322: Society of Petroleum Engineering, presented at the SPE Annual Technical Conference and Exhibition, 17 p.
- Yousef, A. A., Lake, L. W. and Jensen, J. L., 2006, Analysis and interpretation of interwell connectivity from production and injection rate fluctuations using a capacitance model, SPE 99998: Society of Petroleum Engineering, presented at SPE/DOE Symposium on Improved Oil Recovery, 15 p.

APPENDIX A

VBA CODE FOR INPUTTING PARAMETER ESTIMATION

Code:

```
Sub Macro1()
```

```
ThisWorkbook.Sheets("program").Range("J22:L24").ClearContents
```

```
Range("J23") = "5"
```

```
SolverOk SetCell:="$J$19", MaxMinVal:=3, ValueOf:="0", ByChange:="$J$23"
```

```
SolverSolve UserFinisH:=True
```

```
SolverFinish KeepFinal:=1
```

```
ThisWorkbook.Sheets("plot").Select
```

```
mesy = "According to x value, please find and input y value for further calculation! For example:
```

```
for x=-0.0957,y=0.403.Choose y value for your x value now, y="
```

```
y = InputBox(mesy)
```

```
ThisWorkbook.Sheets("program").Select
```

```
Cells(18, 10) = y
```

```
Cells(22, 10) = y / Cells(23, 10) ^ (0.14 / 1.62) * 100
```

```
Cells(23, 12) = Cells(23, 10) * Cells(22, 10) / 100
```

```
Cells(23, 11) = "+/-"
```

```
Cells(24, 10) = Cells(8, 10) / (Cells(23, 10) * (1 + Cells(22, 10) / 100))
```

```
Cells(24, 12) = Cells(8, 10) / (Cells(23, 10) * (1 - Cells(22, 10) / 100))
```

```
Cells(24, 11) = "~"
```

```
Cells(25, 11) = Cells(8, 10) / Cells(23, 10)
```

```
Range("J24:L24").Select
```

```
MsgBox "Calculation finished!"
```

```
End Sub
```

APPENDIX B

MATHEMATICA CODE FOR INTERWELL ESTIMATION

Code:

Default

Directory

```
thisDir = ToFileName[{"FileName" /. NotebookInformation[EvaluationNotebook[]][[1]]];  
SetDirectory[thisDir];
```

Graphics

```
Needs["Graphics`Graphics`"]  
SetOptions[{Plot, LogLinearPlot, LinearLogPlot, LogLogPlot, ListPlot, LogLinearListPlot,  
  LinearLogListPlot, LogLogListPlot}, Frame → True, PlotStyle → {PointSize[0.015], RGBColor[1, 0, 0]},  
  ImageSize → 450, DefaultFont → {"Times", 14}, PlotRange → All, GridLines → Automatic];  
Off[General::"spell1"]  
Off[General::"spell"]
```

Parameters

```
Lmean = 2.44;  
Lmax = 3.48;  
Lmin = 1.42;  
psand = 0.62;  
g = 2.38;
```

Program

```

data1 = {dt → 1.28, a → 1.1, b → 5.0, c → 1.6, ϕ → 3.0, ϕ → 3.0, v → 0.75, pc → 0.6674, κ → 1};
p[tbr_, p_, L_, r_] :=  $\frac{1}{r dt} \left(\frac{tbr}{r dt}\right)^{-a} e^{-a \left(\frac{tbr}{r dt}\right)^{\phi}} e^{-b \left(\frac{tbr}{r dt}\right)^{\phi}} e^{-c \left(\frac{tbr}{\text{Abs}[p-pc]^{\phi}}\right)^{\kappa}}$  /. data1
rI = SetPrecision[Table[i, {i, 0.1, 9, 0.05}], 30];
pI = SetPrecision[0 rI, 30];
L = SetPrecision[{Lmean, Lmax, Lmin}, 5];
Ls = SetPrecision[0 L, 30];
Do[
  Do[
    pI[[i]] = SetPrecision[NIntegrate[p[tbr, psand, L[[j]], rI[[i]], {tbr, 0, 50}, AccuracyGoal → 30], 30]
    , {i, 1, Length[rI]}
  ];
  pPoint = ListPlot[Transpose[{rI, pI}],
    DisplayFunction → Identity,
    GridLines → Automatic,
    PlotStyle → Hue[0.6]];
  pLine = ListPlot[Transpose[{rI, pI}],
    PlotJoined → True, GridLines → Automatic,
    DisplayFunction → Identity];
  Export["percoaltion_mean.xls", Transpose[{rI, pI}], "TSV"];
  Ls[[j]] = Show[ {pLine, pPoint},
    PlotRange → {{0, 4}, {0, 1}},
    ImageSize → 900,
    Frame → True,
    FrameLabel → {"dimensionless well spacing r", "Well pairs connectivity probability p, fraction ",
    "Well pairs connectivity probability p vs dimensionless well spacing r for D1
    horizontal interval", ""},
    TextStyle → {FontFamily → "Times", FontSize → 18},
    DisplayFunction → Identity],
    {j, 1, Length[L]}]

Show[ Ls,
  PlotRange → {{0, 4}, {0, 1}},
  ImageSize → 700,
  Frame → True,
  FrameLabel → {"Dimensionless well spacing r", "Connectivity probability p, fraction ",
  "Interwell connectivity probability p estimation using percoaltion theory", ""},
  TextStyle → {FontFamily → "Times", FontSize → 18},
  DisplayFunction → $DisplayFunction,
  GridLines → Automatic
]

```


APPENDIX C

RESERVOIR PROPERTIES SUMMARY OF D1, D2 AND D3

TABLE C.1 Reservoir Properties Summary of D1 Interval.

Well	Sand per well	D1 Sand Thickness (ft)					Net Sand
		sand 1	sand 2	sand 3	sand 4	sand 5	
4301332219	0	0	0	0	0	0	0
4301331819	0	0	0	0	0	0	0
4301331435	0	0	0	0	0	0	0
4301331716	0	0	0	0	0	0	0
4301330747	0	0	0	0	0	0	0
4301332103	0	0	0	0	0	0	0
4301331268	0	0	0	0	0	0	0
4301331503	0	0	0	0	0	0	0
4301331971	0	0	0	0	0	0	0
4301331499	0	0	0	0	0	0	0
4301332096	0	0	0	0	0	0	0
4301332102	1	4.49	0	0	0	0	4.49
4301331228	1	7.53	0	0	0	0	7.53
4301332098	1	8.48	0	0	0	0	8.48
4301331972	1	11.49	0	0	0	0	11.49
4301331251	1	18.48	0	0	0	0	18.48
4301331250	1	22.04	0	0	0	0	22.04
4301331214	1	29	0	0	0	0	29
4301331270	2	2.53	3.49	0	0	0	6.02
4301331973	2	3.04	4.51	0	0	0	7.55
4301332105	2	3.49	4	0	0	0	7.49
4301331271	2	3.99	15.52	0	0	0	19.51
4301330638	2	4.49	10.5	0	0	0	14.99
4301332104	2	5	1.53	0	0	0	6.53
4301330858	2	6.52	0.51	0	0	0	7.03
4301331225	2	7.99	5	0	0	0	12.99
4301331240	2	9.45	8.99	0	0	0	18.44
4301331277	2	10.52	4.49	0	0	0	15.01
4301331272	2	25.6	1.96	0	0	0	27.56
4301330699	3	1.49	2.99	1	0	0	5.48
4301331205	3	4.48	3.49	6.97	0	0	14.94
4301332132	3	25.4	1.01	3.48	0	0	29.89
4301331229	4	1.5	1.39	2.03	6.52	0	11.44
4301331269	4	3.43	2.98	2.02	3.49	0	11.92
4301331817	5	3.03	4	4.94	0.51	2.48	14.96

TABLE C.2 Reservoir Properties Summary of D2 Interval.

Well	Sand per well	D2 Sand Thickness (ft)					Net Sand
		sand 1	sand 2	sand 3	sand 4	sand 5	
4301330699	0	0	0	0	0	0	0
4301330858	0	0	0	0	0	0	0
4301331205	0	0	0	0	0	0	0
4301331228	0	0	0	0	0	0	0
4301331240	0	0	0	0	0	0	0
4301331251	0	0	0	0	0	0	0
4301331268	0	0	0	0	0	0	0
4301331716	0	0	0	0	0	0	0
4301331817	0	0	0	0	0	0	0
4301331973	0	0	0	0	0	0	0
4301332096	0	0	0	0	0	0	0
4301332098	0	0	0	0	0	0	0
4301332102	0	0	0	0	0	0	0
4301332103	0	0	0	0	0	0	0
4301332105	0	0	0	0	0	0	0
4301332219	0	0	0	0	0	0	0
4301332132	1	0.98	0	0	0	0	0.98
4301331819	1	1.46	0	0	0	0	1.46
4301331270	1	1.95	0	0	0	0	1.95
4301331229	1	2	0	0	0	0	2
4301330638	1	2.01	0	0	0	0	2.01
4301331503	1	2.01	0	0	0	0	2.01
4301331499	1	3	0	0	0	0	3
4301331272	1	3.51	0	0	0	0	3.51
4301331250	1	4.5	0	0	0	0	4.5
4301331225	1	7.5	0	0	0	0	7.5
4301332104	1	7.51	0	0	0	0	7.51
4301330747	1	8.5	0	0	0	0	8.5
4301331214	1	10.98	0	0	0	0	10.98
4301331971	1	11.49	0	0	0	0	11.49
4301331435	2	0.5	4.51	0	0	0	5.01
4301331972	2	6.5	1.55	0	0	0	8.05
4301331269	2	9.04	2.03	0	0	0	11.1
4301331277	2	10.02	8.51	0	0	0	18.5
4301331271	2	10.9	2.5	0	0	0	13.4

TABLE C.3 Reservoir Properties Summary of D3 Interval.

Well	Sand per well	D3 Sand Thickness (ft)					Net Sand
		sand 1	sand 2	sand 3	sand 4	sand 5	
4301330638	0	0	0	0	0	0	0
4301330699	0	0	0	0	0	0	0
4301330747	0	0	0	0	0	0	0
4301330858	0	0	0	0	0	0	0
4301331205	0	0	0	0	0	0	0
4301331214	0	0	0	0	0	0	0
4301331225	0	0	0	0	0	0	0
4301331228	0	0	0	0	0	0	0
4301331250	0	0	0	0	0	0	0
4301331251	0	0	0	0	0	0	0
4301331270	0	0	0	0	0	0	0
4301331271	0	0	0	0	0	0	0
4301331272	0	0	0	0	0	0	0
4301331277	0	0	0	0	0	0	0
4301331435	0	0	0	0	0	0	0
4301331499	0	0	0	0	0	0	0
4301331503	0	0	0	0	0	0	0
4301331716	0	0	0	0	0	0	0
4301331817	0	0	0	0	0	0	0
4301331819	0	0	0	0	0	0	0
4301331971	0	0	0	0	0	0	0
4301331972	0	0	0	0	0	0	0
4301331973	0	0	0	0	0	0	0
4301332096	0	0	0	0	0	0	0
4301332104	0	0	0	0	0	0	0
4301332105	0	0	0	0	0	0	0
4301332132	0	0	0	0	0	0	0
4301332219	0	0	0	0	0	0	0
4301331240	1	2	0	0	0	0	2
4301331268	1	2	0	0	0	0	2
4301332098	1	2	0	0	0	0	2
4301332103	1	3	0	0	0	0	3
4301331269	1	4	0	0	0	0	4
4301332102	1	12.49	0	0	0	0	12.49
4301331229	2	2.5	7.02	0	0	0	9.52

VITA

Weiqiang Li received his degree of Bachelor of Science in Energy and Thermal Engineering in 1997. In June 2005, he entered the Graduate School at Texas A&M University at College Station and studied there under the supervision of Dr. Jensen from May, 2006.

Permanent Address: Hekou Post Office,
Dongying, Shandong,
257000, China

This thesis was typed by the author.